ISBN4-901449-25-7

CNEAS

EXPLOSIVE VOLCANISM IN THE PHILIPPINES

S G. Catane, H Taniguchi, A Goto,
A P. Givero, A A. Mandanas

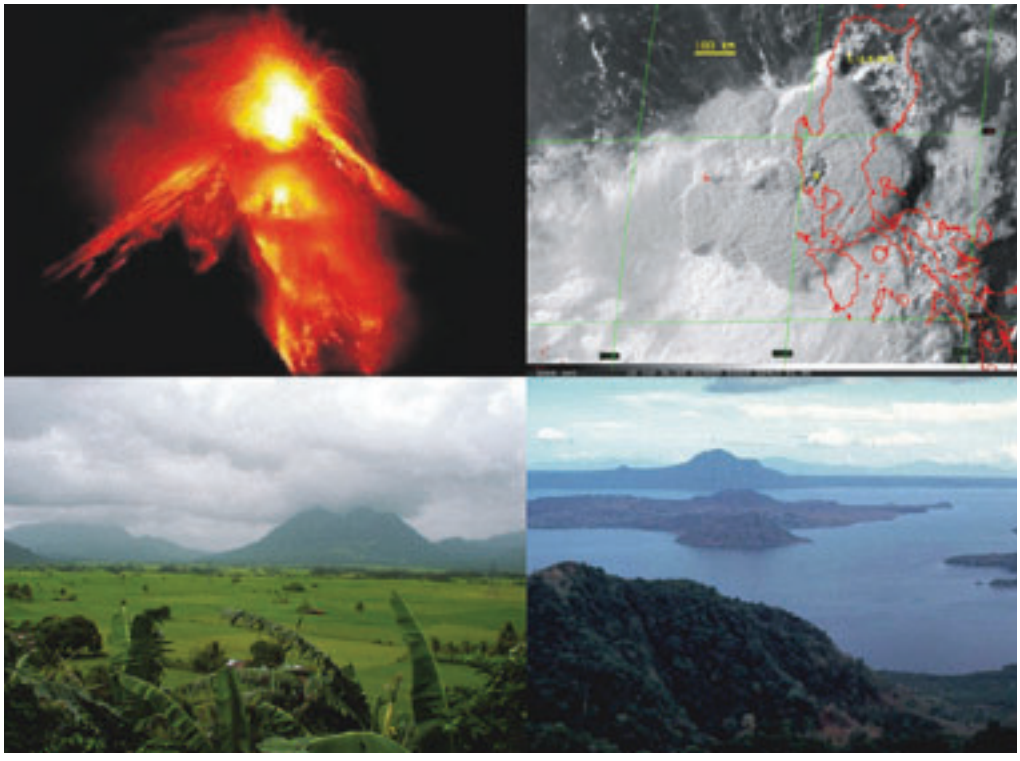

CNEAS Monograph Series No.18

Center for Northeast Asian Studies
Tohoku University

Cover photo:
(A) Strombolian phase of the 2000 eruption of Mayon Volcano. (B) Satellite image of Pinatubo eruption plume at 1630 hrs (local time), three hours after the onset of the climactic eruption on June 15, 1991. Diameter of the plume is about 700 km. (C) A view of the sediment-filled Irosin Caldera floor, post-caldera dome complex Mt. Jormahan (offcenter left) and the lower slopes of active Bulusan Volcano (left). (D) A view of Taal Volcano and its caldera (Taal Caldera). The prominent cone on the island (forefront) is Binintiang Malaki. Formed part of the southern caldera rim, Mt. Macolod (foreground) is a pre-caldera center. Flat topography left of Mt. Macolod is a pyroclastic flow surface. Photo credits: (A) taken by an unknown photographer in Legaspi City, (B) Koyaguchi and Tokuno, 1993 ; Holasek et al., 1996, (C) S. Catane, (D) PHIVOLCS.

Back cover photo:
Exposure of the <27-29 ka Teresa Scoria Flow valley-fill facies showing complex cooling-joint pattern. Correlative units were traced in Metro Manila and surrounding provinces. It is considered as the youngest large-scale pyroclastic flow event associated with Laguna Caldera.

CNEAS

EXPLOSIVE VOLCANISM IN THE PHILIPPINES

S G. Catane, H Taniguchi, A Goto,
A P. Givero, A A. Mandanas

CNEAS Monograph Series No.18

Center for Northeast Asian Studies
Tohoku University

EXPLOSIVE VOLCANISM IN THE PHILIPPINES

Sandra G. Catane*, Hiromitsu Taniguchi**, Akio Goto**,
Andrea P. Givero*, Allan A. Mandanas*

Keywords: volcano, explosive eruption, Mayon, Taal, Pinatubo, Hibok-Hibok, Parker, Philippines

Abstract

The Philippine archipelago lies along the western tectonically active margin of the Pacific Basin. It has a complex volcano-tectonic setting mainly as a result of the oblique convergence of the NNW moving Philippine Sea Plate and the ESE movement of the Eurasian Plate. There are 10 identified volcanic arcs, 9 of which are related to subduction volcanism. The two major subduction zones, the Manila Trench and the Philippine Trench, are sites of most active volcanism and intense seismicity in the Philippines.

There are 22 active volcanoes among the more than 400 volcanoes hosted by the Philippine Islands. Twenty seven are recently identified by the Philippine Institute of Volcanology and Seismology (PHIVOLCS) as potentially active and 359 are inactive. The most explosive volcanoes in recent Philippine history are Mayon, Taal, Pinatubo, Hibok-Hibok and Parker. At least 3 calderas with relatively young caldera-related eruptions have been identified. Taal Caldera and Laguna Caldera is located 60 km and 20 km, respectively, from the nation's capital, Metropolitan Manila (population of about 12 M). The last calderagenic eruption of Taal caldera occurred between 5,380-6,830 yBP.

The Philippines has the most violent volcanoes in the world in terms of casualty. In the 20th century alone, 2,800 lives were lost in the eruptions of the four most explosive volcanoes: 200-300 (Pinatubo 1991), 500 (Hibok-Hibok 1953), 77 (Mayon 1993), 1,335 (Taal 1911), and 200 (Taal 1965). Improved monitoring capabilities, hazard mitigation and intensive hazard

* National Institute of Geological Sciences, University of the Philippines, Diliman, Quezon City, Philippines
** Center for Northeast Asian Studies, Tohoku University, Japan

awareness campaign led by PHIVOLCS during the last two decades significantly reduced the casualties and damages due to volcanic eruptions. For example, casualty could have been higher if no accurate warning was issued during the 1991 Pinatubo eruption where 60,000 people were evacuated to safety and, of these, 20,000 escaped certain death. Moreover, the early detection of precursors prior to the most recent 2001 Mayon eruption allowed volcanologists to issue appropriate warnings to local officials and disaster coordinating agencies and to evacuate over 25,000 people.

Many Philippine volcanoes are explosive because of the general tectonic setting (subduction-related), mostly silicic to intermediate compositions, high volatile contents of magmas, and easy access of water to volcano conduits. Being an archipelago, many explosive eruptions in the Philippines occurred because of water-magma interaction, e.g., Taal, Laguna. Even small phreatic eruptions are equally hazardous and can be regarded as "explosive" due to the wide extent of damage and eruption's ability to kill a number people, as in the case of the 1993 Mayon eruption. Historical eruptions showed that most casualties and property damages were due to of populated communities with active Philippine volcanoes.

Contents

Abstract 1
Acknowledgements 6

1. Introduction 6
2. Volcanic arcs and tectonic elements 9
2.1 Volcanic arcs
2.1.1 Central Luzon Belt
2.1.2 East Philippine Volcanic Arc
2.2 Major tectonic features
2.2.1 Philippine Fault
2.2.2 Manila Trench
2.2.3 East Luzon Trough
2.2.4 Philippine Trench
2.2.5 Negros Trench
2.2.6 Sulu Trench
2.2.7 Cotabato Trench
3. Classification of Philippine volcanoes 22
4. Eruptive histories of the most explosive active volcanoes in the Philippines 23
4.1 Mayon Volcano
4.1.1 Volcano profile
4.1.2 Age estimate
4.1.3 Geochemistry and geochemical variations
4.1.4 Recent explosive eruptions
4.1.5 Style and patterns of eruptions
4.1.6 Volcanic hazards
4.1.7 Hazard zones
4.1.8 Volcano monitoring and eruption prediction techniques
4.2 Taal Volcano
4.2.1 Volcano profile
4.2.2 Morphological and geological features

4.2.3 Historic eruptions, eruptive style, and patterns
4.2.4 Volcanic hazards
4.2.5 Monitoring techniques and devices
4.3 Pinatubo Volcano
4.3.1 Volcano profile and summary of recent activities
4.3.2 Geology and eruptive history
4.3.3 The 1991 Mt. Pinatubo eruption
4.3.4 Pinatubo crater lake artificial breaching － a mitigation measure
4.3.5 Volcanic hazards
4.3.6 Volcano monitoring
4.4 Hibok-Hibok Volcano
4.4.1 Volcano profile and recent activities
4.4.2 Evolution of Hibok-Hibok Volcano
4.4.3 Historical eruptions and eruptive patterns
4.4.4 Volcanic hazards and hazard zones
4.4.5 Volcano monitoring and eruption precursors
4.5 Parker Volcano
4.5.1 Volcano profile
4.5.2 Geology
4.5.3 Historical evidence for the 17th century eruption
4.5.4 C-14 ages in support to historical evidence
4.5.5 Volcanic hazards and monitoring
5. Philippine calderas and associated activities ····· 26
5.1 Taal Caldera
5.1.1 Geologic setting
5.1.2 Caldera features and stratigraphy
5.2 Laguna Caldera
5.2.1 Geologic setting
5.2.2 Age, stratigraphy, and caldera history
5.3 Irosin Caldera
5.3.1 Geologic setting
5.3.2 Geologic history of Irosin Caldera
6. Summary and Conclusions ····· 131

要　　旨

フィリピン諸島は太平洋西縁の活動的な沈み込み帯に沿って位置し，フィリピン海プレートの北北西方向の移動とユーラシアプレートの東南東方向の移動が斜交することにより，複雑な火山・地質環境を有する。そこには10の火山列があり，そのうち9は沈み込みによる火山活動と関係している。主要な沈み込み帯であるマリアナトレンチとフィリピントレンチはフィリピンで最も活動的な火山活動が見られるとともに，地震活動も活発である。

フィリピンにある400以上の火山のうち，22は活動的で，27はフィリピン火山地震研究所（PHIVOLCS）により活動の潜在性が指摘されている。最近のフィリピンで最も爆発的な活動をした火山として，マヨン，タール，ピナツボ，ヒボク-ヒボク，パーカーが挙げられる。比較的最近活動したカルデラが少なくとも 3 つある。タールカルデラとラグナカルデラは人口1200万人の首都マニラからそれぞれ60kmと20kmに位置し，タールカルデラを形成した最後の噴火は5,380-6,830年前とされている。

人的被害の面で考えると，フィリピンの火山は世界で最も危険だと言え，20世紀だけでおよそ2800人が犠牲になっている（200-300人（ピナツボ1991年），500人（ヒボク-ヒボク1953年），77人（マヨン1993年），1335人（タール1911年），200人（タール1965年））。監視態勢の強化，減災対策，20年に渡る PHIVOLCS による啓蒙活動の結果，火山噴火による被害は大きく軽減された。例えばピナツボ1991年噴火では適切に情報が発信され，6 万人が避難し，結果として 2 万人の人命が救われたと推定されている。また最近のマヨン2001年噴火では火山学者からの警告が噴火に先立ち行政に伝えられ，2 万 5 千人が避難した。

フィリピンの多くの火山は爆発的で，その原因は沈み込みに関連した地質的要因，すなわちマグマがシリカと揮発性成分に富むこと，さらに地下水の火道への侵入が容易に起こりうることに起因する。タールやラグナをはじめとし，多くの爆発的な噴火は天水との接触により起こっている。小規模な水蒸気爆発であっても災害を引き起こす可能性は高く，1993年のマヨンのように人を殺傷することもある。過去の噴火は，人的・物的損害の発生は，人々が火山の近くに居住していることに起因することを物語っている。

Acknowlegements

We thank the Prof. K. Yamada, Director of the Center for Northeast Asian Studies, Tohoku University, for supporting our study on explosive volcanism. S. G. Catane would like to thank T. Miyamoto for the helpful discussions on comparative volcanism of Japan and the Philippines. M.H. Mirabueno shared the electronic files of published hazard maps of PHIVOLCS. Some sections of the Pinatubo chapter including geology, 1991 eruption, and crater lake breaching event were referred from the IUGG 2003-A5 guidebook by Catane et al., 2003. This summary paper was prepared while S.G. Catane was visiting the Center for Northeast Asian Studies, Tohoku University, Japan from March-June 2004.

1. Introduction

The Philippines has more than 400 volcanoes mostly distributed in five young and five older volcanic belts or arcs linked to active and inactive subduction zones. Although rare, some young volcanoes may be related to volcanic settings other than subduction, such as the Cuyo Island volcanoes and Amoguis Volcano (30 ka by K-Ar: JICA, 1999) in the continental Palawan Island (Adriano et al., 2002). Among the volcanoes, at least 22 are active, several of which have erupted in recent historic times. The Philippine Institute of Volcanology and Seismology (PHIVOLCS) classified 27 volcanoes as potentially active and 359 others as inactive. Philippine volcanoes dominantly produce andesitic magmas with calc-alkaline affinities, but basaltic to rhyolitic magmas are also generated. Two of the three identified calderas in the Philippines are also of intermediate composition. The dominant volcano landform is composite type.

Among the active volcanoes, Mayon, Taal, Pinatubo, Hibok-Hibok, and Parker are the most explosive. The most recent explosive eruption took place at Mayon Volcano in 2001. Although infrequent, eruptions of Hibok-Hibok in 1951-1953 and Pinatubo in 1991 are among the most explosive events in the Philippine historic record. Mt. Pinatubo's violent eruption in 1991 is considered the largest in Philippine history and the third largest worldwide in the 20th century. The eruption had inflicted long-term and widespread damage in the surrounding provinces. The recent crater-lake break-out on 10 July 2002 signifies the continuing hazards from Pinatubo Volcano. Taal Volcano, a small island volcano in southern Luzon, has had the most number of violent eruptions (e.g., 1754, 1911, 1965), the latest of which occurred

in 1977. Taal is known for its violent base surges. Parker Volcano is one of the less known but one of the most explosive volcanoes in the Philippines. Its eruption in 1641 caused darkness over Mindanao and adjacent islands.

Philippine volcanoes erupt at different styles: phreatic, phreatomagmatic, Strombolian, Vulcanian, Pelean, Merapi, and Plinian. The most explosive volcanoes in recent Philippine history are Taal, Mayon, and Pinatubo. Taal, one of the smallest but deadliest volcanoes in the world, is known for its violent phreatomagmatic activities (e.g., 1911, 1965). Mayon, a volcano famous for its near-perfect symmetry, have erupted 48 times, most of which are Vulcanian. In the climactic 15 June 1991 Plinian eruption of Pinatubo Volcano, the plume intruded the stratosphere to heights beyond 40 km. The head of the giant umbrella cloud expanded laterally to more than 700 km within three hours, covering most of Luzon Island.

Eruption phenomena are variable for each volcano, temporally even in a single eruption episode. The most common hazards directly associated with eruptions are lava flows, lava domes, pyroclastic flows, pyroclastic surges, lateral blasts, tephra falls, and volcanic gases. Base surge, a type of pyroclastic surge, is typical for Taal eruptions, while pyroclastic flow is a common hazard for Pinatubo, Parker, and Mayon. Indirectly-associated hazards are lahars, debris avalanches, tsunamis, subsidence, secondary explosions, secondary pyroclastic flows, and crater-lake breakout. Lahars and debris avalanches can be syn-eruption hazards. Lahars, secondary explosions and pyroclastic flows, and lake breakout, are post-eruption hazards of the 1991 Pinatubo eruption. There is no historical occurrence of debris avalanche in Philippine volcanoes except for the 1628 (?) debris avalanche in Iriga Volcano (Aguila et al., 1986).

Calderas are the most explosive volcanoes in the Philippines based on studies of their deposits. Because of the scarcity of detailed work, only three calderas, Taal, Laguna, and Irosin, will be described herein. These calderas are characterized by the extrusion of andesitic to dacitic magma in the order of tens to hundred cubic meters similar to those erupted by calderas in Japan. The youngest calderagenic event occurred in Taal caldera between 5,380 to 6,830 yBP. This very young activity qualifies Taal caldera as "active", according to the definition of PHIVOLCS.

Volcano and earthquake monitoring is conducted by PHIVOLCS. At least one permanent volcano monitoring station is established in each volcano in the most active category. Additional seismic stations are established when a volcano shows signs of reactivation. Other monitoring methods such as geophysical, geochemical, and visual observations are

conducted on a regular basis. Volcano monitoring activities of PHIVOLCS are augmented by partners abroad, mainly the United States Geological Survey (USGS) and other volcano observatories in Japan.

Each of the active volcanoes in the Philippines has a different set of eruption precursors. The most common precursors include the following: increase frequency of volcanic quakes; increase in steam activity; crater glow; ground swelling; tilting or fissuring; localized landslides and rockfalls; drying of vegetation; increase in temperature of hot springs; crater lakes and wells; variation in chemical content of volcano-related bodies; drying up of wells or springs; and development of new thermal areas and reactivation of old ones. Volcano bulletin summarizing the status of the most active volcanoes are prepared by PHIVOLCS daily. Advisory bulletins are released more frequently during abnormal activities or as the need arises. Alert signals to warn the public of the status of active volcanoes have been prepared and updated after each eruption. Different alert signals were designed for each volcano, owing to the difference in precursors and eruption behavior.

Mitigation measures include hazard zone delineation mainly on the basis geologic mapping and historical eruptive activities. The PHIVOLCS Quick Response Team, virtually available round the clock, is dispatched during volcanic emergencies. Information dissemination and long-term public education are also conducted in the form of lectures, seminars, workshops, and volcano fieldtrips. General information about volcanic eruptions and hazards are provided in posters, brochures, comics, videos and other media.

Here, we present an overview of volcanism in the Philippines, classification of volcanoes, and characteristics of volcanic arcs in relation to their tectonic settings. Detailed review of the explosive activities for the most active and explosive volcanoes - Mayon, Taal, Pinatubo, Hibok-hibok, and Parker, are given. Historically significant eruptions are highlighted. More detailed descriptions of the geology, eruption styles, patterns and recent activities, are summarized for volcanoes where detailed studies are available. Monitoring and eruption prediction techniques for each volcano are outlined. This review paper referred to a significant number of published papers, internal reports, and relevant data on Philippine volcanoes.

2. Volcanic Arcs and Tectonic Elements

2.1 Volcanic Arcs

Volcanoes in the Philippines are distributed in ten volcanic belts. The distribution of ac-

tive and inactive Plio-Pleistocene volcanoes generally reflects the activity along subduction zones bounding the archipelago. With the exception of the East Luzon Trough and Cuyo Belt, all active subduction zones bordering the Philippines have their corresponding volcanic arcs. These are (Fig. 1): (1) Central Luzon Belt in response to the Manila Trench subduction, (2) East Philippine Volcanic Arc associated with the Philippine Trench, (3) Negros Arc related to the Negros Trench, (4) Sulu-Zamboanga Arc corresponding to the Sulu Trench, and (5) Cotabato Belt linked to the Cotabato Trench. Other volcanic belts that may not be related to active subduction include the following: (1) Sta. Ana Belt, (2) Luzon Central Cordillera Belt, (3) Lanao Volcanic Area, (4) Mindanao Central Cordillera, and (5) Cuyo Belt. Cuyo Belt appears to be unrelated to a subduction zone (BMG, 1981).

Several authors described the tectonic features, volcanism, and geochemical characteristics and variations in the two major arcs, the Central Luzon Belt and the East Philippine Volcanic Arc. For the East Philippine Volcanic Arc, only the northern segment, the Bicol Arc, was described by previous authors. In the absence of detailed studies on most Philippine arcs, only the two major arcs will be described herein.

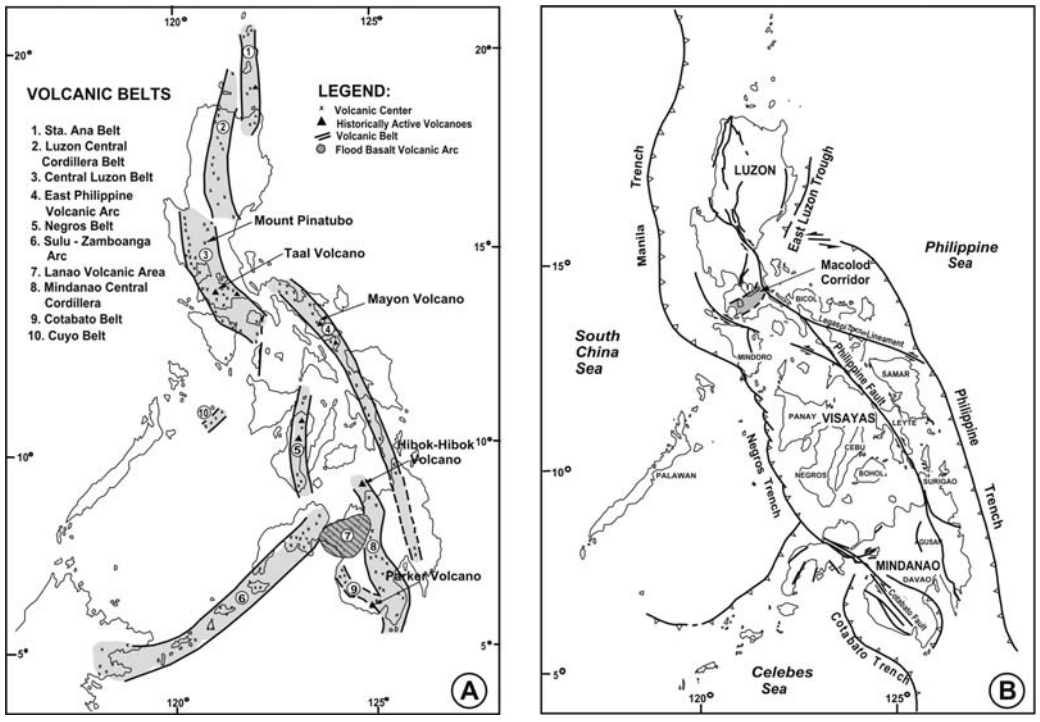

Fig. 1. (A) Volcanic arcs of the Philippines. (B) Tectonic map of the Philippines.

2.1.1 Central Luzon Belt

The Central Luzon Belt (Fig. 2) is an active volcanic arc associated with the subduction of the South China Sea lithosphere underneath the Manila Trench, initiated about 15 Ma (Defant et al., 1988). It is situated approximately above the 100-km depth contour line of the Wadati-Benioff zone (Cardwell et al., 1980; De Boer et al., 1980). A total of 39 volcanic centers

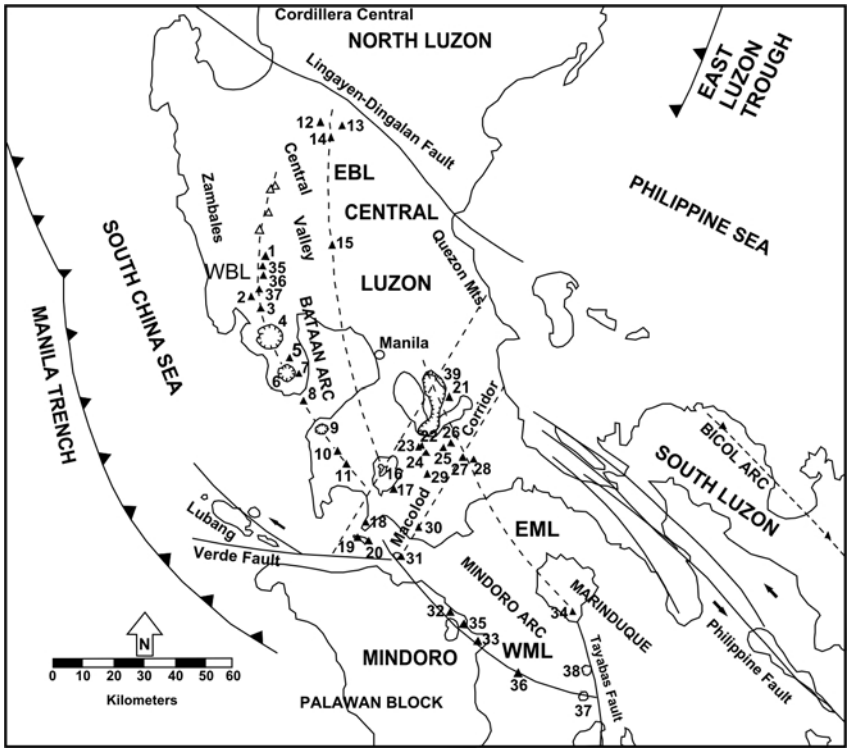

Fig. 2. Map of southern Luzon, Philippines showing major Pliocene-Quaternary volcanoes, arcs and other tectonic elements. WBL-West Bataan Lineament, EBL-East Bataan Lineament, WML-West Mindoro Lineament, EML-East Mindoro Lineament. The numbers on the map correspond to the following volcanoes: 1-Mt. Pinatubo, 2-Mt. Balakibok, 3-Mt. Santa Rita, 4-Mt. Natib, 5-Mt. Samat, 6-Mt. Mariveles, 7-Mt. Limay, 8-Corregidor Complex, 9-Mt. Palaypalay, or Mt. Mataas na Gulod, 10-Mt. Cariliao, 11-Mt. Batulao, 12-Mt. Balungao, 13-Mt. Amorong, 14-Mt. Bangcay, 15-Mt. Arayat, 16-Mt. Taal, 17-Mt. Macolod, 18-Mt. Panay, 19-Maricaban West Complex, 20-Mt. Casapao, 21-Mt. Sembrano, 22-Mt. Makiling, 23-Mt. Mapinggon, 24-Mt. Bulalo, 25-Mt. Nagcarlang, 26-Mt. Atimbia, 27-Mt. San Cristobal, 28-Mt. Banahaw, 29-Mt. Malepunyo, 30-Mt. Lingayen, 31-Verde Island Complex, 32-Mt. Macapili, 33-Mt. Dumali, 34-Mt. Marlanga, 35-Mt. Pola, 36-Mt. Maestre de Campo, 37-Mt. Simara, 38-Mt. Bantoi, and 39-Laguna de bay Complex. Figure adopted from Defant et al. (1988). Several of the tectonic features were adopted from De Boer et al. (1980), Hamburger et al. (1982), Karig (1983), and Wolfe and Self (1983).

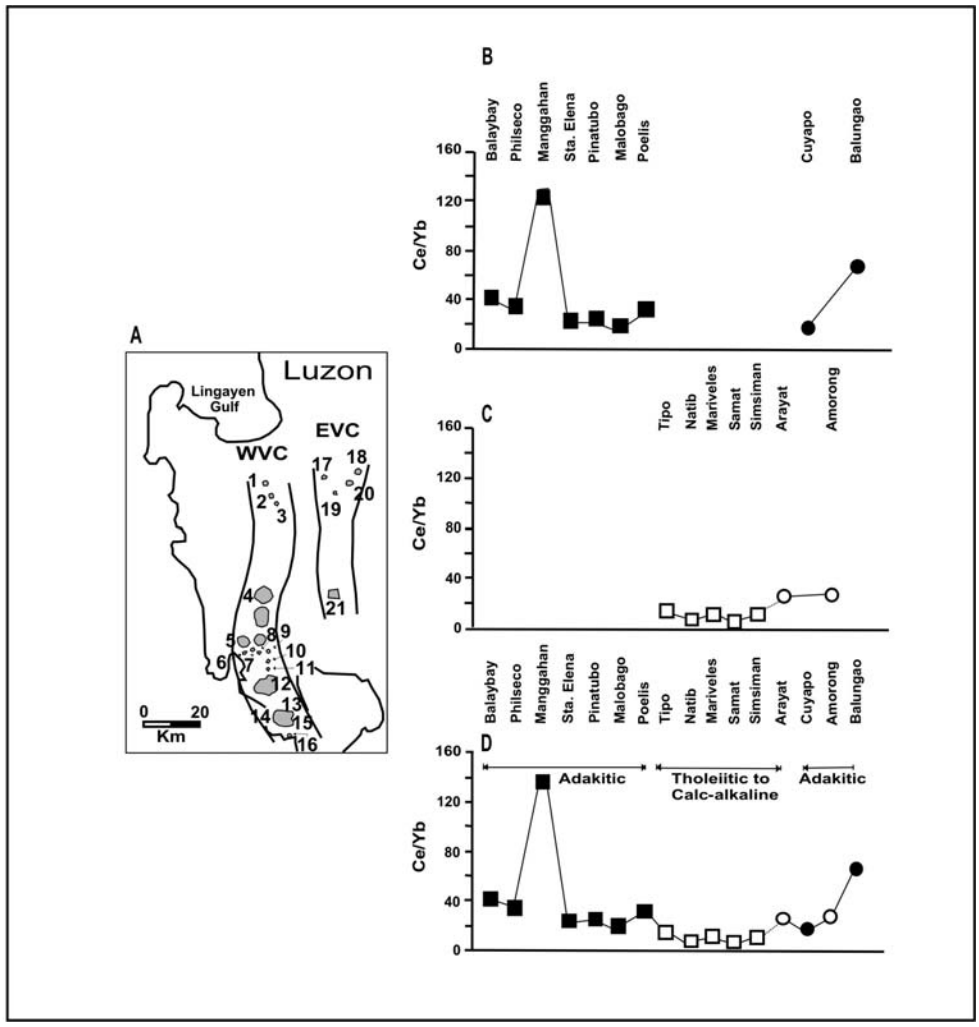

Fig. 3. The Ce/Yb variation in volcanoes and volcanic centers in Central Luzon. (A) Map shows the location of the western (WVC) and eastern (EVC) volcanic chains. Numbers correspond to the names of the volcanic centers: 1-Malobago, 2-Poelis, 3-Pitongbayog, 4-Pinatubo, 5-Balaybay, 6-Philseco, 7-Bubilao, 8-Manggahan, 9-Sta. Elena, 10-Tipo, 11-Sta. Rita, 12-Natib, 13-Samat, 14-Mariveles, 15-Limay, 16-Simsiman, 17-Cuyapo, 18-Balungao, 19-Bangkay, 20-Amorong, and 21-Arayat. (B) The across-arc chemical variations of the silicic rocks in Central Luzon from the west ((WVC) = Balaybay to Poelis) to the east (eastern volcanic chain (EVC)= Cuyapo and Balungao). (C) The across chemical variation of the Central Luzon basalt to basaltic andesites from the west (WBC=Tipo to Simsiman) to the east (EVC=Arayat and Amorong). (D) Combining the basaltic to silicic volcanic centers clearly shows the elevated Ce/Yb of the latter compared to the former. A longitudinal variation of adakitic-tholeiitic-calc-alkaline-adakitic spatial zonation is recognized. Symbols: *closed boxes* -western volcanic chain adakitic rocks, *open boxes* -western volcanic chain normal volcanic rocks, *closed circles* -eastern volcanic chain adakitic rocks, *open circles* -eastern volcanic chain normal volcanic rocks. Adopted from Yumul et al. (2003).

(Fig. 2) define the arc, extending from the Balungao volcanic group on the north to Mt. Simara on the south (Defant et al., 1988). Volcanism in the arc is predominantly andesitic with calc-alkaline affinities, although individual volcanoes can be basaltic to rhyolitic (Defant et al., 1989). Defant and Ragland (1988) suggested that the dominant process in the magmatic evolution of some volcanoes along this arc is crystal fractionation.

Defant and others (1989) proposed five segments for the Manila Trench-related arc: Taiwan (Taiwan Coastal Range and the islands of Lutao and Lashu), Babuyan, northern Luzon, Bataan, and Mindoro (Fig. 2). Bataan and Mindoro constitute the Central Luzon Belt (De Boer et al., 1980). The northern segment is the Bataan Arc (BA), which extends from Lingayen-Dingalan Fault Zone southward to Verde Passage Fault Zone. The southern portion is the Mindoro Arc (MA), which extends from the latter tectonic feature to the Tablas Fault Zone. A major volcanic zone trending NE-SW, called the Macolod Corridor (MC), divides the arc into two (Defant et al., 1988). A shift in the location of volcanism eastward in both of the segments suggests that the subducting slab initiated partial melting of the mantle during its eastward downward migration (Fig. 3; Defant et al., 1988). Melting at two specific depths resulted to sub-parallel chains of volcanoes along Bataan Arc, the Western Bataan Lineament (WBL) and Eastern Bataan Lineament (EBL) (Defant et al., 1988). These two constitute the forearc-main arc and back arc regions (Fig. 3) with respect to Manila Trench, respectively (Yumul et al., 2003).

Bataan Arc

The Western Bataan Lineament (WBL) is one of the areas with the greatest clustering of volcanoes in the Philippines (Wolfe and Self, 1983), among which are Mt. Pinatubo, Mt. Natib, and Mt. Mariveles. Older and eroded volcanoes (0.19-5.93 Ma) consisting of andesitic to dacitic plugs and necks, which developed on ophiolites of the Zambales complex, are also present in this volcanic chain (Defant et al., 1988). In contrast, the Eastern Bataan Lineament (EBL) developed on predominantly clastic sediments of the Central Valley Basin (Defant et al., 1988). The EBL consists of volcanic centers including Mts. Balungao, Cuyapo, Amorong, and Arayat, and whose age ranges from 0.32-0.78 Ma (Yumul et al., 2003). Volcanic centers in this side of the arc are sparse and smaller compared to the adjacent forearc (Yumul et al., 2003). The dominant magma type in the volcanic belt ranges from augite-hypersthene andesite, biotite-hornblende andesite to minor hornblende-biotite dacite (Divis, 1980).

Several workers (e.g., Balce et al., 1979; De Boer et al., 1980; Datuin, 1982; BMG, 1981) have discussed the across-arc variation in the Bataan Arc. A recent work by Yumul and others (2003) shows this variation in terms of Ce/Yb values. Silicic rocks with adakitic affinity and basaltic to andesitic volcanoes constitute the two sets of volcanic centers in Bataan Arc. Across-arc geochemical variation in terms of Ce/Yb is readily seen among the former set (WBL) but is not very clear among the latter (EBL). When arranged in the field, the easternmost and westernmost volcanic centers exhibit higher Ce/Yb compared to those in between (Fig. 3C). The resulting across-arc variation from west to east is adakitic-tholeiitic-calc-alkaline-adakitic zonation (Yumul et al., 2003). The across-arc geochemical variation signifies the contributions from the slab, mantle, and crust compounded by the effects of geochemical processes such as partial melting, fractionation, magma mixing, and mantle-melt interaction (Yumul et al., 2003).

Volcanoes of the Bataan Arc do not only display a general younging from west to east (De Boer et al., 1980) but also show a specific compositional trend. Volcanic centers that are approximately 5 Ma are silicic; those between <5 to 1 Ma have basaltic to andesitic geochemical composition, while those whose age is <1 Ma show a broad range of composition from basaltic to andesitic to dacitic (Yumul et al., 2003). Yumul and others (2003) interpreted the observed spatial and temporal relationships of the different volcanic centers in Central Luzon as related to the change in dip of subduction of the South China Sea crust.

Mindoro Arc

The Mindoro Arc is composed of two parallel volcanic chains, the Western Mindoro Lineament (WML), consisting of volcanoes namely Verde Island, Mt. Macapili, Mt. Pola, Mt. Maestre de Campo, and Mt. Simara, and the Eastern Mindoro Lineament (EML) which includes the Laguna de Bay Complex, Mt. San Cristobal, Mt. Banahaw older volcanics (>0.7Ma), and Mt. Marlanga (Fig. 2; Defant et al., 1988). The WML was formed along the eastern margin of the north-trending Mindoro basin while the EML probably developed on a basement composed of Angat ophiolites (Defant et al., 1988). The shift of volcanism eastward is the result of the active subduction along the Manila Trench as in the case of the Bataan Arc (Defant et al., 1988).

Unlike its northern arc counterpart, geochemical variation within the WML and EML is difficult to assess. The incorporation of crustal component from the North Palawan Continental Terrain contaminated magmatism in the area, producing magmas with higher radio-

genic Sr, which is present only in the Mindoro Arc. Aside from Sr, MA rocks also exhibit the highest radiogenic Rb, Ba, Th and large-ion lithophile elements (LILE) compared with all the other Central Luzon Arc rocks (Defant et al., 1988). Alternatively, this unique geochemical signature can be due to subduction of a terrain composed of ophiolites and metamorphic complexes (Hamilton, 1979; De Boer et al., 1980; McCabe et al., 1982; Karig, 1973).

The geochemical variation was both across and along the Central Luzon Arc. Recent volcanism along this arc shows systematic regional variation (Knittel et al., 1988; Knittel and Defant, 1988; Defant et al., 1990 and 1991). The Central Luzon Arc (i.e. EBL) shows a progressively decreasing radiogenic Nd and increasing radiogenic Sr values towards the south. Knittel and others (1988) and Defant and others (1991) suggest that this variation could have resulted from the incorporation of crustal materials, most likely from a fragment of North Palawan Continental Terrain or sediments derived from it into the source regions of these mantle-derived magmas (Bernard et al., 1996).

Macolod Corridor

Macolod Corridor, the third major volcanic zone that separates the northern and southern segments of the Central Luzon Belt, is a 40-km wide NE-SW trending tectonic depression. It extends from Maricaban Island to Mt. Sembrano (volcanoes 19 and 21: Fig. 2) and is characterized by volcanic centers that are relatively closely spaced and vary significantly in size (Defant et al., 1988). These include Taal Volcano, Taal Caldera, Laguna Caldera (within Laguna de Bay Complex) and three other stratovolcanoes as well as several monogenetic scoria cones and maar craters. Defant and others (1988) interpreted that the recent activities of Mt. Banahaw and Mt. San Cristobal complex as well as Taal Volcano are related to the MC. Volcanism in this region began at about 300 ka (Defant et al., 1988). Radiometric dates compiled by Oles (1991) within the MC indicate that volcanism began at least 2.3 Ma.

There are a number of ideas as to the possible mechanism of generation of magmas in this region. Divis (1980) related volcanism in this area to a leaky transform fault joining the most active parts of the Philippine and Manila Benioff zones. Defant and others (1988) proposed a rift-related magmatism for MC. This NE-SW zone of extension controls the formation of basaltic volcanoes within the MC (Forster et al., 1990).

Defant and others (1988) have shown that the geochemistry of Macolod Corridor volcanics is distinct from that of Mindoro Arc and Bataan Arc. MC volcanics plot primarily in the subalkaline field but have clearly elevated alkali values compared to the WBL. The MC mag-

mas also have higher LIL elements values than those of WBL. These geochemical signatures are a consequence of lower degrees of partial melting in the MC source than that of EBL or WBL. The radiogenic Sr value obtained is lower than or equal to any of the samples collected from BA or MA (Defant et al., 1988). Defant and others (1988) attributed the alkali-enrichment in the Macolod Corridor volcanics to rifting. They also argued that the lower $^{87}Sr/^{86}Sr$ ratio as compared with the Bataan and Mindoro segments is due to the same tectonic process. Defant and others (1988) believe that Sr values in MC are not affected by fluids from the slab as the EBL and WBL and are not affected by the slivers of continental crust, as the MA volcanics are. Thus magmas originating in this zone are the result of processes other than those in the subduction zones below Central Luzon and Mindoro-Marinduque. Defant and others (1988) proposed that MC is a rift zone.

Subsequent workers (i.e. Knittel and Defant, 1988; Knittel et al., 1988; Milklius et al., 1991; Sudo et al., 2000) interpreted that volcanism in the MC as subduction-related. The isotopic and trace element studies of the lavas erupted in the Macolod Corridor, including the recent Taal eruptive products, suggest source enrichment by contamination of a melt fraction of the North Palawan Continental Terrain (Knittel and Defant, 1988; Knittel et al., 1988; Miklius et al., 1991). Sr and Nd values of MC magmas are actually intermediate between Bataan and Mindoro Arc magmas, which contain continent-derived materials (Knittel and Defant, 1988; Knittel et al., 1988). MC magmas therefore may also contain continent-derived materials associated with the South China Sea plate subduction and that magmatism in this region may also be subduction-related and does not necessarily need a rifting mechanism (Sudo et al., 2000). Moreover, the migration of active volcanism from the Laguna de Bay area to monogenetic volcano areas, about 1.6-1.0 Ma, is difficult to explain by rifting. A plausible explanation for this shift is the steepening of the subducted slab at the Manila Trench with time (Sudo et al., 2000). The Benioff zone indicates that subducted slab along the Manila Trench is very steep that it does not extend beneath the cluster of young and active volcanoes, e.g., Taal. It remains controversial as to whether the present subducted slab produces the concurrent volcanism.

As a whole, the evolution of the Central Luzon Arc through space and time is a complex one, producing geochemical signatures distinct for each volcanic zone across and along the length of the arc.

2.1.2 East Philippine Volcanic Arc

The Southeastern Luzon Volcanic Arc (SELVA) or Bicol Arc (Fig. 4), is part of the linear chain of volcanoes, the East Philippine Volcanic Arc, stretching from southeastern Luzon, thru the Samar-Leyte islands in the Visayas, to eastern Mindanao. The SELVA itself is within the enclosure of 122° 30' E to 124° 30' E longitude and 12° 30' N to 14° 60' N latitude, a NW-SE oriented landmass about 250-km long and 50-km wide, encompassing an area of about 15,000 km^2. It is located between the Philippine Trench to the east, and the active, left-lateral strike-slip Philippine Fault Zone to the west. Arc volcanism in the SELVA is related to the westward subduction of the Philippine Sea Plate at the Philippine Trench (Aurelio, 2000), approximately 210-280 km off shore to the east, at an average rate of 8 cm/yr (MGB, 1996).

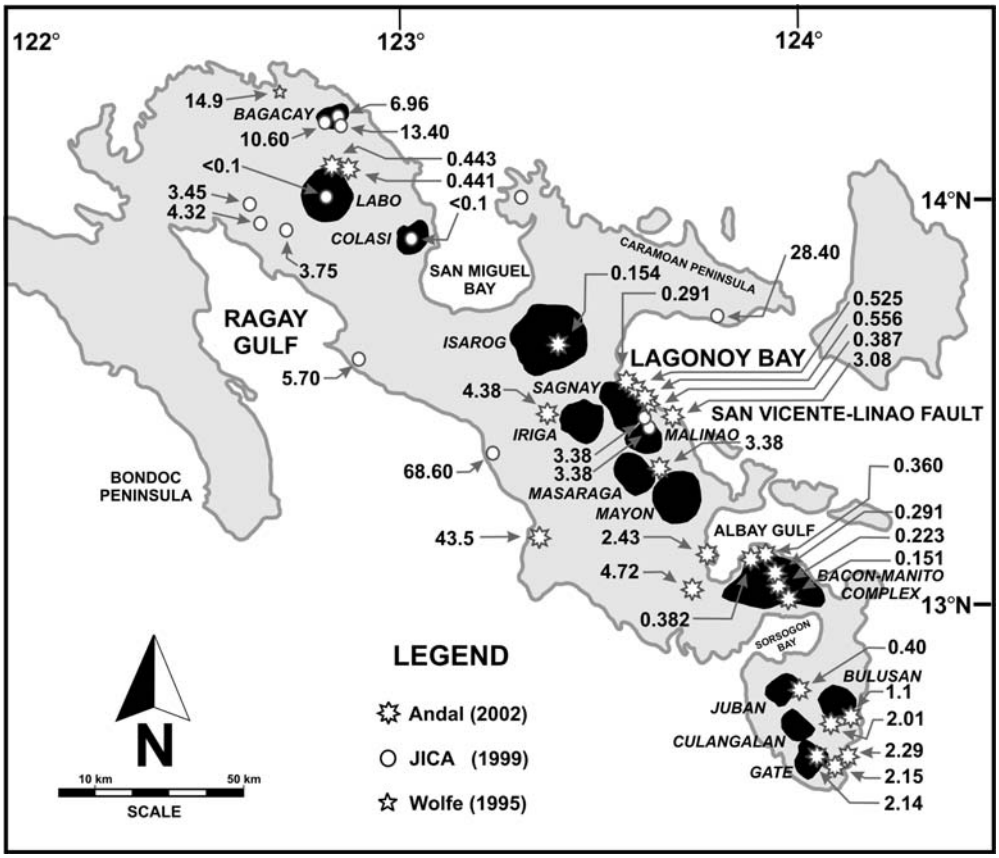

Fig. 4. Volcanoes of the Southeastern Luzon Volcanic Arc (SELVA) and their corresponding K-Ar ages. Radiometric data were taken from JICA (1999), Wolfe (1995) and Andal (2002). Modified from Andal (2002).

The Philippine Fault Zone and the Philippine Trench control local structures within the arc and the general elongate shape of the region. Another major fault known as the San Vicente-Linao Fault transects the arc through the Pocdol mountains, southwest of Legaspi and Mt. Mayon, in a west-northwest orientation (Fig. 5). Several northwest-southeast trending faults can also be found in the Albay and Lagonoy Gulf vicinities (Newhall, 1977; JICA, 1999).

The SELVA is composed of twelve major volcanic centers, mostly stratovolcanoes with single eruption craters and steep-sided cones (Fig. 4). Of the twelve, three are classified by PHIVOLCS as active, namely Mt. Iriga, Mt. Mayon, and Mt. Bulusan & Bulusan Volcano Complex. The other nine are Mt. Bagacay, Mt. Labo, Mt. Culasi & Mt. Cone, Mt. Isarog, Mt. Sangay, Mt. Malinao, Mt. Masaraga, Bacon-Manito Volcanic Complex, and Mount Bintacan. New K-Ar dating of rocks, as well as earlier age data throughout the SELVA

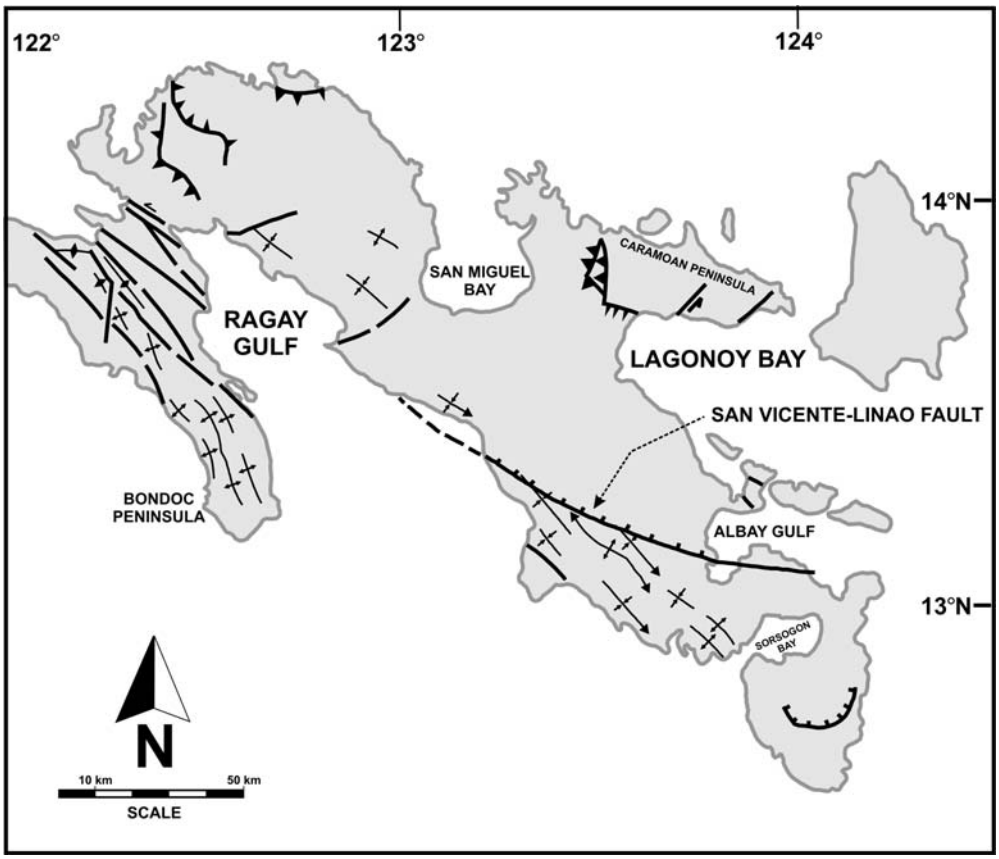

Fig. 5. Major structures in the Southeastern Luzon Volcanic Arc. Extracted from BMG (1981) and Delfin (1991).

from Wolfe (1981), Delfin (1991), and JICA (1999), led to the recognition of three magmatic episodes in the arc (Andal, 2002).

The first magmatic episode is represented by rocks ～70 to ～ 6 Ma old (Figs. 4 and 6). The deposits are composed mainly of granodiorite & diorite intrusive rocks and andesite flows (Andal, 2002). The rocks have SiO_2 and K_2O compositions ranging from 51 to 63 wt% and ～0.1 to 2.5 wt%, respectively, indicating basalt to transitional andesite-dacite compositions. Multi-element plots of samples standardized to the Primitive-Mantle values of Sun and McDonough (1989) display patterns found in typical island-arc volcanic rocks (Arculus, 1994). The pattern shows a steady increase from heavy rare-earth elements (HREE) towards LILE. Breaking these patterns are strong negative Nb and Ti anomalies, and slightly positive Sr anomalies. The first episode rocks exhibit geochemical affinity with calc-alkaline basalt and island arc tholeiite.

Volcanic rocks with ages ranging from 5.7 to 1.1 Ma were deposited during the second magmatic episode (Figs. 4 and 6) (Andal, 2002). These rocks are composed of rhyolite flows, dacites, and massive basaltic andesite to andesite lava flows. Volcanic rocks have 52 to 66 wt % SiO_2, 1.2 to 2.8 wt % K_2O, and low MgO wt % & FeO/MgO ratios. The multi-element patterns from normalized samples display a general increase from HREE to LILE, interrupted by strong negative Ti and Nb anomalies, and positive Sr and Pb anomalies. Hornblende borders, opacite rims, and dusty & oscillatory zoned plagioclase crystals observed in thin sections, as well as the pyroxene + plagioclase + hornblende ± biotite ± apatite crystallization order suggest the island-arc affinity of the second magmatic episode (Andal, 2002).

Less than 1.0 Ma volcanic rocks represent the third magmatic episode. Basaltic andesite and andesite are the dominant rock types (Andal, 2002) (Figs. 4 and 6). The samples have SiO_2 compositions ranging from 48 to 73 wt%. They also range from low-K arc tholeiite to high-K calc-alkaline rocks, with the majority belonging to the boundary between the calc-alkaline and high-K calc-alkaline series. The standardized multi-element plots of rock samples from the third magmatic episode show patterns characterized by a steady increase in HREE towards LILE and depletion in HSFE' s, with strong negative Nb and Ti anomalies, and positive Sr and Pb anomalies breaking the patterns.

In summary, the first magmatic episode emplaced silicic rocks. Silicic and intermediate rocks were extruded during the second episode. Deposited during the third episode were intermediate to mafic rocks. All the three episodes exhibit calc-alkaline affinities and have geochemical signatures typical of island-arc magmas.

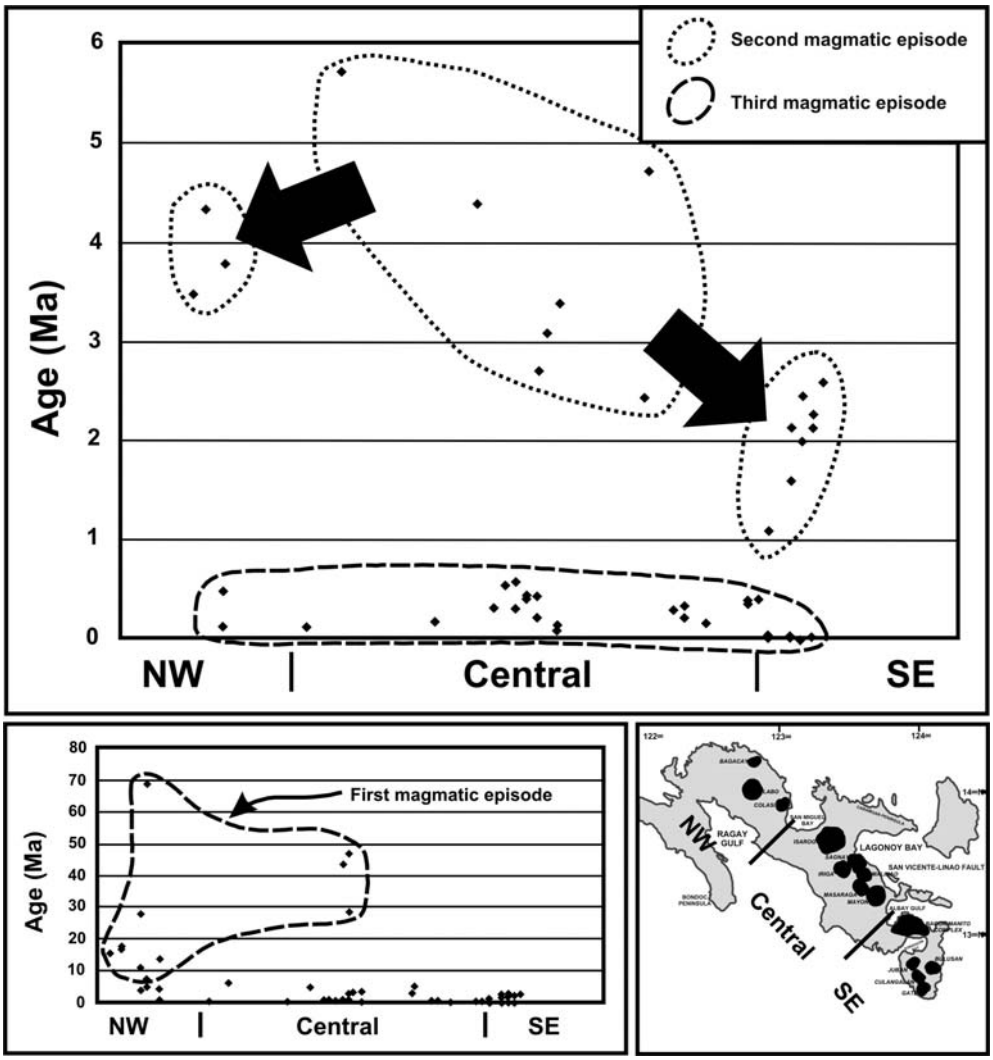

Fig. 6. *Top:* Diagram showing the second and third magmatic episode with their geographic position with respect to the arc. Arrow shows possible propagation direction of volcanism. *Bottom left:* Diagram showing all the dated volcanic rocks in the volcanic arc. Highlighted are the first magmatic episode samples. *Bottom right:* Reference map illustrating the NW, central, and SE portion of the volcanic arc. From Andal (2002).

2.2 Major Tectonic Features

The Philippine Mobile Belt (PMB) is a zone of active deformation. It is a complex system of subduction zones, collision zones, and marginal sea basins, bounded on the east by the Philippine Sea Plate, and the eastern margin of the Eurasian Plate on the west. The major tectonic features related to volcanism are: (1) the Philippine Fault, (2) Manila Trench, (3)

East Luzon Trough, (4) the Philippine Trench, (5) Negros Trench, (6) Sulu Trench, and (7) Cotabato Trench (Fig. 1). Three active collision zones exist at the northern, western, and southern margins of the Philippines. They are: Northern Luzon-Taiwan (continent-arc collision), Mindoro-Panay (arc-continent collision), and Moluccas Sea (arc-arc collision).

2.2.1 Philippine Fault

The Philippine Fault or the Philippine Fault Zone is a 1,200 km-long structure traversing the length of the archipelago from Luzon to Mindanao. The fault is generally left-lateral (Nakata et al., 1977). Slip rates differ from 0.55 cm/yr to 6.85 cm/yr. Estimates of the Philippine Fault's age range from Tertiary to Upper Pliocene.

The Philippine Fault has three varying structural regimes. As a result, three distinct segments can be distinguished based on structural character and data availability:

1. Northern segment: Northwest Luzon to Lamon Bay

   This segment of the Philippine Fault is the one responsible for the 16 July 1990 earthquake. Unlike the central segment that is restricted to a narrow zone, the northern segment branches out into several strike-slip faults generally oriented N-S. Furthermore, it is characterized by a transgressional regime with a dominant vertical thrust component relative to strike-slip movement (Ringenbach, 1992).

2. Central segment: Bontoc Peninsula to Leyte

   The central segment of the Philippine Fault exhibits a relatively simple structure, with only 2-3 well-defined branches. This segment is characterized by a left-lateral strike-slip movement as implied by observational features such as truncated surfaces, fault planes, and ruptures during earthquakes.

3. Southern segment: Mindanao and the Moluccas

   Field studies and remote sensing measurements conducted in 1991 indicate that the southern segment of the Philippine Fault bounds the Agusan-Davao Basin on its eastern flank (Pubellier et al., 1991). This segment strikes N10° -20° W in Surigao and N-S in Davao. More recent structural investigation of the Philippine Fault in this region has shown that this segment cuts across the Agusan-Davao Basin (Quebral, 1994).

2.2.2 Manila Trench

The Manila Trench represents the morphologic expression of the South China Sea's sub-

duction under the Luzon Arc (Cental Luzon Belt) (Karig, 1973; Cardwell et al., 1980). The trench reaches depths of up to 5,100 m in the latitude of Manila (Ludwig et al., 1967), with a corresponding Benioff zone that is steep on its southern portion but flattening to the north.

2.2.3 East Luzon Trough

The northern tip of the Philippine Trench cuts across a still poorly understood structure, which is often referred to as the East Luzon Transform Fault. The East Luzon Trough (Fig. 7) is located north of this transform fault and east of Luzon Island. It is considered as a newly forming subduction zone (Karig, 1973; Lewis and Hayes, 1983) since compressive structures are generally absent on the eastern flank of Luzon and that the corresponding volcanic arc has not yet formed.

2.2.4 Philippine Trench

The Philippine Trench accounts for the westward subduction of the Philippine Sea Plate under the eastern Philippine Arc (Fitch, 1972; Cardwell et al., 1980; Hamburger et al., 1983). It is suggested that the Philippine Trench is young and is presently propagating to the south. This is due to its relatively shallow Benioff zone corresponding to a maximum of 250 km for the length of the subducted slab. Furthermore, seismic reflection profiles and bathymetric data (Karig and Sharman, 1975; Karig, 1973) show that a well-developed accretionary prism related to the trench does not exist.

The Eastern Philippine Volcanic Arc, which can be traced from Bicol to Leyte, is linked to the Philippine Trench. Traces of this volcanic arc, however, are not found in Mindanao.

2.2.5 Negros Trench

The Sulu Sea Basin subducts under Negros Trench. The corresponding Benioff zone is poorly manifested, with a subducted slab reaching a depth of only about 100 km and dipping slightly under the islands of Negros and Panay. An active volcanic chain (Negros Arc) related to the Negros Trench, however, can be traced in these islands.

2.2.6 Sulu Trench

The Pliocene-Pleistocene magmatic activity of Zamboanga Arc is linked to the southward subduction of the Oligocene-Miocene Sulu Sea back-arc basin along the Sulu Trench.

2.2.7 Cotabato Trench

Subduction along the Cotabato Trench is relatively young as shown by an underdeveloped Benioff zone. An active volcanic arc related to the trench, however, can be found on the western margin of Mindanao Island (Divis, 1983; Cruz, 1987).

3.0 Classification of Philippine volcanoes

Philippine volcanoes are classified as active, potentially active, and inactive based on their current activities and eruptive histories. At least 22 are considered active, and several have erupted in recent times (Table 1). Volcanoes are active if they satisfy at least one the fol-

Table 1. Active volcanoes in the Philippines. Modified from PHIVOLCS (2002).

Name	# historical eruptions	Last eruption or activity	Latitude	Longitude	Locality	Elevation (km)	Type of activity	Main rock type
1. Babuyan Claro	4	1917	19 31.4N	121 56.4E	Babuyan Island	0.843	Strombolian, phreatomagmatic	basaltic
2. Banahaw	3	1843	14 04.0N	121 29.0E	Laguna-Quezon Province	2.169	Explosive with lahar	andesite
3. Biliran	1	1939	11 01.4N	124 32.1E	Biliran Island	1.34	Presently solfataric	hb andesite
4. Bud Dajo	2	1897	06 01.0N	121 03.0E	Jolo Island, Sulu	0.62	Presently solfataric	basalt
5. Bulusan	15	1994-1995	12 46.2N	124 03.0E	Sorsogon	1.565	Phreatic, phreatomagmatic and strombolian eruptions	andesite
6. Cagua	2	1907	18 13.3N	122 07.4E	Cagayan	1.16	Presently solfataric	andesite
7. Camiguin de Babuyanes	1	1857	18 50.0N	121 51.6E	Babuyan Island Group	0.712	Presently solfataric	andesite
8. Didicas	6	1978	19 04.6N	122 12.1E	Babuyan Island Group	0.843	Phreatic eruption and formation of domes and spines (explosive)	andesite
9. Hibok-hibok	5	1948-1953	09 12.2N	124 40.5E	Camiguin Island	1.332	Pelean	olv-bearing andesite and dacite
10. Iraya	1	1454	20 27.0N	120 01.1E	Batan Island, Batanes	1.009	Plinian	andesite
11. Iriga	2	1642	13 27.4N	123 27.4E	Camarines Sur	1.143	Phreatic eruption, debris avalanche	basaltic andesite
12. Kanlaon	21	1996	10 24.7N	123 07.9E	Negros Island	2.435	Phreatic, phreatomagmatic and strombolian eruptions	andesite
13. Leonard	*no data*	1800 yBP (C-14)	07 22.9N	126 02.8E	Davao	0.2	Presently solfataric	andesite to dacite
14. Makaturing	7	1882	07 38.8N	124 19.0E	Lanao del Sur	1.94	no data	no data
15. Matutum	1	1911	06 22.0N	125 06.5E	South Cotabato	2.286	Plinian	andesite
16. Mayon	48	2001	13 15.4N	123 41.1E	Albay	2.46	Strombolian, Vulcaniaand Plinian	andesite
17. Musuan (Calayo)	2	1867	07 52.6N	125 04.1E	Bukidnon	0.646	no data	olv-bearing andesite and dacite
18. Parker	1	1640	06 06.8N	124 53.5E	South Cotabato	1.784	Plinian	dacite
19. Pinatubo	3	1992	15 07.4N	120 20.0E	Zambales-Pampanga-Tarlac	1.445	Plinian	dacite
20. Ragang	7	1916	06 40.0N	124 30.0E	Lanao del Sur-Cotabato	2.815	Explosive with lava flows	no data
21. Smith	5	1924	19 32.4N	121 54.7E	Babuyan Island	0.688	Phreatic (?) / explosive (?)	basalt
22. Taal	33	1977	14 00.1N	120 59.1E	Batangas	0.311	Phreatic, phreatomagmatic and strombolian eruptions	andesite, basalt

lowing conditions: (1) has erupted in historic times (e.g., Mayon, Taal), (2) has oral folkloric history which suggests that an eruption took place (e.g., Parker), (3) has shown indications of seismic activity (e.g., Musuan), and (4) has volcanic deposits less than 10 ka (e.g., Pinatubo prior to its 1991 eruption). Considered most active are the volcanoes which have short repose periods, namely: Mayon, Taal, Bulusan, Canlaon, and Hibok-Hibok. Pinatubo Volcano has been included among the most active in view of its recent activities.

Potentially active volcanoes are characterized by one or several of the following features: (1) geologically young (<10,000 yrs for composite volcanoes; <25,000 yrs. for calderas), (2) geomorphologically young (i.e. little vegetation cover, low degree of dissection, young vent features), (3) presence of solfataras/fumaroles, (4) suspected seismic activity, (5) documented local ground deformation, (6) geochemical indications of magmatic involvement, and (7) geophysical proof of magma bodies. There are 27 identified potentially active volcanoes.

Volcanoes with no record of eruption and whose landforms have been modified by weathering and erosion are classified as inactive. There are 359 volcanoes identified in this category. Given the short span of recorded Philippine history (600 yrs), some volcanoes which are classified at present as potentially active or inactive may be reclassified as active when new data become available.

4.0 Eruptive History of the Most Explosive Active Volcanoes in the Philippines

4.1 Mayon Volcano

4.1.1 Volcano Profile

Mayon Volcano, the most active volcano in the Philippines, lies in the eastern portion of Albay Province, southeast Luzon Island (13° 15.4' N, 123° 41.1' E). Known for its beauty and highly symmetrical cone, it is one of the prime tourist destinations of the country. Mayon rises to about 2,462 m above sea level and covers an area of 250 km^2 encompassing Legaspi City and seven towns. About 900,000 people live around the volcano. Mayon Volcano is part of the local chain of volcanoes known as the Bicol Arc. The Bicol Arc is the northern segment of the East Philippine Volcanic Arc (Fig. 4), which is related to the active westward subduction of the Philippine Sea Plate along the Philippine Trench.

Mayon is an andesitic stratovolcano with a history of at least 48 eruptions since 1616 (Table 2). It is built by four major types of volcanic processes, namely, tephra fall, pyroclas-

tic flows, lahars, and lava flows. Its most explosive eruption occurred on 01 February 1814 and devastated the towns on the southwestern slope of the volcano. The eruption was Plinian, characterized by widespread fallout deposition, pyroclastic flows, and surges around the volcano. As a result, at least 1,200 people were killed. The most recent eruption occurred in 2001. This eruption is characterized by both explosive and non-explosive activities. The eruption was commenced by dome intrusion, followed by dome explosion and collapse, producing pyroclastic flows and surges with minor ashfalls. It was terminated by lava flow effusion. Most of the flows were emplaced along the gulleys facing Legaspi City, at the southeastern slope of the volcano.

Mayon's eruptions, though sometimes destructive, bring long-term benefits to people living around it. Its fertile slopes and surrounding plains, coupled by abundant rainfall through the year, have made the province of Albay a rich agricultural region. Pyroclastic flow and lahar deposits are very much suitable for coconut, rice, abaca, cassava, tomatoes, and legume cultivation, with minimal fertilizer requirements.

4.1.2 Age Estimate

Mayon is one of the youngest stratovolcanoes within the Southeastern Luzon Volcanic Arc. It was formed during the third magmatic episode (<1 Ma) (Fig.4) of the arc, characterized by the extrusion of basaltic to andesitic volcanic rocks (see section 2.1.2).

Most of the earliest deposits of Mayon are probably buried beneath its edifice, thus precise age of Mayon is unknown. The oldest exposed deposit was dated to be 5,050±250 yBP by ^{14}C method (Meyer, 1985). The first age estimate was given by Newhall (1977) using three methods: (1) by estimating the rate of addition of new volcanic products and the total volume of the cone, (2) by extrapolating downward from ^{14}C dates to an assumed base of the cone, and (3) by studying folkloric legends of the early inhabitants of the area. The first method, using addition rate estimates from the 1928 and 1968 eruptions (Faustino, 1929; Moore and Melson, 1969), yielded an age of approximately 5,500 yBP. The second method, using two ^{14}C dates of charred wood (Hamada, 1976), and working under the assumptions that the rate of past construction is similar to the recent rate and that the base of Mayon lies approximately at sea level, gave an age of about 69,000 yBP. The third method is a rather crude estimation that relies heavily on religious faith and local folklore (Espinas, 1968), and thus cannot give a reliable age for Mayon. Similarly, possible errors in the assumptions adopted by the first two methods could be the reason for the crude order of magnitude agreement between the

Table 2. Historic eruptions of Mayon Volcano. From Ramos-Villarta et al. (1985).

Date Range			Precursory Signs				Type of Activity				Associated Phenomena				Type of Eruption	Places Affected	Remarks
Year	Start mo/d	End mo/d	Q	R	G	S	AF	TF	PF	LF	L	RS	VL	EQ			
1616	2/19	2/23					x	x	x	x	x			x			Earliest recorded eruption
1766	7/20	7/25					x		x	x	x				VULC	AF, PF, & LF - East	Crater glow for 4 months
1766	10/23	10/24														Malinao destroyed, Cagsaua, Guinobatan, Budiao, Polangui, Ligao - major damages	Destructive L due to heavy typhoon rains - Oct. 23-24 30 deaths - Malinao 19 deaths - Albay
1800	10/30	10/31					x	x	x						VULC	Cagsaua, Budiao, etc.	Multiple pyro-eruptions
1811	10/5	10/6	x				x	x	?						VULC		Forceful ejection of a column of ash & rocks "Big river of fire"
1814	2/1	2/1	x				x	x	x		x	x	x		PLIN	PF - southern slopes Camalig, Cagsaua, Budiao, Guinobatan, half of Albay L - Cagsaua & Budiao AF/L? - Ligao, Guinobatan, Libog, Tabaco & Tiwi	Most violent and destructive eruption; powerful ejection of ash & lapilli; major PFs Crater reduced = 40 m Major L generated
1827-1828	6	2		x	x		x	x	x		x		x	x	VULC	L - Camalig	Lasted until Feb. 1828. Column of fire rose 300 m
1834-1835	5(?)			x	x		x	x	x	x	x	x			VULC		Lasted until May 1835; more or less continuous
1839							x										Minor ash eruption
1845	1/21	1/21		x			x	x	x		x	x			VULC	AF - southwest Camalig, Guinobatan & Ligao	Eruptions 15-30 min. interval One ash cloud with pumice
1846	5/11	5/11					x								VULC	Camalig - 12 cm ash	Strong ash eruption CG continuous for many nights
1851	5/26	6					x							x			Two minor ash eruptions
1853	7/13	8/26		x			x		x		x				VULC	PF - Camalig, Guinobatan; L - Ligao, Oas, Polangui AF - Malilipot, Bacacay, Libog, Guinobatan, Camalig, Albay, Cagsaua	Major eruption; heavy coarse airfall on Aug. 26
1855	3/22				x		x			x							Minor eruption
1857					x		x										Minor ash eruption
1858	1	12					x			x	x			x	STRM		Initial 150 m lava fountaining with small ash emissions
1861																	Minor ash eruption
1862							x				x						Minor ash eruption

1868	12/17						x	x	x		x	x			VULC		Large ash cloud with lapilli & bombs
1871-1872	12/8	1		x			x	x	x			x	x	x	VULC	PF - S to SE; Albay, Legazpi AF - Camalig, Guinobatan (SW)	"Streams of lava" - S & SE
1872	9/5	9/9		x			x			x		x					Emission of ashes & "lava"
1873	6/20	7/22		x			x			x							Minor eruption with sudden 30 cm subsidence in Malinao Rain triggered lahar in Nov. 1875
1876	4	11/26					x										Minor ash eruption
1881	7/6	8		x	x		x		x	x	x				STRM	AF - Camalig & Guinobatan LF - S, SE & SW slopes	Gentle extrusion of lava Craterial outburst started Nov. 21 '81 Repeated lahar
1885	11/21	12/2					x			x						LF - SSW, W & SSE slopes	Minor overflow of "lava"
1886-1887	7/8	3/10					x		x	x	x				STRM	AF - Camalig, Guinobatan & Libog	Gentle continuous eruption followed by ash & scoria eruption; violent activites on Jul 8, 1886; Feb 22 & 27; Mar 1 & 9, 1887; Lahar - Mar '87 continued > 1 year
1888	12/15			x			x					x					Two minor ash eruptions
1890	9/10	9/30	x		x	x	x			x					VULC-STRM	LF - threatened Libog	Sep 30 - moderately strong ash eruption
1891	10/3	12/3	x		x	x	x			x						LF - S & SW	Minor explosions
1892	2/3	2/29	x		x	x	x	x	x	x		x			VULC	PF - E & ESE slopes	Activity in full blast Feb 21 Emissions every 15 -20 mins Cone lowered by 100 m Activity waned Feb 29
1893	10/4	10/31		x			x	x		x	x	x		x		LF - eastern slopes	Minor ash, lapilli & bomb eruption Strong tremors on 11th & 19th of long duration Minor eruption on Oct 31
1895	7/20	11/26	x	x	x		x			x	x	x	x	x			Minor eruption & lahar Crater glow - whole of Aug Emission of lava Nov 25-26
1896	8/31	9/27					x			x	x						Minor ash & lava eruption Minor lahar
1897	6/4	7/23	x	x	x	x	x	x	x	x	x	x	x		Strong VULC	PF - seashore of Sto. Domingo, barrios of Sto. Niño, San Isidro, San Roque, San Antonio, Sta. Misericordia, Ligao & parts of Bigaa; San Fernando, Legazpi overwhelmed; L - Basud River (Sto. Domingo) ENE, Camalig	Next to 1814 eruption in destructiveness Violent phase lasted 17 hours L/PF reached Albay Gulf Most deaths likely due to PFs
1900	3/1	3/6	x	x	x	x	x	x	x	x	x	x	x	x	VULC	LF - Legazpi & Libog AF - Ligao, Guinobatan, Tabaco, Libog & Camalig	Preceded by abnormal animal behaviour Emission of numberless incandescent lapilli

1902							x			x	x						Minor ash eruption Lahars probably part of 1900 eruption
											x					Camalig, Bongabong, Tabaco	Non-volcanic floods in 1915
1928	1	8			x	x	x		x	x					VULC	PF - San Antonio, Malilipot AF - San Antonio, Tabaco; Amtic, Ligao; TF - Bonga, Bacacay; LF - Libog	Climax reached July 20 Gas phase July 22 Pyroclastic flow
	3																Rain triggered lahar in 1930
1938	6/5						x		x	x					VULC	Foothill barrios of Legazpi & Libog; AF - Guinobatan, Ligao, Camalig, Daraga & Tabaco LF - Sto. Domingo	Several strong explosions caused small scale pyroclastic flow
1939	8/21						x										Minor explosion
1941	9/13						x										Minor emission of steam and ash
1943							x										Minor emission of steam and ash
1947	1/8	2			x	x	x		x	x					VULC	LF - Sto. Domingo; Calbayog, Malilipot; PF - San Vicente, Malilipot; AF - Masarawag, Guinobatan, ankle-deep ash	Activity not as strong as 1938
1968	4/20	5/20	x	x	x	x	x		x	x	x				VULC	AF - Camalig & Guinobatan LF - Camalig; PF - Tinobran, Quirangay, Miisi, Bonga	Pyroclastic flow Frequency of eruption 3-4 hrs. to 0.5-1 hr
1978	5/3	7/4			x	x	x	x		x		x		x	STRM	LF - Camalig	Lava emission lasted July 4 CG & occasional ash puffs after eruption; Lahar - Jun 30, '81 height of typhoon
1984	9/9	10/6			x	x	x	x	x	x	x	x	x	x	VULC	LF - Camalig; AF - Sto. Domingo, parts of Legazpi; PF - SE & E; Bonga, Sto. Domingo	Sept 23-25 peak of eruption
1993	2/2	4/4					x	x	x	x	x	x		x	VULC-STRM	PF - Mabinit, Bonga; AF - Camalig, Sto. Domingo, Legazpi; LF and L confined to gullies	1-5 km eruption column Casualties: 77 dead, 5 injured
2000	2/12	3/1		x	x	x	x		x	x	x	x		x	STRM-VULC	AF - Guinobatan, Ligao, Camalig; LF and PF confined to gullies	0.5-17 km eruption column
2001	1/9	10/10	x	x	x	x	x	x	x	x	x	x		x	STRM-VULC	PF - Bonga, Basud, Miisi, Anoling; AF - Camalig, Guinobatan, Daraga, Legazpi, Sto. Domingo; LF and L confined to gullies	Explosive eruptions on 24 & 29 June and 26 July; 10 km - max. eruption column

Legend:

Precursory Sign
Q — Quake
R — Rumble
G — Glow
S — Smoke

Type of Activity
AF — Ash Fall
TF — Tephra Fall
PF — Pyroclastic Flow
LF — Lava Flow

Associated Phenomena
L — Lahar
RS — Rumbling Sounds
VL — Volcanic Lightning
EQ — Earthquakes

Type of Eruption
PLIN — Plinian
VULC — Vulcanian
STRM — Strombolian

age estimates of both methods. In the case of the second method, the age obtained by ^{14}C dating on samples correlated with the 1814 eruption was 1,370 ± 85 yBP, thus suggesting that 69,000 yrs may be erroneous. Newhall (1977) concluded that the estimates from the first method are more likely correct, but also cautioned that they should be taken only as order of magnitude estimates because of poorly documented assumptions.

Subsequent age approximation done by Ramos-Villarta et al. (1985) using crude backward extrapolation based on recent growth rate, resulted to an age estimate of 25,000 yBP. This is similar to the age of 24,000 yBP obtained by Punongbayan (1985) based on volume of ejecta per eruption and on the assumption that only major eruptions significantly contribute to the cone building process.

4.1.3 Geochemistry and geochemical Variations

Basaltic andesite rocks are the most common eruptive products of Mayon. Their SiO_2 contents typically range from 53 to 56%. However, occasional basaltic eruptions manifest that basaltic magma is supplied in batches to a shallow reservoir beneath the edifice, approximately once every 100 yrs, and is differentiated to basaltic andesite and andesite during succeeding eruptions (Newhall, 1977). The most recent basaltic magma influxes occurred just before the 1814 and 1818-82 eruptions. As in the 1814 eruption, Plinian eruptions may accompany basaltic influxes, and may be succeeded by periods or relatively frequent volcanism. Basaltic eruptions occur after parameters such as vesicularity, phenocrysts/groundmass ratios, and oxide concentrations (MgO, FeO, and TiO_2) reach minimum values (Newhall, 1977).

The best model that can account for the general aspects of the cyclical variation in the mineralogy and chemistry of the lavas is the periodic influxes of basaltic magma from depth into a shallow magma system (Newhall, 1977). Successively more andesitic lavas are produced by the fractional crystallization of olivine, augite, hypersthene, calcic plagioclase, magnetite, and possibly pargasitic hornblende, until a new supply of basaltic magma is introduced. The general trend toward more basic composition may be best explained by differentiation in a deep zone of magma generation by fractional fusion of eclogite or peridotite (Newhall, 1977). Using a new set of geochemical data from recent eruptions (1968-1993), Listanco and others (1999) reaffirmed Newhall's interpretation that magmatic differentiation is the dominant mechanism for the observed compositional variation at Mayon.

The SiO_2 contents of recent lava flows from the 1984, 1993, and 2000 eruptions are

54.09%, 54.36% and 53.22-53.93%, respectively (Table 3 and Fig. 7) (Listanco et al., 1999; Arpa et al., 2001). The very little compositional variation between these recent eruptions suggests that their magmas came from a single batch of basaltic andesite magma (Listanco et al., 1999). Petrographic evidence pointing to possible magma mixing was observed in the 1968-1993 volcanic rocks (Listanco et al., 1999) and in the 2000 deposits (Arpa et al., 2001). XRF analyses, however, showed that the light gray and dark gray pyroclasts in the 2000

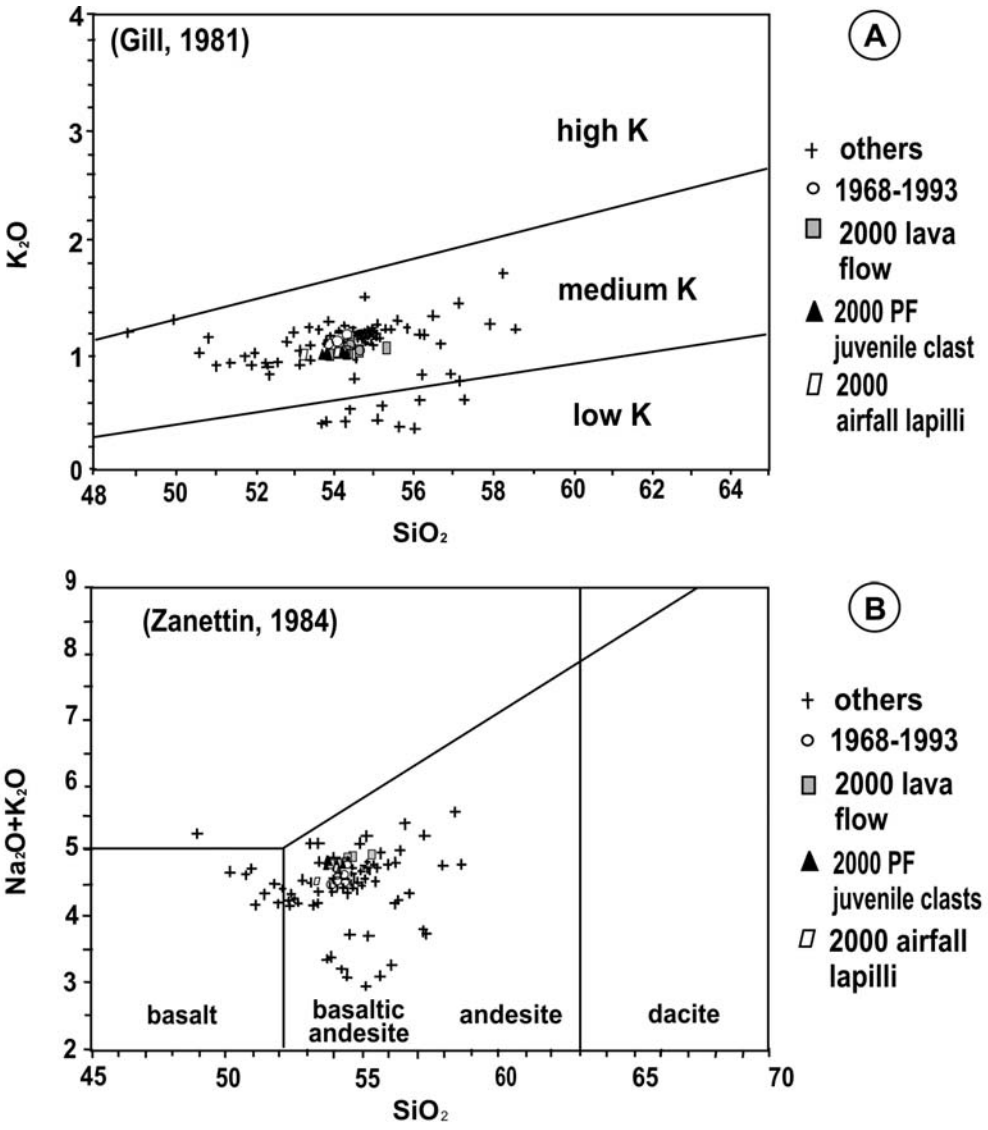

Fig. 7. (A) K_2O vs. SiO_2 and (B) $Na_2O + K_2O$ vs. SiO_2 plots for Mayon volcanic rocks. 2000 Mayon eruption geochemical data taken from Arpa et al. (2001). Modified from Listanco et al. (1999).

Table 3. Major and trace element geochemistry of the 2000 lava flow, lapill: fall and pyroclastic flow deposits. From Arpa et al. (2001).

Major element compositions	SiO_2	TiO_2	Al_2O_3	Fe_2O_3	MnO	MgO [low <15wt%]	CaO	Na_2O	K_2O	P_2O_5	Total	Remarks
BMAL-00-01A	54.60	0.73	19.53	8.38	0.16	4.10	8.65	3.71	1.11	0.31	101.28	lava flow
BMAL-00-03	55.47	0.75	19.87	8.61	0.16	4.28	8.76	3.73	1.12	0.31	103.06	lava flow
BMAL-00-06	54.42	0.73	19.30	8.49	0.16	4.25	8.57	3.59	1.10	0.31	100.92	lava flow
BMLV-00-1W	54.17	0.72	19.24	8.42	0.16	4.16	8.57	3.59	1.10	0.31	100.44	lava flow
BMAL-00-11W	54.46	0.73	19.13	8.28	0.16	4.06	8.43	3.64	1.15	0.31	100.36	lava flow
BMAL-00-12W	54.36	0.73	19.45	8.43	0.16	4.11	8.56	3.60	1.10	0.31	100.79	lava flow
BMAL-00-10	53.97	0.73	19.12	8.50	0.16	4.23	8.61	3.61	1.09	0.30	100.33	lava flow
BMAL-93-09	54.49	0.73	19.49	8.45	0.16	4.19	8.57	3.58	1.10	0.31	101.08	1993 lava flows
BMPF-00-01	54.41	0.72	19.51	8.38	0.16	4.14	8.56	3.64	1.09	0.31	100.92	pyroclast
BMPF-00-02A	53.95	0.72	19.23	8.42	0.16	4.21	8.56	3.62	1.09	0.31	100.29	pyroclast
BMPF-00-03A	53.77	0.73	19.53	8.50	0.16	4.19	8.72	3.71	1.09	0.31	100.71	pyroclast
BMPF-00-05A	54.26	0.73	19.36	8.47	0.16	4.19	8.57	3.59	1.10	0.31	100.74	pyroclast
BMPF-00-05B	54.05	0.73	19.27	8.60	0.17	4.32	8.63	3.66	1.05	0.31	100.78	pyroclast
BMPF-00-06	53.89	0.72	19.30	8.32	0.16	4.09	8.51	3.60	1.09	0.31	99.97	pyroclast
BMPF-00-07	54.22	0.72	19.44	8.35	0.16	4.10	8.64	3.59	1.09	0.31	100.62	pyroclast
BMASH-00-04A	53.28	0.80	19.50	8.82	0.16	4.09	8.58	3.56	1.02	0.29	100.11	airfall lapilli
BMASH-00-04B	54.05	0.75	18.51	8.78	0.17	4.52	8.47	3.55	1.11	0.31	100.24	airfall lapilli
Accuracy [%]	0.20	0.90	0.30	0.40	2.30	3.80	0.30	3.40	0.80	2.50		

Trace Element Compositions	Ba [>350ppm]	Nb	Ni	Rb [>5ppm]	Sr [>500ppm]	Th	Y	Zr
BMAL-00-01A	355.38	2.85	0.79	19.42	749.21	1.88	20.41	104.48
BMAL-00-03	356.02	3.01	1.14	19.16	747.23	2.41	20.13	103.92
BMAL-00-06	352.22	3.02	2.91	19.08	739.93	1.86	20.37	104.74
BMLV-00-1W	356.94	3.13	1.74	18.92	748.42	2.21	20.48	104.37
BMAL-00-11W	398.58	3.18	2.21	20.16	723.56	2.08	20.62	108.27
BMAL-00-12W	361.98	3.14	1.83	18.97	747.23	1.93	20.22	104.82
BMAL-00-10	384.96	3.19	2.38	19.15	739.23	2.00	21.25	104.50
BMAL-93-09	367.07	3.17	2.10	19.26	746.36	1.73	20.88	105.65
BMPF-00-01	354.73	2.93	0.59	19.41	749.36	2.09	19.92	105.16
BMPF-00-02	358.21	2.94	1.41	19.36	745.10	2.35	20.34	104.34
BMPF-00-03	354.50	3.03	1.70	19.33	741.08	2.22	19.93	103.92
BMPF-00-05A	352.20	3.06	1.74	19.32	746.11	1.72	19.83	103.94
BMPF-00-05B	400.95	2.88	2.34	19.09	750.71	2.35	20.28	102.24
BMPF-00-06	364.50	3.12	1.71	19.10	740.43	2.36	19.95	104.13
BMPF-00-07	374.81	3.20	1.53	19.15	748.86	2.19	20.57	104.21
Accuracy [%]	2.10	7.00	5.80	7.20	0.60	9.80	1.80	1.20

pyroclastic-flow deposit have a similar composition despite their color and textural difference (Arpa et al., 2001).

4.1.4 Recent Explosive Eruptions

Some of the 48 eruptions recorded are explosive in nature resulting to significant number of casualties and property damage around the volcano. About 1,200 people died in the most destructive Plinian eruption in 1814. Lives were lost even in smaller and less explosive eruptions. For example, 77 farmers were killed by surges in the unanticipated phreatic explosion that occurred at the initial phase of the 1993 eruption. No one was killed during the most recent 2000-2001 eruptions of Mayon, but it caused considerable damage to agriculture and other properties, most of which were due to syn- and post-eruption lahars.

The 02 February 1993 phreatic explosion

In 1993, Mayon Volcano erupted after nine years of repose. The eruption started with an explosive phreatic eruption on 02 February 1993, followed by dome intrusion and subsequent generation of block-and-ash flows from dome growth, explosion and collapse. Increased magma intrusion rate gave way to quiet emissions of lava flows which marked the end of the eruption. Seventy seven farmers were instantly killed by the initial blast that devastated the southeast side of the volcano (Fig. 10A, 10B). The eruption sequence departed from the more common open-vent eruptions (e.g., 1978, 1984) that are accompanied by high-rising eruption plumes, generating column-collapse type and/or boiling-over type pyroclastic flows.

In most of its activities, Mayon had showed signs of unrest, days to months prior to eruption. However, except for pronounced changes in the groundwater level, one to two months before 1993 (Newhall, 1993), the volcano erupted without significant precursory seismic activity. Seismic patterns indicated that prior to each eruption, i.e. 1978, 1984, and 1993, Mayon prepared for the next, in the form of small periodic magma intrusions (Newhall, 1993). Seismic swarms in 1985, 1988, 1991, and 1992 could have been manifestations of magma influxes near the surface in preparation for the 1993 eruptive phase. The absence of seismicity shortly before the 1993 event suggests that magma had reached the summit crater at least months before the February 1993 eruption.

A phreatic explosion at 1311 hrs on 02 February 1993 at the summit of Mayon produced a small pyroclastic flow and a surge that moved down the Bonga gully at the southeastern flank of the volcano (Fig. 8) (Catane and Mirabueno, 2001). Eyewitness accounts indicated

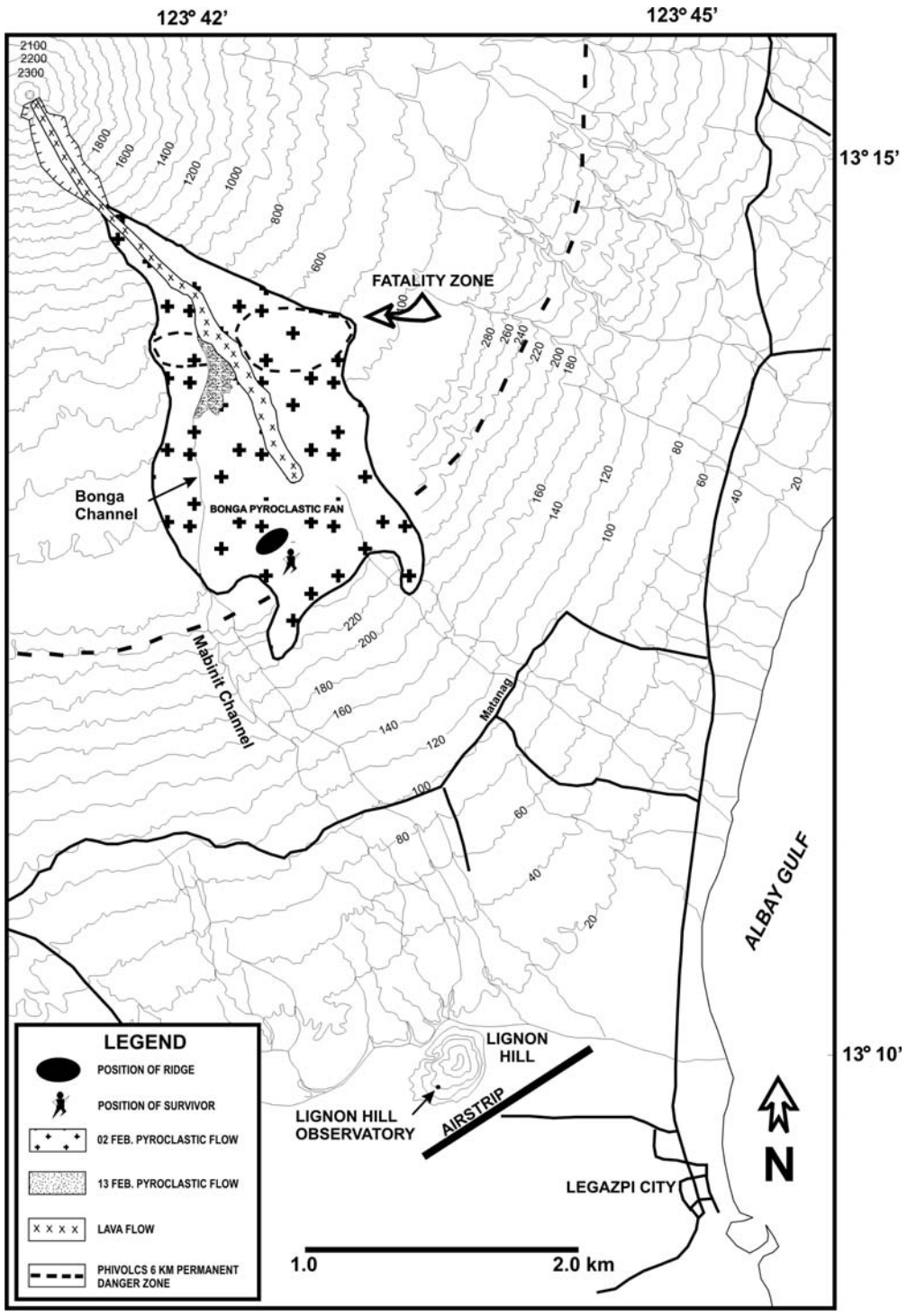

Fig. 8. Distribution map of the 1993 Mayon Volcano eruptive products. The fatality zone and the position of one of the survivors are also indicated. Adopted from Catane and Mirabueno (2001).

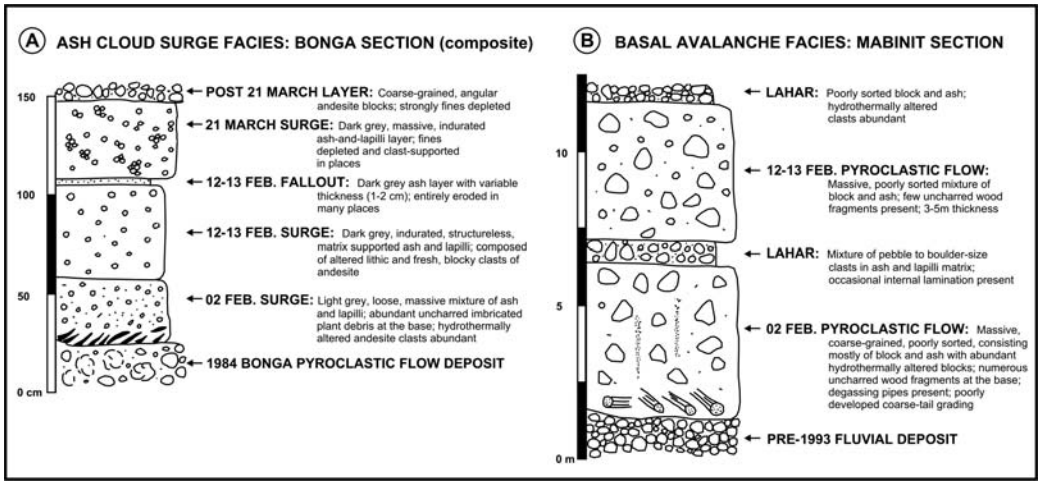

Fig. 9. Composite sections of the 02 February 1993 phreatic explosion surge deposits and succeeding events. (A) Deposits of the ash-cloud facies covered mostly the surface of the 1984 Bonga pyroclastic fan, southeast slope of the volcano, (B) Basal avalanche deposits emplaced at the upper reaches of Mabinit channel. From Catane and Mirabueno (2001).

that it took only 1-1.5 min for the initial flow to travel from the summit down to the base at 600 m above sea level (Newhall, 1993). The deposit consists of in-channel basal avalanche and overbank surge facies (Fig. 9) (Catane and Mirabueno, 2001). The basal avalanche unit is 2-5 m thick, massive, and coarse-grained, consisting of hydrothermally altered blocks set in a lapilli and ash matrix (Fig. 10C). It includes many pieces of uncharred trees and plant debris, suggesting that the flow moved across the vegetated pre-1993 eruption surface, and that it is indeed related to the first explosion. Degassing pipes were observed, indicative of hot emplacement (Fig. 10D). The associated surge layer mantled the surface of the 1984 Bonga pyroclastic fan. Its thickness varied from a few millimeters at the margins to about 50 cm at the central part of the Bonga fan, approximately 600 m elevation. Similar to the basal avalanche facies, the surge deposit is composed of hydrothermally altered lapilli and ash with variable amounts of uncharred plant debris. Juvenile material is absent in both avalanche and surge facies. The 02 February 1993 surge differs from a typical cross-bedded surge deposit by its massive internal structure. Interestingly, the event is a rare example of a phreatic explosion generating both pyroclastic flow and surge. Catane and Mirabueno (2001) hypothesized that the initial explosion generated sufficient volume of coarse and fine fragments, producing high particle concentration flows, allowing the formation of the basal avalanche deposit. High particle concentration and high momentum of the flow due to strong explosion energy

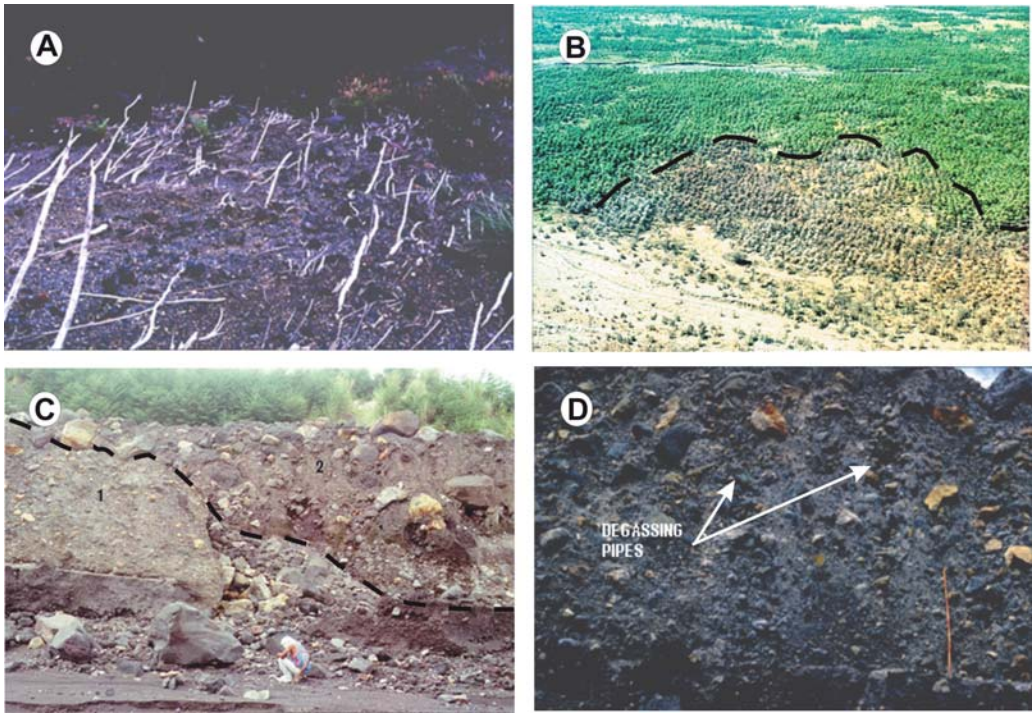

Fig. 10. Effects and pyroclastic products of the 1993 Mayon eruption. (A) Surge deposit and imbricated blown-down trees on the surface of the Bonga pyroclastic fan. Flow direction is away from the viewer. (B) Singed vegetation at the edge of the pyroclastic surge. The flow was from left to right. (C) Basal avalanche deposits exposed at the bottom of the Mabinit channel. Flow unit 1, the basal unit of the 02 February pyroclastic flow, contains abundant hydrothermally altered clasts (yellow). Flow unit 2 contains altered blocks as well as juvenile clasts (andesite). Flow unit 2 is related to the 12-13 February pyroclastic flow. (D) A close up view of the 02 February basal avalanche deposit showing degassing pipes and abundant lithic components. Modified from Catane and Mirabueno (2001).

and steep upper slope of Mayon prevented deposition of particles until the flow reached the break-in-slope at 600 m elevation. Flow separation took place at this point, allowing the overlying surge to spread and move as an independent flow.

The emplacement temperature range of the 02 February 1993 pyroclastic flows and surges was estimated at 100-300℃, based on evidence in the deposit (e.g., segregation pipes, rock components) and the degree at which objects and human bodies were exposed to heat (Fig. 11A) (Catane and Mirabueno, 2001). The explosive nature of the phreatic eruption is evidenced by the following: (1) blown-down trees (Fig. 10A), (2) splintered and blasted objects (Fig 11B, Fig. 11C), and (3) on-ramping of surge deposits on barriers and topographic highs.

Only two people survived the 02 February blast (Fig. 11A). Rapid expansion of superheated steam and magmatic gases, whose temperature is close to magmatic temperatures, could

Fig. 11. Impact of surges on human and objects. (A) One of the two survivors of the 02 February pyroclastic surge who suffered up to third degree burns. The most severe burns were incurred on different parts of her body that were directly exposed to the moving surge. (B) Impact and penetration marks on a coconut tree (person in photograph is 1.5 m tall). (C) A fragment of a blasted skull found at the edge of Buyuhan channel, about 5.5 km from Mayon's crater. Modified from Catane and Mirabueno (2001).

have generated the fatal explosion (Catane and Mirabueno, 2001). Although rare, the experience from the 1993 Mayon eruption showed that there is a chance of surviving a surge, within a narrow zone (about 500 m inward from the surge margin), but as long as the person can avoid direct surge impact, by seeking refuge behind topographic barriers/objects or with the use of protective cover.

2000-2001 Eruptions

A combination of Strombolian and Vulcanian type of eruptions characterized the February to March 2000 unrest of Mayon Volcano. The eruption began with quiet lava effusion, culminating to explosive a Strombolian phase (Table 4, Fig. 12A), which generated small pyroclastic flows.

The 28 February to 1 March 2000 Vulcanian eruptive phase of Mayon also generated pyroclastic flows (Fig. 12B). The total volume estimate of the pyroclastic flow deposits emplaced in 14 channels around the volcano is 13.9 M m^3. Bornas et al. (2000) documented the following lithofacies for the 2000 pyroclastic flow deposits (deposition channels are in parentheses): (1) juvenile cauliflower bomb-rich units (Mabinit, Buyuan, Basud, Buang), (2) lithic clast-rich block-and-ash unit (Mabinit, Basud, West Bulawan, Buang),

Fig. 12. (A) Strombolian phase of the 2000 eruption of Mayon. (B) Multiple pyroclastic flows generated during the initial Vulcanian phase of 2000 Mayon eruption. Photo A was taken in Legaspi City by an unknown photographer; photo B by PHIVOLCS.

Table 4. Chronology of the 2000 (Bornas et al., 2000) and 2001 (Corpuz and Laguerta, 2003) Mayon eruptions. From Bornas, et al. (2000); Corpuz and Laguerta (2003).

Date	Time	Activity	Areas affected	Other observations
2000 MAYON ERUPTION				
12 Feb		Emergence of a lava pile at the summit vent; incipient lava flow and rockfall.	Bonga Gully	
24, 26 and 27 Feb		Lava effusion progressed into Strombolian activity; pyroclastic eruptions produced 200 m - 3 km high ash columns and small volume pyroclastic flows	Bonga and Miisi Gullies	
28 Feb to 1 Mar		Culmination of eruption with an explosive Vulcanian activity; eruption columns reached 12 km; pyroclastic flows generated from eruption column collapse were emplaced along 14 major channels.	All sides of Mayon in a ~3 km radius.	
3 Mar		Lahar Activity	Anoling-Salvacion, Tumpa, Quirangay, and Maninila Channels	
2001 MAYON ERUPTION				
January to April		Lava dome growth on the summit; sporadic ash explosions; edifice deformation, and very high gas outputs.		Apparent ascending magma, Alert Level 2 was raised.
11 May	5:52 PM	Series of explosions ejecting mostly ash and bombs.		
12 May		Partial collapse of the SE portion of the summit.		
13 May		Ascending magma extruded on the southeast flank of the growing lava dome.	Bonga Gully	
17 June		A stubby lava flow was formed.		
20 June		Lava extrusion was more or less continuous; gas discharge became more voluminous and contains more ash particles.		
22 June		Lavas had partially buried the summit dome.		
23 June		Conspicuous summit glows.	Bonga Gully	COSPEC readings of Sulfur Dioxide reported about 7,000 tonnes per day (t/d). Alert Level was raised from 3 to level 4; hazardous eruption imminent within days.
	7:09 PM	Low-level lava fountaining and descent of lava flow units from the summit to about 500 m elevation.		
	8:00 PM	Minor lava fountaining commenced.		
24 June	3:17 AM	Series of explosions formed a 1-km ash column; ash fell on the northern flank of the volcano.	Barangays Amtic and Tambo of Ligao and Barangays San Vicente, San Antonio, Quinastillojan, Bantayan, Tabiguian, and Buang of Tabaco.	
24 June	1:00 PM	First major pyroclastic flow.	Bonga Gully and Barangay Buyuan	Alert Level 5 was raised.

	2:44 PM	Large explosions generated multiple pyroclastic flows around the cone.	Ash blanketed the northern areas, particularly the cities of Ligao and Tabaco.	Eruption column rose to about 10 km altitude.
29 June	4:05 PM	Small pyroclastic flow within the Bonga Gully.		
30 June - 19 July		Mayon's activity waned.		Volcano status eventually lowered to Alert Level 3.
20 July		Seismographs around the volcano again recorded high frequency-type short duration tremor related to rockfalls.		
21 July		Sulfur Dioxide flux increased threefold to 7,400 t/d.		Crater glow increased and rockfalls intensified.
25 July	4:18 AM	Continuous high-frequency tremors; lava boulders detached from the blocky lava flow, causing rockfalls.		
26 July	2:19 AM	Mild lava fountaining		Alert Level 4 was in effect.
	5:38 AM	Explosion formed 500-meter high ash cloud accompanied by low-frequency type earthquake.		
	7:45 AM	Another ash explosion.		
	7:56 AM	First large explosive eruption; column rose to about 10,000 meters altitude.	Pyroclastic flows along Bonga (southeast) and Basud (east) Gullies. Small volume pyroclastic flows descending the Mi-isi and Anoling Gullies (generally southern flanks).	
	2:20 PM	Another episode of eruption.		
	5:49 to 6:10 PM	Third and final eruption episode.	Ashfall of about 7mm thick in Camalig (southwest); thinner ashfalls in Daraga to the south and Guinobatan to the southwest; 5 mm thick in Legazpi (southeast) and Lidong (east-southeast).	
27 July		Effusive state; SO_2 flux remained at 6,450 t/d.		
10 August onwards		Decline of seismic activity; SO_2 fluxes are still high - up to 6,600 t/d.		
End of August				Evacuees returned to their homes.

(3) ash-rich massive to stratified block-and-ash unit (Buyuan, Basud, West Bulawan, Buang), and (4) lithic clast-rich block-and-ash unit. Geochemical analysis of the 2000 lavas and pyroclasts revealed a basaltic andesite composition, with SiO_2 contents of 53-54 wt% (Arpa et al., 2001). Two types of pyroclasts were recognized in the pyroclastic flow deposits - light gray and dark gray pyroclasts (Arpa et al., 2001). Mineral assemblage is the same for both types (clinopyroxene, othopyroxene, plagioclase, olivine, and magnetite) but differs in crystallinity and groundmass texture. Dark gray pyroclasts exhibit lower degree of crystallinity and have brown glass in the groundmass. They are chemically similar except for higher Ba content in the light gray pyroclast.

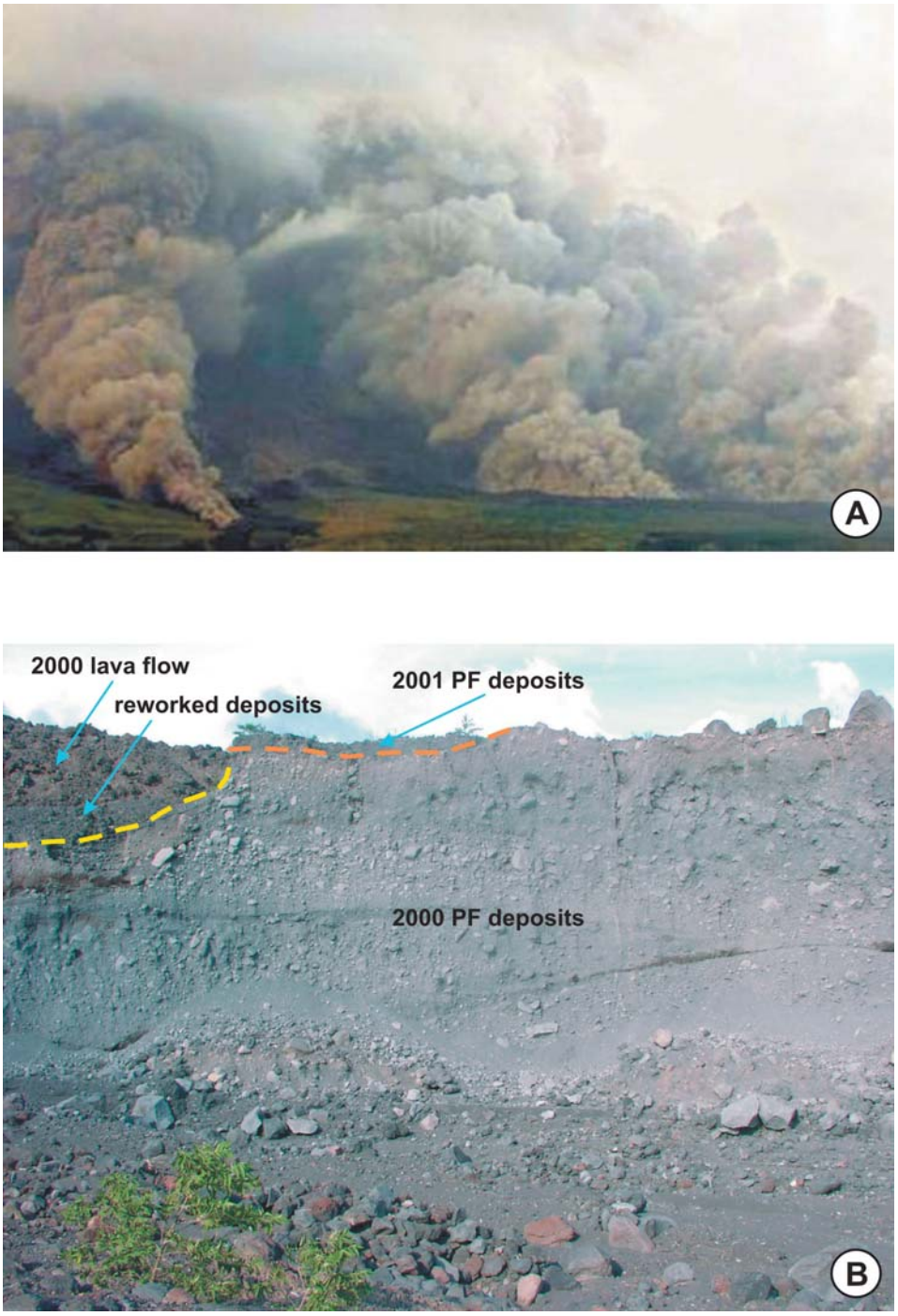

Fig. 13. (A) Pyroclastic flows of the 2000 Mayon eruption. Photo by PHIVOLCS. (B) Pyroclastic-flow deposits of the 2000-2001 eruptions along Mabinit channel. The lower 90% of the outcrop constitutes the 2000 products. The upper left of photograph is the 2000 lava front. Photo by S. Catane.

The 2001 Mayon eruption occurred in two episodes (Table 4). The first unrest was recognized in early January, culminating to explosive eruptions on 24 and 29 June (Fig. 13). Resurgent magmatic activity began on 20 July and climaxed on 26 July. In the morning of 26 July, Mayon Volcano ejected a 10 km high ash column, generating pyroclastic flows that went down mainly in Bonga and Basud channels (Arpa, 2001; Corpuz and Laguerta, 2003). It was followed by two more explosive events in the afternoon of the same day. Fortunately,

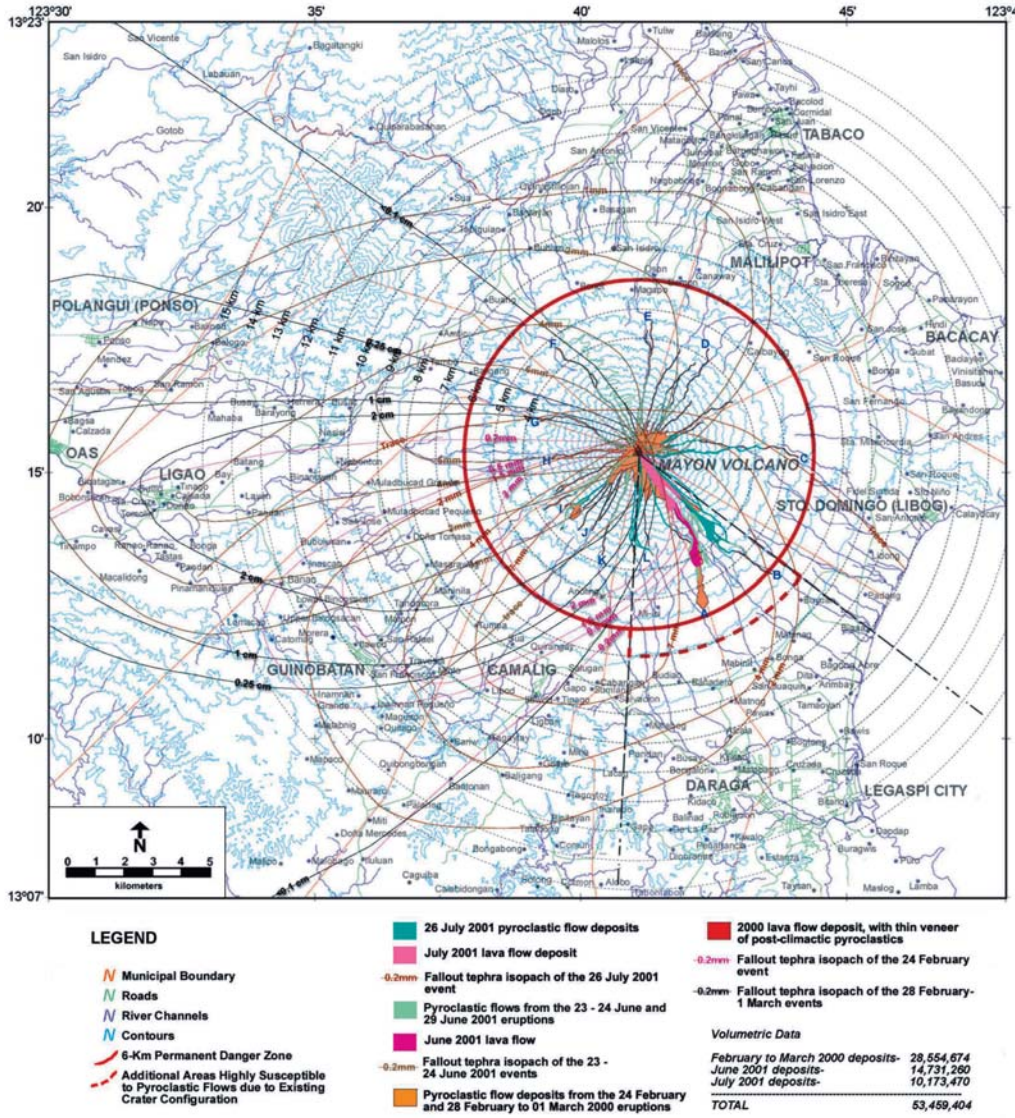

Fig. 14. Distribution of the eruptive products of 2000 and 2001 Mayon eruptions. From PHIVOLCS: *In* Arpa (2001).

Fig. 15. Lava flows of the 2000 (dark gray) and 2001 (black), overlying units with prominent flow levees) Mayon eruptions. Photo by S. Catane.

early detection of precursors allowed volcanologists to make warnings, giving sufficient lead time for local officials to evacuate over 25,000 people (Corpuz and Laguerta, 2003). Low-level lava spattering and active degassing continued until mid-August of the same year.

The total volume of the July 2001 eruption is about 10 M m^3. Most eruptive products were emplaced at the southeastern slope of the volcano (Figs. 14 and 15). The most voluminous pyroclastic flow deposits are found in Buyuan, Basud, and Miisi and were formed within the 6 km radius Permanent Danger Zone. The lava flow effused on July 2001was estimated to be 3.8 M m^3.

4.1.5 Style and Patterns of Eruptions

The eruptions of Mayon are mostly explosive. In many of its historical eruptions, the dominant style is Vulcanian, characterized by the emission of ash and ash-laden gases, forming huge cauliflower-like ash columns, and extrusion of basaltic andesite to andesite magma. One large Plinian eruption occurred in 1814, ironically producing basaltic tephra

(Fig. 16). The occurrence of Plinian eruptions is roughly 100 yrs as a result of injection of basaltic magma in the magma reservoir (Newhall, 1977). Mirabueno (2001), however, obtained a basaltic andesite composition for the 1814 tephra, in the range of 53.5-55wt% SiO_2.

Mayon exhibits one or more eruption styles for the entire duration of a single eruption. Two contrasting sequences in Mayon were recognized based on historical accounts (Ramos-Villarta et al., 1985): (1) airfall to pyroclastic flows (and lahars), and finally to lava flows, and (2) quiet emission of lava flows to relatively explosive ejection of ash and lapilli which produced tephra falls and pyroclastic flows. The first pattern is interpreted to be a result of progressive decrease of magma vesiculation rates. In the second sequence, extrusion of relatively degassed magma remaining in the conduit after a previous eruption resulted to lava flows, followed by explosive eruption as new batch of fresher and volatile-rich magma is replenished in the vent. The recent 2001 eruption followed the second pattern, tapping proba-

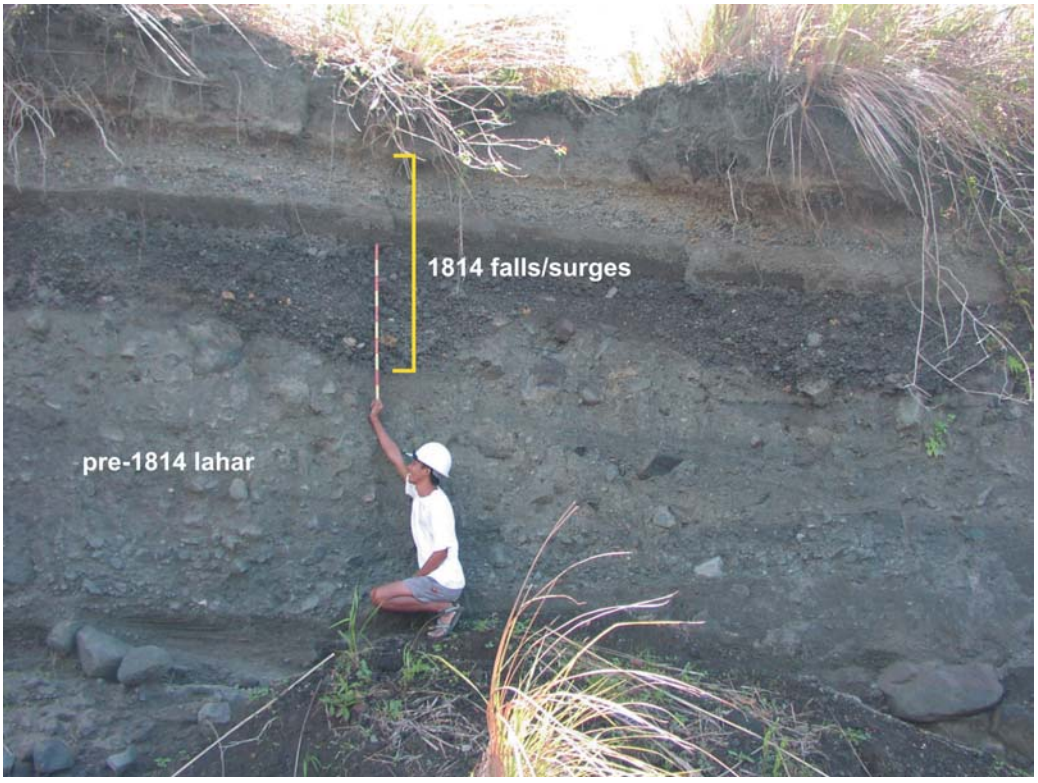

Fig. 16. The lapilli-rich surge/fall(?) layer (dark gray to almost black bed in the middle) of the 1814 Plinian eruption exposed along the lower reaches of the Mabinit channel. Note the irregular thickness and erosive base of the deposit. The two layers just above it are fallout or surge beds probably associated with the same eruption. Thick, massive unit below the 1814 layer is an older lahar deposit. Photo by S. Catane.

bly residual magmas of the 2000 eruption. The third type of eruptive sequence is solely Strombolian, which starts with minor ash ejections and terminates with quiet lava effusion, as in the 1978 eruption.

More detailed visual and instrumental monitoring of the 1993 and 2000-2001 eruptions provided opportunities to observe more discrete eruption patterns of Mayon. The 1993 eruption commenced with a phreatic explosion resulting to a widening of the notch at the southeastern side of the volcano. This was followed by viscous extrusion of lava, forming a steep dome. Instability due to continued dome growth resulted to the collapse and emplacement of block-and-ash flows for more than a month, followed by an influx of more degassed lava flows that marked the end of the eruption. This is considered as the fourth pattern.

The formation of a dome makes the 1993 eruption distinct from the other patterns. Mayon has been regarded as an open-vent system until 1993 when the summit crater was plugged and virtually "closed" by a dome for almost two months. The mechanism for pyroclastic-flow generation was controlled by the existence of the dome, from which pyroclastic flows were derived, and the breaching of the crater rim on the southeastern side, which became pathways for the flows. Pyroclastic flows were emplaced via explosive disruption of the dome, instead of the collapse of a Vulcanian plume common in an open-vent system. The possible implications of open and closed vent systems in relation to the varying eruption styles of Mayon have not been fully investigated.

Unlike the 1993 eruption, the 2001 occurred in two phases (Table 4):

a) *Phase 1*- The eruption started with lava dome growth and stubby lava flow. Low-level lava fountaining ensued before explosions began, followed by a series of pyroclastic flows. Mayon's activity waned from 30 June to 19 July.

b) *Phase 2*- Resurgent magmatic activity began on 20 July and climaxed on 26 July. Low-level lava fountaining on July 26 was followed by explosive eruption and formation of a 10-km eruption column and pyroclastic flows. Low-level lava spattering and active degassing continued until mid-August.

The June and July 2001 eruptions occurred so close in time that they must have tapped a single batch of magma (Corpuz and Laguerta, 2003). From accounts of previous activities, a major eruption of Mayon may be preceded one or two years by minor explosions or seismic precursors, presumably as the magmatic system is reactivated. This places the 2000 and 2001 eruptions in the same time span for which a beginning precursor (e.g., 22 June 1999 or earlier) is followed by one or more episodes of eruptions and eventually a distinct waning phase

(Corpuz and Laguerta, 2003). The interval between the 2000 and 2001 eruptions was initially considered a waning phase, but upon re-examination of tiltmeter data and seemingly persistent summit explosions in the months following March 2000, it appeared that this interval was in fact inflationary (Corpuz and Laguerta, 2003). Thus, trends and events prior to the discovery of the lava dome on 08 January 2001 should have been viewed as precursors and not as post-eruption events. However, this is not clear because high seismicities, elevated SO_2 fluxes and above-average summit activities such as thermal outputs and rockfalls, often occur for some time after a major eruption. A promising discriminant between precursor and post-eruption activity is ground deformation (Corpuz and Laguerta, 2003). The placement of tiltmeters on one flank at varying elevations resolved a general inflation trend that strongly suggested that continued intrusion was taking place (Corpuz and Laguerta, 2003).

Based on the chemical and petrographic analyses of 51 sequential lava flows, Newhall (1977) detected a cyclical variation in modes and chemical compositions that can be related to the eruptive styles of Mayon. The two most recent cycles are from 1800 to 1876 and from 1881 to the present. The cycles can be explained by geochemical-temporal variations in Mayon rocks. Although basaltic andesite (53-56 wt% SiO_2) is the most common eruptive product of Mayon, occasional basaltic eruptions related to basaltic magma injection in a shallow magma chamber beneath the edifice, occur approximately every century (Newhall, 1977). Basaltic magma is differentiated to basaltic andesite and andesite during succeeding eruptions. Newhall (1977) inferred that the next two to three eruptions from 1978 should be similar to the 1928-1978 eruptions and should end that cycle. Most recent influxes occurred just before the 1814 and 1818-82 eruptions.

Using erupted magma volume data, Punongbayan (1985) recognized cyclical patterns in Mayon's major eruptions involving at least 20 M m^3 of volcanic ejecta. Completed cycle durations range from 41 to 47 years. The 1968 cycle is the latest and is only on its 37^{th} year. He predicted that within 3 to 5 years after the 1984 eruption, there will be one or two major eruptions to complete the cycle.

Lizardo (1986) conducted statistical analysis of the eruptive events of Mayon Volcano from 1766 to 1984. The existence of two phases characterized by generally decreasing repose patterns was identified. The period from 1800 to 1897 constitutes the first phase, while the second spans from 1900 to 1984. The transition from the first to the second phase implies that a minor change in the volcanic system or the triggering mechanism, possibly took place between 1897 and 1900. In the second phase, it was found out that explosivity is dependent to

the repose period. Longer repose periods tend to be succeeded by more explosive eruptions.

Goto (1993) compared the viscosity of ash and volcanic bombs from the 1993 Mayon eruption with essential ejecta of 1988-1989 Tokachi-dake eruption and Unzen dome-1 lava. The viscosity of Mayon ash is a little higher than that of Tokachi-dake's, but about one order lower that that of Unzen's. Mayon and Tokachi-dake exhibit the same eruptive style. The viscosity of magma of the destructive 1814 Plinian eruption of Mayon is lower by a factor of three than that of the less explosive 1993 eruption (Pelean and Merapi types). This implies that factors other than viscosity control the explosivity of volcanic eruptions at Mayon.

The near-perfect symmetry of the volcano indicates that eruptions have repeatedly utilized the central vent and that these have never been sufficiently violent to destroy its cone. Recent eruptions were directed toward the southwestern, southern, and eastern sectors, in contrast with older deposits distributed in the northern and western quadrants. The location of the notch on the crater rim may have been variable throughout Mayon's eruptive history to allow an almost even distribution of deposits in all quadrants. In the recent eruptions, gravity flows have utilized the lowest part of the rim of the crater. The present notches, which are connected to the largest gullies, Bonga and Basud, are facing the southeastern and eastern sectors of the volcano. They have been utilized and progressively enlarged by pyroclastic flow erosion and summit explosions during the 1993, 2000, and 2001 eruptions. Although much of the lower segment of the Bonga gully was filled with lava flows, its upper section was severely widened and deepened, leaving a narrow, pie-shaped segment of the cone bounded on the east by the other deeply incised Basud gully. The seemingly unstable chunk of the cone faces the side of Legaspi City. This warrants further studies on the potential hazards due to cone instability and collapse.

On the basis of the recent eruptive activities of Mayon, the resulting morphology of the crater rim formed during a previous eruption, mainly controls the direction of gravity flows in the succeeding eruptions.

4.1.6 Volcanic Hazards

Volcanic hazards in Mayon vary greatly in type, lateral extent, duration, and destructive potential. The hazards are the consequence of Mayon's three eruption types namely Strombolian, Vulcanian, and Plinian as well as dome-formation related hazards. Hazards of Mayon are ballistic fragments, lava flows, pyroclastic flows and surges, tephra falls, and lahars.

Lava flows

Lava flows of Mayon are relatively large, coherent and elongated streams of incandescent molten volcanic rock materials that originate from the summit crater or a point near the summit area. Some lava flows may originate from lava fountain activity during Strombolian eruptions, or from domes at the summit crater. Lava flows cascade down along gullies and ravines in the steep upper cone, but slow down upon reaching the basal slopes. At the initial phases of the 1993 and 2001 eruptions, lava outflow started out as a viscous dome inside the crater. Lobate morphology, steep flow margins, prominent flow levees, and blocky surface are typical of Mayon lava flows. The moderately high viscosity of the lava flows tends to retard lateral spreading. The farthest distance attained by lava flows is only 6 km from Mayon's summit.

Because lava flows of Mayon move slowly, they can be avoided and thus they do not pose as a direct hazard to people. However, lava flows destroy everything along their path, and grounds covered by lava flows may remain barren and useless for decades. When lavas move on steep slopes, red-hot blocky fragments detach from the moving flow and roll down the front and sides, endangering people and property. Cascading lava flows may have indirect hazards. Active moving flows may trigger landslides and rockfalls. The 1984 lava flow triggered a small earthflow on the southwestern slope of the volcano.

PHIVOLCS has delineated the lava flow hazard zone at Mayon as an array of narrow zones radiating outwards from the summit crater. These areas define the gullies and crevices radiating from the volcano's summit crater and extend from 6-7 km downwards. There are at least 23 of these gullies around Mayon Volcano. The three largest gullies have been formed in 1984 mainly due to erosion by pyroclastic flows, making them most susceptible to lava encroachment. The largest and deepest gully, the Bonga gully, has been repeatedly utilized by lava flows during the last three eruptions of Mayon Volcano. The volume of lava flows varies significantly in each eruption. The estimated volume of the 1928 lava flow was 60 M m^3; 20 M m^3 for each of the 1968 and 1984 eruptions, and 3.8 M m^3 for the 2001 eruption. With the Bonga gully's estimated channel capacity of 15 M m^3 (pre-1993 eruption estimate), overflow is expected if this volume is exceeded. Because of the significant channel capacity reduction of the Bonga channel due to the deposition of lava flows during the 1993, 2000, and 2001 eruptions, the other gullies on the eastern and southwestern slopes of the volcano may funnel the lava flows in the next eruptions.

Pyroclastic flows

Pyroclastic flows from Mayon originate in four ways: (1) collapse of pyroclastic materials from a tall eruption column during Vulcanian and Plinian eruptions (Moore and Melson, 1969; Cruz et al., 1985; Ramos-Villarta et al., 1985); (2) boiling-over directly from the vent (Cruz et al., 1985); (3) dome explosion and collapse (Pelean-type) (Catane and Mirabueno, 2001); and (4) passive dome/lava collapse (Merapi-type) (Catane and Mirabueno, 2001). The first and second types were typical of the 1814 Plinian, and 1968, 1978, 1984 Vulcanian eruptions, while the 1993 and 2001 produced types 3 and 4. Pyroclastic flows generally follow gullies and low-lying areas along the flanks of the volcano. They are channel-confined on the upper slopes, but overflow and spread at the break-in-slope, forming broad pyroclastic fans, e.g., Bonga pyroclastic fan (Cruz et al., 1985). Pyroclastic flows associated with Vulcanian and Plinian eruptions are commonly emplaced in all directions around the summit crater. The direction of pyroclastic flows related to dome disruption, however, depends on where on the slope of the volcano a dome has grown. Dome-derived pyroclastic flows are confined along channels adjacent to the dome. In the case of the 1993 eruption, the dome that was growing inside the summit crater was exposed by breaching on the southeast side of crater by the 02 February phreatic explosion. Consequently, pyroclastic flows were emplaced in this direction.

An expanded, less dense, more mobile ash-cloud surge overrides the main body of pyroclastic flow. Because of higher mobility, ash-cloud surges may separate from the main flow and follow different path. In the 1993 eruption of Mayon, while the main flows followed the base of channels, the surges climbed and hugged channel levees, and some even overtopped ridges. The initial surge of the 1993 eruption killed 77 farmers.

Pyroclastic flows and surges pose a major threat to life and property because of their high temperature, mobility, and direct impact. There is but a slim rate of survival if caught by an advancing flow or surge. Mayon pyroclastic flows commonly reach 5-8 km from the crater. In 1897, however, pyroclastic flows extended to the sea, east of the volcano, at a distance of 12 km. Pyroclastic flows travel at great speeds. It took only 1-1.5 min for a small pyroclastic flow/surge during the 1993 phreatic eruption to move down from the summit to the base of the volcano (Newhall, 1993). Many of the boiling-over type pyroclastic flows were emplaced at higher velocities in the order of a few minutes at an aerial distance of 6-7 km from the summit crater (Cruz et al., 1985). The volume of pyroclastic flow and surge deposits varies in each eruption. The 1984 eruption deposited a volume of 40 M m^3, 10 M m^3 for the 2001

eruption, and only 2 M m^3 of pyroclastics (mostly from surges) was emplaced during the 1993 eruption.

The pyroclastic flow hazards zone (Fig. 17) is the outward extension of the lava flow hazard. This zone extends downward to an elevation of 200 m. The zone is extended on the east side along Basud gully in Sto. Domingo village since it has been severely affected by his-

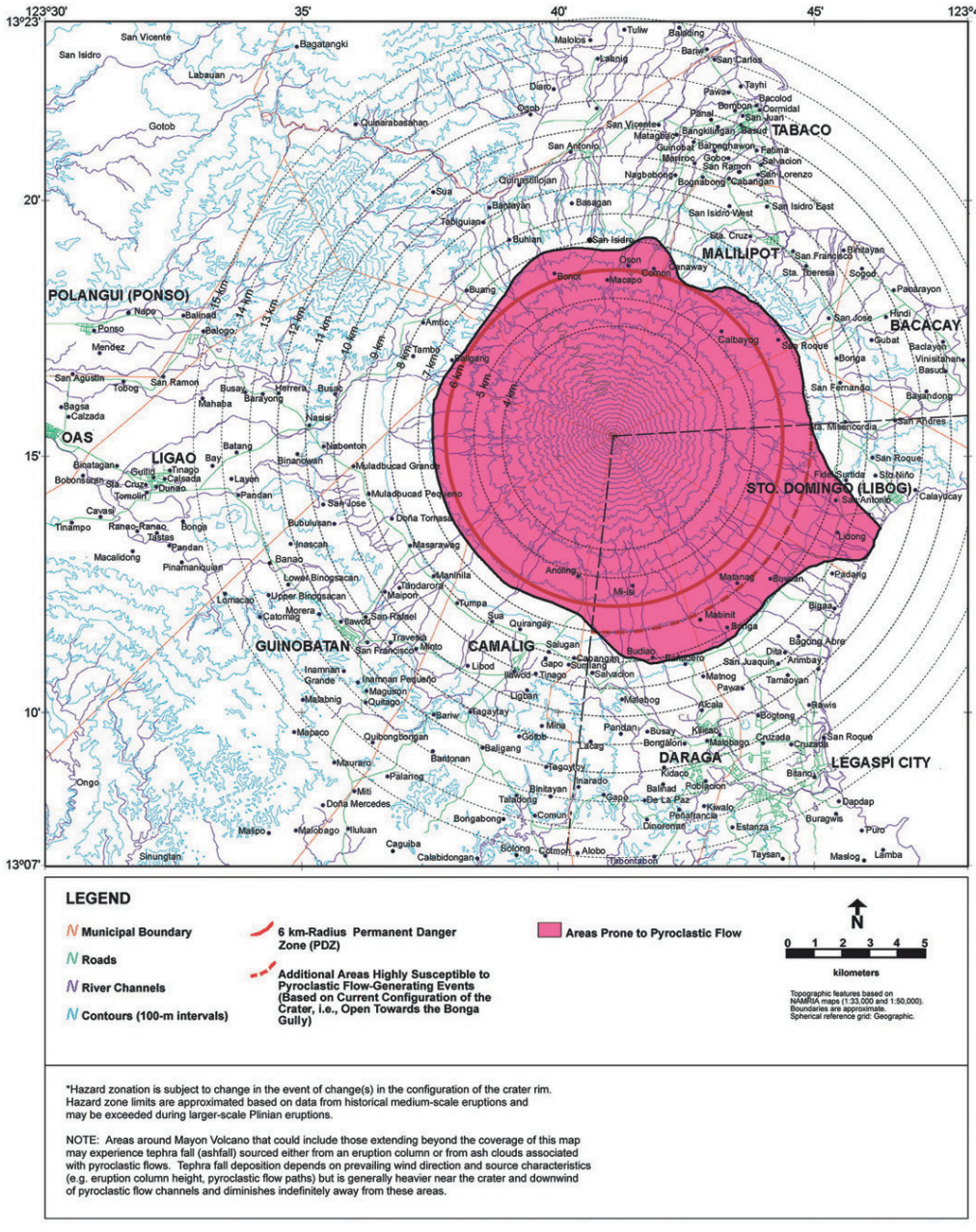

Fig. 17. Pyroclastic flow hazard map of Mayon Volcano by PHIVOLCS as of April 2003.

toric eruptions. Currently, the area of greatest hazard lies along the 3 largest gullies lying on the eastern, southeastern and southwestern flanks of the volcano. The Bonga gully faces the villages of Mabinit, Bonga, Matanag and Buyuan - all of Legaspi City. The vulnerability of this area is compounded by the tilt of the crater rim to south. Other likely paths of deadly pyroclastic flows are Basud gully (E side) and the Daraga-Camalig gully (southwest side). The notches connected to the two gullies, Bonga and Basud, were further widened during the latest eruption in 2001, thus making them convenient pathways of pyroclastic flows in the future.

Ballistic fragments, lapilli fall, and ashfall

Tephra consists of explosively ejected clots of incandescent magma or fragments of older solid rock. These particles are explosively thrown up into the air from the crater by explosion. Tephra particles are of various sizes, from ash (< 2 mm), to lapilli (2-64 mm), to blocks/bombs (> 64 mm). Tephra derived from fresh magma are termed juvenile.

Bombs/blocks are large tephra derived from either new fresh molten materials or old rocks that are blown out from the vent with ballistic trajectories. Spasmodic ejection of volcanic bombs occurs during Mayon's Strombolian phase. Large blocks ripped off from the vent and crater walls by explosions are emplaced in the same manner but are more common at the early, vent-clearing stage of eruption. These falling debris can damage any object or structure present in the area of direct impact. Hazard zones for ballistic projectiles cover only areas near Mayon's crater at distances of 0.5-1 km depending on the explosivity of the eruption.

Lapilli fall are smaller than bombs and blocks (a few milimeter up to 8 cm for Mayon). Unless eruption is phreatic type, most are derived from newly erupted magma. The 1814 Plinian eruption produced abundant lapilli, some of which reached as far as 18 km from the crater. Up to 8 cm diameter of juvenile fragments fell out on the southwest slope of the volcano during the 2001 eruption. The relatively high temperatures of lapilli may ignite objects or cause forest fire. It may also cause burns, scalding and other physical injuries related to their relatively high impact velocities.

Ash fall is a variety of tephra consisting of particles mostly < 2 mm in diameter. They are produced by explosive fragmentation of the magma. Because of their small size and low density they can hurled up high in an eruption column and can be entrained in the atmosphere for prolonged periods. They can be transported away from the volcano by prevailing

winds. Ash falls are derived from both vertical eruption column and overlying ash cloud of pyroclastic flows. In Mayon, ash fall is the most common hazard from Mayon and they are mostly associated with Vulcanian and Plinian eruptions.

Heavy downfall of volcanic ash poses a direct threat to people, animals, crops, houses, buildings, machineries, and aircrafts. Fine volcanic ash is often respirable and inhalation of ash may result to or aggravate respiratory ailment. Other effects of ash fall are: (1) extreme darkness during the day, (2) aviation accidents or damage to aircraft engines, (3) crop damage by burial and introduction of chemical substances in the ash, (4) collapsing roofs due to heavy accumulation of ash, (5) metal corrosion by acid-bearing ashes, and (6) inhibition of water infiltration due to ash mantling newly erupted pyroclastic materials, thus promoting initiation of lahars.

PHIVOLCS defines high hazard zone as areas that will likely receive heavy ash fall of at least 20 cm. This definition assumes that eruptions are similar to the 1968 and 1984 Vulcanian eruptions. The hazard zone forms an overlapping elliptical-shaped pattern with a prominent northeast-southwest elongation, following the prevailing wind stream in Albay province. However, dispersion of ash from an eruption column is dependent on the prevailing wind speed and direction at various altitudes.

Lahars

Lahars, sometimes called mudflows or volcanic debris flows, are flowing mixtures of volcanic debris and water. It is a spectrum of different flow types depending on the water-sediment ratio. High sediment concentration flows have high viscosities (debris-flow type), while low sediment concentration flows behave more like normal stream flows (hyperconcentrated stream flows). There are two types of lahars in Mayon: (1) primary lahars are rain induced and occur during volcanic eruptions; and (2) secondary lahars are those that occur after eruption has ceased. Primary lahars are hot and often larger in volume and more destructive than secondary lahars. Debris-flow type lahars are more common during eruptions. Lahars originate from the upper and middle slopes of Mayon Volcano. Loose, unconsolidated, and newly deposited pyroclastic materials on the slopes, are remobilized by heavy rains, producing a debris-water mixture that flow down along gullies on the slope of the volcano. Lahars at Mayon generally follow pre-existing gullies and ravines, but upon reaching the lower slopes, spread out and leave thick and extensive deposits. The build-up of deposits by series of lahar events, produce a fan-shaped morphology. At least two major lahar deposits fans

were formed during the 1984 eruption. Pre-historic lahar fans with well-preserved surface morphologies are common at the lower basal slopes of Mayon.

Lahars are considered as the most destructive and persistent hazards in Mayon. Lahars destroyed and buried houses, buildings, and infrastructures with mud and pyroclastic debris. They blocked drainages, raised river beds, and caused flooding adjacent to flat areas.

Rockfalls and landslides

Rockfalls at Mayon are triggered by ground deformation due to pressure exerted by rising magma near the crater, just before an eruption. They are also associated with actively moving lava flows, where huge incandescent blocks break, detach and roll down from the steep front and margins of flows. Cascading lava flows on steep slopes can destabilize rocks and soil and trigger landslides, i.e. the 1984 Camalig earthflow. Another potential source of landslides in the future is the seemingly unstable side of the cone bounded by the deeply incised Bonga and Basud gullies. This was a result of progressive erosion of the notches during the last three eruptions of Mayon. Collapse can be triggered by an eruption, explosion or a strong earthquake and may endanger the villages at the southeastern slope of Mayon. Considering that relatively large volume of rock debris can be dislodged from the summit, assessment of the cone stability is deemed necessary.

4.1.7 Hazard Zones

For Mayon, the area surrounding the volcano within 6-km radius from the summit is regarded as the Permanent Danger Zone, where the danger is present at all times and the hazard involved is high during an eruption (Fig. 17). This area is risky for habitation and permanent settlement should not be allowed. The area within 6-8 km from the summit is considered a moderate hazard zone during eruption periods. At the onset of an eruption, people living within this hazard zone are alerted for possible evacuation. PHIVOLCS recommends specific areas for evacuation, depending on the possible course and nature of volcanic activity. The area up to 10 km from the summit is endangered only if Mayon erupts violently. Once a sign of violent eruption is observed, the towns covered by the 10 km radius will be alerted for possible evacuation. PHIVOLCS has also prepared maps for specific volcanic hazards such as ballistics, lava flows, pyroclastic flows, airfall, and lahars. These maps are updated after each eruption or as the need arises.

4.1.8 Volcano monitoring and eruption prediction technigues

In 1955, the first seismograph installed was a three-component Ishimoto acceleration seismograph at the Bureau of Air Transportation office in Legaspi City, located about 10 km south of the volcano' s summit. In 1957, the Commission on Volcanology (COMVOL), the predecessor of PHIVOLCS, installed a water-tube tiltmeter at Mayon Resthouse Observatory (MRHO), situated about 4 km north-northwest of the summit at an elevation of 760 m above sea level. An Askania Vertical Magnetometer was also obtained, and this facilitated routine magnetometric survey. A Hilger and Watts (Wilmore) electromagnetic-type seismograph was acquired in 1965, and installed at the Legaspi Station. One component Hosaka Vertical Seismograph was added at MRHO, and a three-component Akashi seismograph was established at the Sta. Misericordia Station (SMS) located 8.5 km east of the summit.

Prior to the 1984 eruption, PHIVOLCS has been maintaining the two volcanological stations, the MRHO and the SMS. Both stations are equipped with 3-component Hosaka electromagnetic seismograph with a natural period of 1.0 second. MRHO operates normally at a magnification range of 4,000 to 10,000x, while at SMS, the range is lowered (1,000 to 4,000x) due to high noise level brought by traffic. A Philippine Atmospheric, Geophysical & Astronomical Services Administration (PAGASA) local weather station, also maintains a Teledyne seismograph in the Legaspi Seismic Station (LSS) with a magnification of 56,000x and located about 12.5 km south of the summit.

At the height of the 1984 eruption, the SMS station was abandoned since it was within the danger zone and along the direct path of pyroclastic flows. A monitoring station was temporarily established in Legazpi City. After the eruption, a permanent observatory, the Lignon Hill Observatory (LHO), was established on the promontory of Lignon Hill in Legazpi City.

Several types of volcanic quakes and tremors are being received in the seismic stations. They are classified as LT/S-, SX-, B-, A-, E- and SDH-type quakes or tremors (Peña, 1986). The LT/S or local tectonic quake is believed to be associated with fracturing as magma forces its way up. The SX-type has no distinct p and s phases and has several appearances. The A- and B-types have no distinct p and s waves, but differ in period: the A-type ranges from 0.5 to 0.8 s while the B-type varies from 0.8 to 1.0 s. The X-type is a series of A-type tremors that lasts for several minutes. SDH-types are short duration harmonic tremor.

The seismic records obtained by the different stations are rather incomplete during the early 80s due to frequent power shortages and instrument breakdown. This resulted to the

very late issuance of warning and evacuation order during the 1984 eruption. In the previous eruptions (i.e. 1968 and 1978), it was found out that seismicity usually begin to increase at least six months prior to the eruption, but discernable trends or sharp increases occur at least one to two months before (Peña, 1986).

Seismic monitoring was also applied in the detection of mudflows/lahars after the 1984 eruption of Mayon. The seismic signals generated by mudflows are high frequency non-monochromatic tremors with fluctuating amplitudes belonging to spasmodic type of tremors (Bautista et al., 1986). A lead-time of approximately 20 minutes upon detection of mudflows is available for warning the people that are threatened.

Monitoring of SO_2 emission rates was first carried out on Mayon Volcano during the 1978 eruption and later during the 1993 eruption. SO_2 measurements were conducted using a Barringer correlation spectrometer (COSPEC), lent by the USGS, and a COSPEC Model V donated by the Canadian government. SO_2 flux ranged from 300 − 4,000 t/day during the first eruption phase from 3 February to 19 March. It increased to 3,000 − 6,000 t/day starting 18 March, coinciding with vigorous lava outpouring. It was observed that in Mayon, periods of explosive eruptions are preceded or accompanied by sharp increases in SO_2 flux (Tubianosa et al., 1999). COSPEC measurements were also proven useful in forecasting explosive phases of the most recent 2001 eruption.

When Mayon was declared abnormal on August 1988, a summit thermal anomalies survey was conducted remotely, using a handheld Minolta/Land infrared radiometer, and directly at the summit, by recording fumarole temperatures using a chromel-alumel type thermocouple. Moderately high temperatures recorded (maximum in excess of 285℃) suggest that magma is present at relatively high levels within the volcano (Oppenheimer, 1988).

At present, PHIVOLCS is maintaining three observatories - LHO, MRHO, and SMO. MHRO has a three-component Hosaka seismograph. The MHRO also houses a watertube tiltmeter. LHO has a three-component Kelunji seismograph and receives telemetered data from SMO and MHRO annually. Three tiltmeters on a radial line through MRHO are telemetered to LHO. Recently LHO has begun monitoring the water table on the southeastern side of Mayon. Binoculars are used for 24-hour visual observations such as the presence of crater glow, bluish fumes, and volume of steam emission. A leveling line is located in the northwest sector while two EDM lines are in the northwest and southeast. Surveys are conducted every quarter and during crises. Plume monitoring of Mayon using a video capturing system was set-up in 2003 by Prof. Kisei Kinoshita of Kagoshima University, Japan. This

can be accessed via real-time video streaming through the internet.

Ramos-Villarta and others (1985) enumerated the eruption precursors of Mayon as follows: (1) increase in the frequency of volcanic earthquakes; (2) ground tilt and deformation; (3) fissuring at or near the crater; (4) increase in frequency of rockfalls in the summit area; (5) change in steam color (from white to brown to grey) indicating increase in volume of entrained ash; (6) volume increase of steam emission; (7) rumbling sounds; (8) crater glow; and (9) abnormal animal behavior (i.e. descent of wild pigs and other wild animals into populated areas).

4.2 Taal Volcano

4.2.1 Volcano Profile

Taal Volcano (14° 02' N, 120° 57' E) is the most destructive and violent among the active volcanoes in the Philippines. The last two major eruptions in the 20th century alone killed at least 1,525 people. Taal is located in the province of Batangas in southwest Luzon, about 60 km south of Metro Manila. It is one of the volcanoes in the Central Luzon Belt associated with the subduction along the Manila Trench. Volcanism in Taal and the rest of the Southern Tagalog Volcanic Field is related to the northeast-southwest cross-arc lineament referred to as the Macolod Corridor, an apparent pull-apart rift zone separating the Philippine and West Luzon shear zones (Defant et al., 1988; Knittle and Oles, 1995).

Taal Volcano is an island that lies inside a 25 km caldera lake now occupied by Taal Lake (Fig. 18). Its highest point is 311 m above sea level making it one of the world's lowest volcanoes. There are about 47 eruptive centers within the island consisting of tuff cones, tuff rings, scoria cones, and cinder cones.

Fig. 18. A view of Taal Volcano Island and its caldera (Taal Caldera). The prominent cone on the forefront of the island is Binintiang Malaki. The volcano at the foreground is Mt. Macolod which forms part of the southern margin of the caldera. This photo was taken from the northern caldera rim (PHIVOLCS).

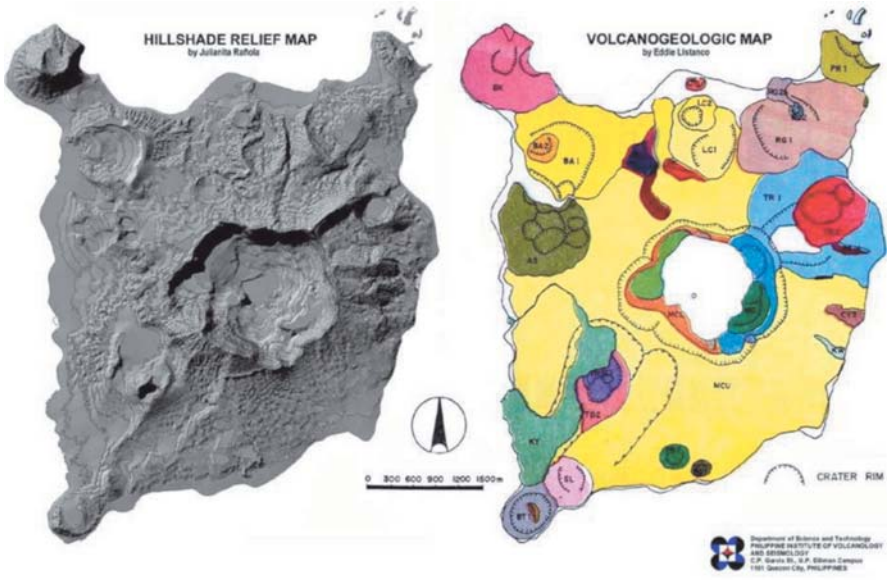

Fig. 19. Geomorphologic (left) and geologic (right) map of Taal Volcano Island. From Listanco (1994).

The most prominent volcanic cones are Binintiang Malaki, Binintiang Munti, Pira-piraso, Calauit, and Mt. Tabaro eruption site (Fig. 19). Underwater topography suggests the existence at least 35 other volcanic centers at the bottom of the caldera lake. At least one of the historic eruptions occurred underwater, off Calauit in 1716. Roughly in the middle of the Volcano Island is the freshwater-filled 2-km wide Main Crater, which has been the site of historic and the most explosive eruptions of Taal. Twelve of Taal Volcano' s eruptions, from 1749 to 1911, occurred here. Mt. Tabaro eruption site, on the southwest flank of the island, is the locus of the most recent eruptions from 1965 to 1977.

The Taal topographic depression now largely occupied by Taal Lake is a result of at least two overlapping calderas within a graben setting. Taal Lake has an area of 267 km^2 and rises 2 m above sea level. It is 100 m deep at the northern portion and 150-260 m deep at the southern portion (PHIVOLCS, 1997). It is drained by the Pansipit River into Balayan Bay on the southwestern shore. Taal Caldera is 25 km across and was formed by piecemeal collapse between 140,000(?)-5,380 yBP (Listanco, 1994). The youngest calderagenic activity determined using ^{14}C is 5,380-6,830 yBP (Listanco, 1994; Martinez and Williams, 1999). This eruption produced the Taal Scoria Flow. The volume estimate of the deposit is 50 km^3 and it can be traced at the northern side of the caldera (Listanco, 1994). Several pre-caldera inactive volcanoes namely Macolod, Batulao, Sungay, Makiling and Malepunyo sit around the caldera. Taal

Volcano Island is considered as a post-caldera feature.

A total of 33 eruptions were recorded at Taal. The most violent and catastrophic eruptions occurred in 1754 and 1911. In 1754, the towns of Sala, Lipa, Tanauan and Taal, then bordering Taal Lake, were destroyed and were re-established to their present sites. The 1911 eruption completely devastated the entire Volcano Island and led to a casualty of 1,334. Ash fallout covered an area of 2,000 km^2 and reached as far as Metro Manila.

Historic eruptions of Taal are mostly explosive and typically phreatic or phreatomagmatic. Base surges are commonly associated with these eruption types. A few of the eruptions such as in 1968 and 1969 were Strombolian, characterized by lava fountaining from several active vents and effusion of lava from the base of the cones.

Despite the hazards posed by the volcano, Taal Volcano Island has been attracting migrants because of its fertile soil and rich fishing grounds. The island has been declared as a national park in the early 80s by then President Ferdinand Marcos. In spite of this, the population continues to grow. The island had a population of 5,800 as of 1991 (PHIVOLCS, 1992).

4.2.2 Morphological and Geological Features

Taal Volcano Island, whose center is the Main Crater, is a low stratovolcano with tuff-ring-like morphology and high tephra to lava ratio (Listanco, 1994). The ratio of at least 9:1 is high compared to the typical stratovolcano, and can be attributed the magma system's easy access to water. The main cone structure and stratigraphy is virtually unexposed due to its youthfulness and active tephra deposition. Inside the Main Crater are mostly inaccessible exposures of airfall and base surge sequences, indicating the importance of magma-rock-water interaction even at the early stage of eruptive history. At least four lava flows and a thick lava agglutinate are exposed along the nearly vertical crater wall. Plug and/or dike-like bodies are exposed on the south-southeastern walls and northern side of the crater (Listanco, 1994).

Most of the flank cones can be classified as monogenetic tuff rings on the basis of parameters including height, basal diameter, crater width, crater depth, and crater floor height (Listanco, 1994). They occupy the northern half of the island and are conspicuously less in the southern part (Fig. 19). This may be partly due to the presence of a more dominant northeast-southwest trending structure. The only two tuff cones include the more prominent Binintiang Malaki (BK) and Look 2 (LC2) (Figs. 19, 20). Of the flank tuff rings, the Pulang Bato (PB1) seems to be peculiar: it has the morphological parameters of a tuff

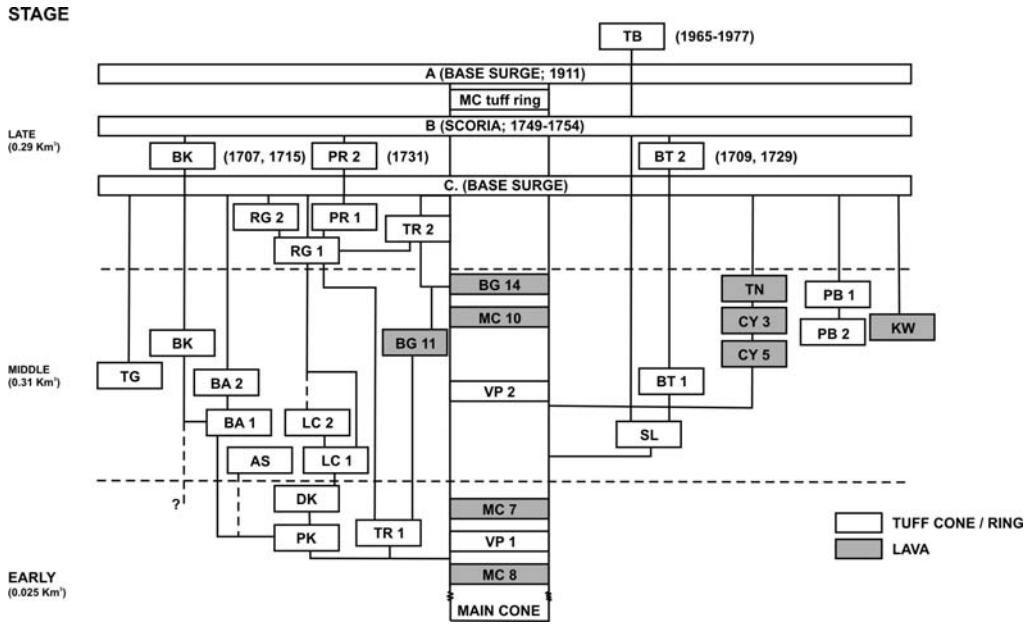

Fig. 20. Block diagram for the evolution of Taal Volcano Island. From Listanco (1994).

ring, but dominated by scoriaceous spatter bombs. Thus, it may be better described as a "scoria ring" (Listanco, 1994).

Figure 20 shows the spatial and temporal patterns in the location of eruption centers at Volcano Island (Listanco, 1994). Based on its volume and stratigraphic relation with other edifices, the main cone must have played a central and major role as an eruption center through time. The overall pattern is one of general outward migration of eruption centers, accompanied by a strong northeast-southwest trending structural control.

The rock composition of Taal Volcano varies from basalt to basaltic andesite. Miklius and others (1991) recognized two distinct and contemporaneous series at Volcano Island: the calc-alkaline and magma-mixed BM, and the iron-enriched Tauran series. They further suggested that the two series were derived from discrete, separately evolving primitive melts, with mixing confined within each.

Only a few geophysical works have been conducted to reveal the subsurface structure and magma source of Taal Volcano. Nishigami and others (1994) reported a fan-shot seismic profile indicating increased S-wave attenuation below 1 km and strong reflectors at 7±10 km depth beneath the island. The authors interpreted these seismic properties as evidence of a magma chamber between 1 and 7 km depth. Lowry and others (2001), however, interpreted

the abovementioned anomalies as corresponding to hydrothermal overpressuring and alteration of volcaniclastics similar to other large caldera systems, because those depths are too shallow for such a widespread partial melt system to remain in stable equilibrium. Besana and others, (1995) interpreted the presence of partial melt at 18 km depth beneath the northern caldera rim as inferred from 15% reduction of shear wave velocity using receiver function analysis.

4.2.3 Historic Eruptions, Eruptive Style, and Patterns

Taal Volcano has erupted 33 times since its first recorded outburst in 1572. Its last eruption was in 1977. Accounts of historical eruptions were given by Centeno (1885), Saderra Maso (1911), and Worcester (1912), and reviews by Andal and Yambao (1978), Masigla and Ruelo (1987), Newhall and Dzurisin (1988), and PHIVOLCS (1991b). Table 5 shows a summary of the historical eruptions of Taal Volcano. The center of eruption within historical times has shifted from the Main Crater to different locations within Volcano Island and Taal Lake. Masigla and Ruelo (1987) divided the historic eruptions into four series based on spatial relationship (Table 5): (1) A- series (central and main crater), (2) B-series (flank: Binintiang Malaki, 1707 and 1715; Binintiang Munti, 1709 and 1929 A; Calauit, 1716; near Pirapiraso, 1731, (3) C-series (central: 1749-1911), and (4) D-series (flank: Mt. Tabaro eruption site, 1965-1977). The duration of Taal eruptions lasts from 1-2 days (e.g., 1977) to more than 6 months (e.g., 1754). Repose period varies from 1 yr to 62 yrs.

Taal had four very explosive eruptions in historical times, i.e. 1749, 1754, 1911 and 1965. The short-lived 1749 eruption extruded 100 M m^3 of volcanic debris, devastated the whole of Volcano Island and nearby lakeshore towns, and resulted to casualties. The six month long 1754 eruption destroyed the old towns of Sala, Lipa, Tanauan, and Taal, then located on the margins of Taal Lake, and were subsequently relocated to their present sites. Ramos (1986) deduced that syn-eruption underwater landslides may have been responsible for the destruction of some of these towns, based on lake underwater investigation. The eruption produced a volume of 150 M m^3 of tephra. In 1911, the volcano claimed 1,334 lives and completely devastated the entire Volcano Island. The greatest destruction was due to a rapidly expanding eruption cloud (base surge) at the base of the eruption column that swept down the slope of the Main Crater and out across the surrounding lake. Eruption column height was about 15 km and the volume of ejecta was estimated at 80 M m^3, severely affecting an area of 230 km^2. More than fifty years later, another explosive eruption took place in 1965. Violent base

Table 5. Summary of Taal Volcano historic eruptions. From Masigla and Ruelo (1987); PHIVOLCS (1997).

Date of eruption	Center or activity	Precursory signs	Type of eruption	Intensity of eruption	Associated phenomenon	Effects & areas affected
ERUPTION SERIES A - MAIN CRATER						
1572	Main Crater		Phreatomagmatic			
1591	Main Crater		Phreatic			
1605 - 1611	Main Crater					
1634	Main Crater					
1635	Main Crater					
1641	Main Crater		Phreatic		Tephra fall	Houses destroyed
1645	Main Crater	Rumbling sounds				
ERUPTION SERIES B - FLANK CRATERS						
1707	Binintiang Malaki		Phreatic		Shock waves	
1709	Binintiang Munti		Phreatomagmatic			
1715	Binintiang Malaki					
1716 21 Sept.	Off Calauit (underwater)	Tremors, rumbling sounds, inc. in lake temp.	Phreatomagmatic	Violent	Earthquakes, seiches, toxic gases, tephra fall, base surge	Fatalities, destruction of vegetation & livestock
1729	Binintiang Munti					
1731	Pira-piraso (underwater)	Rumbling sounds	Phreatomagmatic (?)		Earthquakes, seiche, tephra fall, base surge, bombs	Destruction of houses an livestock
ERUPTION SERIES C - MAIN CRATER						
1749 11 Aug.	Main Crater	Booming sounds, crater glow, tremors	Phreatomagmatic	Very violent	Earthquakes, subsidence, fissuring, lightning, shock waves, seiches, acid rain, tephra fall, projectiles, base surge	Fatalities, destruction of houses and vegetation - Volcano Island; lakeshore towns of Taal, Sala & Tanauan
1754 15 May	Main Crater	Rumbling sound, tremors	Phreatomagmatic	Very violent	Earthquakes, fissuring, solfatara, shock waves, seiches, acid rain, tephra fall & projectiles, base surge	Fatalities, destruction of houses & vegetation - Volcano Island, Taal, Lipa, Sala & Tanauan
1790	Main Crater					
1808	Main Crater		Phreatomagmatic	Moderate		

1825	Main Crater					
1842	Main Crater					
1873	Main Crater					
1874	Main Crater		Phreatomagmatic	Moderate	Tephra fall, toxic gases	Destruction of vegetation
1878	Main Crater	Tremors	Phreatic	Moderate	Tephra fall	Ashfall - Volcano Island
1903	Main Crater					
1904	Main Crater		Phreatic	Mild	Earthquakes, tephra fall & projectiles	
1911 27 Jan.	Main Crater	Tremors	Phreatic	Very violent	Earthquakes, subsidence, fissuring, solfatara, lightning, shock waves, seiches, acid rain, tephra fall and projectiles, base surge	Fatalities, destruction of houses, vegetation and livestock - Taal Volcano Island, Tanauan, Talisay and other lakeshore towns
ERUPTION SERIES D - MT. TABARO						
1965 28 Sept.	Mt. Tabaro	Change in lake color, inc. in lake temp. & level	Phreatomagmatic	Violent	Solfatara, shock waves, seiches, acid rain, tephra fall & projectiles, base surge	Fatalities; destruction of houses, vegetation and livestock
1966 5 Jul.	Mt. Tabaro	Inc. in lake level	Phreatomagmatic	Moderate	Tephra fall and projectiles	Destruction of houses and vegetation & livestock
1967 16 Aug.	Mt. Tabaro	Tremors, changes in lake color, inc. in 1966 crater lake temp., inc. in seismicity	Phreatomagmatic	Mild	Tephra fall & projectiles	
1968 Jan.	Mt. Tabaro	Inc. steaming & bubbling activity in crater lake, inc. in seismicity, change in color of 1966 crater lake	Strombolian	Moderate	Tephra fall, lava flow	
1969 29 Oct.	Mt. Tabaro	Inc. in seismicity, harmonic tremors, inc. in steaming activity, change in crater lake color	Strombolian	Moderate	Tephra fall, lava flow	
1970 3 Sept.	Mt. Tabaro		Phreatic	Mild		
1976 3 Sept.	Mt. Tabaro	Fissuring, inc. in steaming activity, inc. in probe hole temp., inc. in seismicity	Phreatic	Mild	Tephra fall	
1977 3 Oct.	Mt. Tabaro	Hissing sounds, inc. in steaming activity, fissuring, inc. in probe hole temp., inc. in seismicity	Phreatic	Mild	Tephra fall	

Fig. 21. The 1966 phreatic eruption of Taal Volcano. Note the base surges that laterally move out from the base of the eruption column. COMVOL 1966 photo: *In* PHIVOLCS (2003).

surges similar to the 1911 eruption swept out the southwest sector of the island, affecting towns across the lakeshore. The eruption opened up a new vent (1.5 km x 1.3 km) at Mt. Tabaro eruption site, on the southeastern portion of the island. Eruption column heights reached 15-20 km and deposited fine ash as far as 80 km downwind.

Taal Volcano eruption style is primarily phreatic (Fig. 21) and phreatomagmatic, and rarely, Strombolian and Plinian. The infrequent Plinian activities in 1749 and 1754, characterized by extensive tephra fallout, were the most explosive within historic times (412 years

for Taal). The two other explosive eruptions, 1911 and 1965, were phreatomagmatic, dominated by base surges. The 1911 eruption has been classified as phreatic, but a more recent study shows that the deposits contain fresh and quenched juvenile scoria fragments and glass shards (Knittel, 1998, pers. comm.), thus, it can be described as phreatomagmatic. If so, it explains the relatively wide area of devastation by the eruption. Most of Taal's eruptions have been phreatic and phreatomagmatic mainly due to easy access of lake and groundwater into the vent system. Only two eruptions, 1968 and 1969, were Strombolian, characterized by lava fountaining and non-explosive lava effusion.

4.2.4 Volcanic Hazards

The entire Volcano Island has been declared as a Permanent Danger Zone, barring from permanent settlement. Nonetheless, it is inhabited by more than 5,800 people. Hazardous areas shown in the hazard map in the foregoing section are based on areas previously affected by Taal Volcano's historic eruptions. In particular, lakeshore towns west and northwest of the island are threatened by explosive eruptions similar to the 1754, 1911, and 1965.

Hazards from Taal Volcano can be either direct or indirect. Direct hazards are processes and events directly resulting from an eruption. These are: base surges, ashfalls, ballistic projectiles, lava flows, toxic gases, and acid rain. Indirect hazards are consequences of the direct hazards, they include: seiche/tsunami and flooding, fissuring, ground subsidence, and lakeshore landslides (Ramos, 1986).

Base Surges

Base surges are low-concentration, turbulent mixtures of volcanic debris, steam and gas, that flow rapidly outward in all directions from the base of the main eruption column. Base surges of Taal have lower emplacement temperatures but in general more mobile than pyroclastic flows. The 1911 eruption devastated the whole island and lakeshores across Taal Lake, while two-thirds of it was destroyed in 1965, including mainland lakeshore villages on the southwest. The main characteristics and effects of the base surges based on accounts of the 1911 and 1965 eruptions are: (1) surges travelled at speeds of more than 50 m/s; (2) base surges carried all sizes of pyroclasts but dominated by ash and lapilli; (3) surges were non-incandescent, (4) surges travelled a maximum of 6 km from the vent (1965 eruption); (5) wet mud and ash were plastered on standing objects such as walls and tree trunks; (6) sandblasting effect of surges (removed and shredded bark of trees); and (7) survivors suffered minor

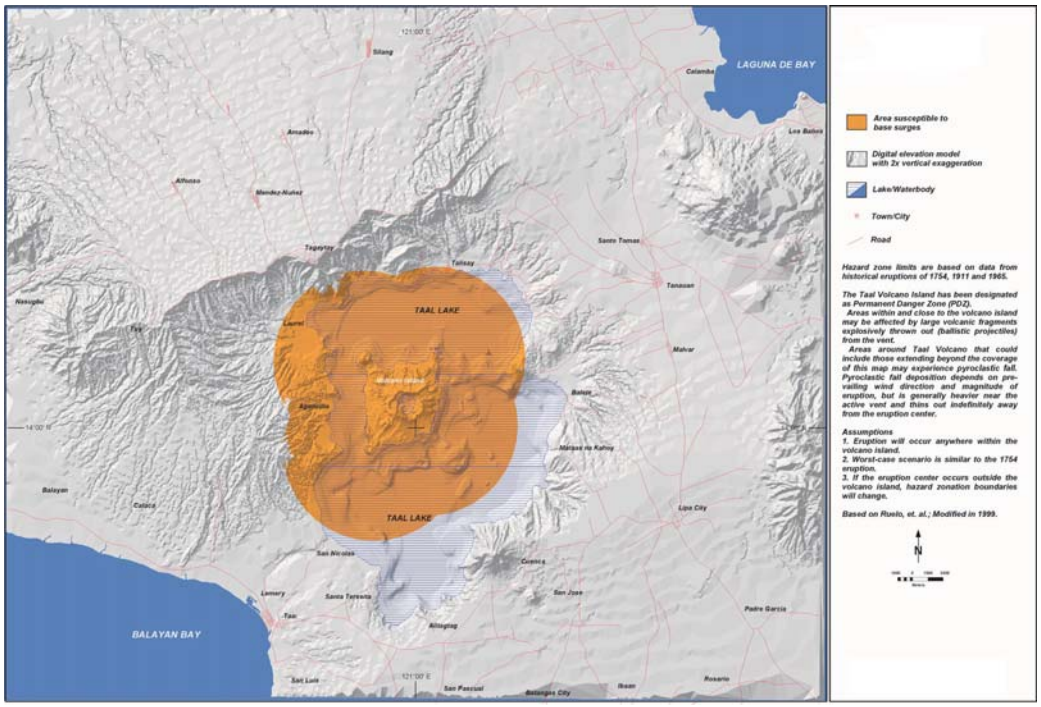

Fig. 22. Taal Volcano base surges hazard map by PHIVOLCS as of 1999.

degree burns indicating low temperatures (<100℃).

Figure 22 shows the hazard zonation map for base surges. The high danger zone corresponds to the areas that had been affected by the most explosive eruptions such as the 1754, 1911, and 1965 base surges. These areas will likely experience the severest damage in case eruptions of similar magnitude will occur. The area within a 6-km radius from the Main Crater corresponds to the places highly prone to base surges.

Ashfall

Taal has a 9:1 pyroclastic-lava ratio. Great quantities of ash and lapilli are released during explosive eruptions. Release of steam and gas pressure during explosions causes these tephra to be thrown vertically upward and become entrained in the eruption column, as high as 20 km from the crater. Coarser materials immediately fall back to the surface but the finer ash remains suspended for some time and dispersed by prevailing wind. The dispersal of ash and affected areas depend much on the prevailing wind direction at the time of the eruption and wind vectors at different altitudes. In the eruptions of Taal, ashfall constitute the second greatest hazard. Deaths and injuries have been attributed to heavy ashfalls.

Heavy ashfalls caused collapse of many houses and structures, damaged crops, killed animals, and affected people's health mostly due to respiratory ailment. Ashes from the 1754 eruption blocked the Pansipit River (lone outlet of Taal Lake) causing water level to rise, inundating the towns located along the lakeshores. In this eruption, one-meter thick ash was dispersed in an area of 400 km^2. Both the 1911 and the 1965 eruptions deposited 25-cm thick ash over an area of 230 km^2 and 60 km^2, respectively.

Prevailing wind direction and eruption column height were the primary basis for the hazard zonation for ashfall. Two sets of hazard maps were prepared by PHIVOLCS corresponding to eruption column heights of below three kilometers and greater than three kilometers. In both cases, the high danger zone is the area likely to receive at least 10 cm thick ashfall; 1-10 cm thick for moderate danger zone; and <1cm thick for low danger zone. The axes of the lobes are parallel to the seasonal northeast-southwest wind vectors.

Ballistic Projectiles

Projectiles of Taal eruptions include volcanic lapilli to bombs and blocks (>2 cm). They can destroy objects or inflict injury by direct impact or by rolling down the slopes of the volcano. In the 1911 eruption, a 250 kg block was thrown out and settled on the Main Crater rim. Projectiles have destroyed houses and crops on the island according to accounts. The high danger zone for ballistic projectiles covers an area within a radius of 5 km from the Main Crater on the basis of historic eruptions and studies on explosive eruptions worldwide.

Lava Flows

Lava flows in Taal Volcano are quiet, non-explosive effusions of molten rock from a vent or fissure. Taal extruded lava twice during historical times, first in 1968 the other in 1969. The lava flows moved slowly, about tens of meters per hour, but had high temperatures, sometimes as high as 1,175 C. Probable path and damage by Taal Volcano lava are limited within Volcano Island. Thus, the entire Volcano Island is succeptible to lava encroachment. Another potential hazard associated with lava flows are secondary explosions generated by hot lava-lake water interaction as they encroach the shore. Pyroclastic fragments generated by the explosive fragmentation of lavas can cause injury to people and destroy structures in the immediate vicinity.

Toxic Gases and Acid Rain

The Main Crater lake is highly acidic with a pH of 2.8-3.0. There have been no direct measurements on the acidity of ash particles or reports of acid rain during the historic eruptions, but fallout from the eruption cloud emanating from the Main Crater would have high a probability of being acidic because airborne particles can easily absorb gases and compounds present in the eruption cloud. Some survivors of the 1911 eruption sustained acid burns. In 1904, people on the lakeshore felt strong burning sensations when showered with acidic mud rain settling out of an eruption cloud. Acids can also be carried by base surges and can cause scalding. Volcanic gases killed all livestock on Volcano Island and damaged vegetation on the leeward side of the crater during the 1874 eruption. Gas dispersion is controlled by gas density and wind pattern. It also depends on the location of the gas vents. Gases denser than air will tend to crawl along gullies and topographic lows, thus the hazard zone is restricted in these areas. Also, gas odor such as sulphur stench has annoying effect. The danger zone for acid rain and gases adhering to airborne particles follows the danger zone for airfall.

Seiches/Tsunamis and Flooding

Incoming tsunamis and waves induced by seiches can cause considerable damage to life and property especially along the lakeshore. They can engulf and wash away structures along these areas. Seiches in Taal had been due to the impact of surges on Taal Lake. Boats fleeing the island capsized due to seiches, accounting for some of the deaths during Taal eruptions. Places succeptible to tsunamis, seiches, and flooding are low-lying areas less than 20 m above sea level on the island and lakeshores of the mainland.

Fissuring and Ground Subsidence

Earthquakes usually accompany eruptions of Taal Volcano. Strong quakes were felt during the 1749, 1754, and 1911 eruptions. During the earthquakes, fissures and ground subsidence occurred in many places, e.g., 1749 eruption. After the 1911 eruption, the Taal Volcano Island had subsided by 2 to 3 meters. Areas that subsided were flooded or submerged like what happened to an island northeast of the volcano that sunk. Fissures had caused damages to properties particularly infrastructures. In the 1911 eruption, fissures were observed as far as Sto. Tomas located northeast of Taal caldera. Areas prone to fissuring and ground subsidence had been confined between the two previously defined sub-parallel fissure

lines trending N35-40E. The upper line extends from Sinisian to Cabuyao, and the lower line from Lemery to Calamba. The fissure zone is parallel to the general trend of the Macolod Corridor.

4.2.5 Monitoring Techniques and Devices

PHIVOLCS maintains two volcano observatories in Taal Volcano: Pira-piraso Volcano Observatory and Buco Volcano Observatory. Both observatories have 3-component Hosaka electromagnetic seismographs. Pira-piraso station, located in Volcano Island, has a water tube tiltmeter and a telescope. Around Taal Lake are installed tide gauges as part of the lake tilt system. Precise leveling and EDM benchmarks are located in the southwest of Volcano Island near the 1965 eruption site. These sites are revisited quarterly to record any changes in ground condition. Several ground probe holes whose temperatures are determined every other day are located in this site. The Main Crater, site of the violent 1911 activity, is also being monitored using water level and temperatures of the lake and surrounding fumaroles. Water samples from the Main Crater and Taal lakes are collected twice a month and analyzed for its geochemistry. Eruption precursors at Taal Volcano include the following: rumbling/booming sounds, tremors, increase in lake temperature, crater glow, change in crater lake color, increase in lake level, increase in steaming and bubbling activity on crater lake, fissuring, and increase in probe hole temperature.

4.3. Pinatubo Volcano

4.3.1 Volcano Profile and Summary of Recent Activities

Mount Pinatubo (15° 7.4N, 120° 20.0E) belongs to the chain of composite volcanoes along the Luzon Volcanic Arc (Fig. 23). The arc parallels the west coast of Luzon Island and reflects eastward-dipping subduction along the Manila Trench to the west (Defant et al., 1989). The other major volcanic centers forming the chain are Mts. Natib and Mariveles, and smaller cones including Mts. Malasimbo, Balakibok and Negron. Mount Pinatubo is among the highest peaks in west-central Luzon. Its former summit, at 1,745 m elevation, may have been the crest of a lava dome that formed about 500 years ago, during the most recent pre-1991 major eruptive episode (Newhall et al., 1996). After the 1991 eruption, the summit height was reduced to 1,445 m above sea level and replaced by a 2-km wide, 600-800-m deep summit caldera. The volcano's lower flanks that are highly dissected and covered by dense vegetation prior to the 1991 eruptions are composed largely of pyroclastic deposits from vo-

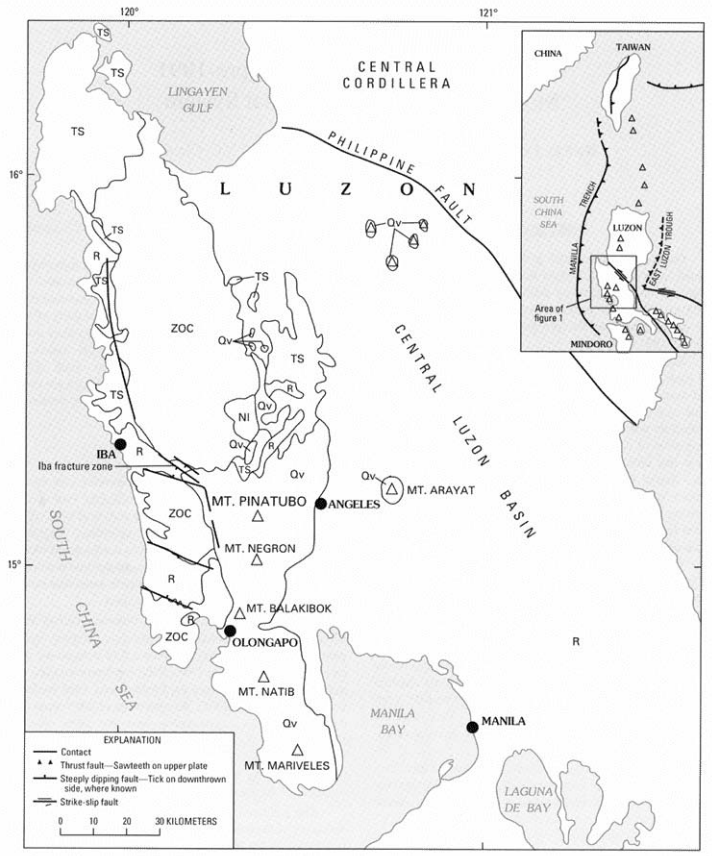

Fig. 23. Regional geologic map of the Mt. Pinatubo area. Inset shows major tectonic features of Luzon. Volcanoes are indicated by triangles. Major geologic units: R-recent sdiments, Qv-Quaternary volcanics, TS-Tertiary sediments; N-Neogene intrusive, ZOC-Zambales Ophiolite Complex. From Delfin et al. (1996).

luminous, explosive pre-historic eruptions (Wolfe and Hoblitt, 1996). Older Quaternary andesitic-dacitic volcanic deposits (Pinatubo volcanics), consisting of lava flows and pyroclastics, comprise the older sequence of Mount Pinatubo and adjoining peaks.

In June 1991, Pinatubo Volcano erupted after 450 years of repose. The eruption was the third largest in the 20th century. At least 4.8-6.0 km^3 of tephra were deposited around Pinatubo and in the South China Sea (Wiesner et al., 2004). A 2-km diameter caldera was formed due to the collapse of the volcano's summit during a lateral blast in the 15 June climactic phase. Much of the pyroclastic deposits emplaced on the slopes of Pinatubo were subsequently reworked to form lahars. A lake began to form in September 1991 from groundwater inflow and rainfall. In July 1992, a small mud cone (5 m x 100 m size) was formed near the

center of the caldera lake. The initial mud cone developed into a dome which grew sporadically, and by September of the same year, the dome's size was 300 m x 400 m. The dome was totally submerged in 1997 due to continuous rise in lake level. Lahars ensued from the 1991 eruption until 1999, causing widespread destruction of properties and infrastructures around the volcano. The Pinatubo giant ash cloud intruded the stratosphere and resulted to slight global cooling. The caldera lake continued to rise through the years, leaving a cliff-edge freeboard of 45 m on 07 May 1998 to only 2 m on 30 August 2001 at the Maraunot Notch, the lowest point of the crater rim. Aware of the possibility of a natural catastrophic crater-lake breaching, PHIVOLCS and the Department of Public Works and Highways (DPWH) decided to construct a drain canal to induce artificial breaching at a predetermined time, after people had been evacuated for safety. On 06 September 2001 the breach was opened at 6:53 am (local time), but breaching did not occur because the water discharge rate of 0.1 m^3/s is too slow to induce erosion. A year later, on 10 July 2002, at the height of southwest monsoon rains, the notch gave way unleashing about 65 M m^3 of water along Bucao and Botolan Rivers (Bornas, 2002). The lahars and flood waters overtopped the Bucao Bridge and damaged Botolan's river spur dikes northwest of the volcano. The breakout event, however, did not cause fatalities and damages were insignificant.

On January 2004, an unusual change in color of the crater-lake water took place, from bluish or emerald green to dark brown and almost blackish. PHIVOLCS gave two possible explanations for the change in water color: (1) the effect of increased dissolved Fe- and Mg-oxides in water from sediments inside the crater, or (2) due to increase in biogenic activity as a result of decline in volcanic activity since 1995 (PHIVOLCS, 28 Sept. 2004). As of this writing, PHIVOLCS, along with the assistance of the Industrial Technology Development Institute-Department of Science and Technology (ITDI-DOST), University of the Philippines-Institute of Biology (UP-IB), and others, is still undertaking more exhaustive investigations to pinpoint the most probable cause of the lake's coloration and to assess potential hazards if any.

4.3.2 Geology and Eruptive History

The eruptive history of the volcano has been divided into two major periods, namely, the ancestral and modern Mount Pinatubo (Fig. 24) (Newhall et al., 1996). The ancestral Mount Pinatubo was a Pleistocene andesite-dacite stratovolcano whose remnants are preserved in topographically elevated terrain surrounding the pre-1991 Pinatubo dome. Contemporane-

ous with this ancestral Mount Pinatubo stratocone are the domes of Mounts Negron, Cuadrado, and Mataba, and the Bituin plug (Delfin, 1983). Modern Mount Pinatubo is a dacite-andesite dome complex surrounded by sheets of dacitic pyroclastic flows and related lahars. New ^{14}C dating and stratigraphic analyses (Newhall et al., 1996) revealed at least six distinct eruptive episodes of modern Pinatubo, beginning with a caldera-forming event (Inararo episode) >35,000 ^{14}C yBP.

The Pinatubo volcanic rocks are cut by predominantly northwest- and north-trending

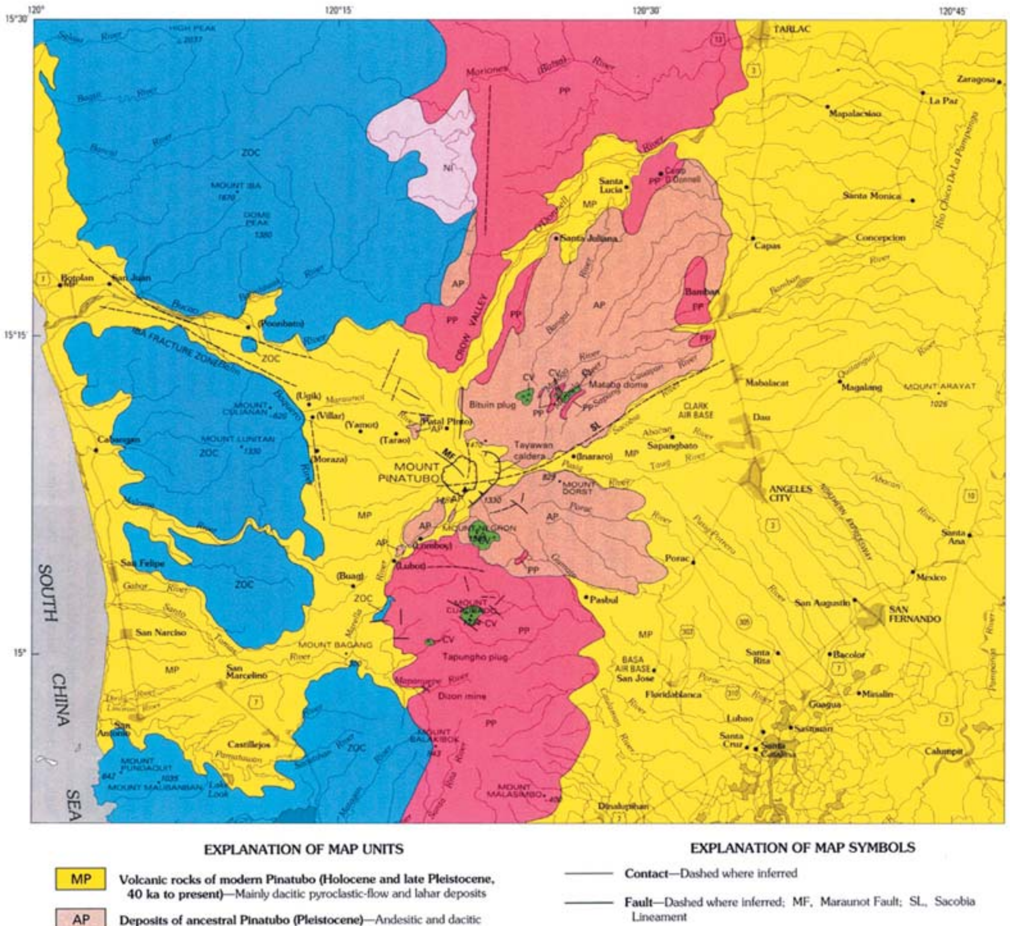

Fig. 24. Geologic map of Mt. Pinatubo and vicinity. From Newhall et al. (1996).

dip-slip faults (Figs. 23, 24). De Boer and others (1980) proposed the existence of a major northwest-striking structure, the Iba Fracture Zone, passing beneath Mount Pinatubo, which manifests as the Maraunot Fault, the Dagsa Fault, and the northwest-southeast alignment of surface hydrothermal discharges on Mount Pinatubo (Delfin, 1983). Shorter and less dominant northeast- and east-trending faults cut the major structures without any apparent offset. These shorter and easterly trending faults are particularly well defined near the summit region of the volcano.

Ancestral Pinatubo

Ancestral Pinatubo was an andesite and dacite stratovolcano whose center was in roughly the same location as the modern Pinatubo. It was as high as 2,300 m from the projection of dip slopes upward from the existing terrain. A high-silica andesite intrusive on the east flank of Pinatubo (UTM 1675.7N, 220.5E) yielded a K-Ar age of 1.10±0.09 Ma (Ebasco Services, Inc., 1977). A similar age of 1.09±0.10 Ma (Bruinsma, 1983) was obtained from a hornblende andesite lava flow on the western slope of the volcano.

Ancestral Pinatubo is exposed in relict walls of an old 3.5 x 4.5-km caldera, recognized by Delfin (1983) and named the Tayawan Caldera (Fig. 24). Such size is expected from an eruption of 10 to 15 km^3 dense-rock equivalent (DRE) of magma (Newhall et al., 1996). Prominent points on the relict rim of that caldera include Mount Donald Macdonald (southeast caldera rim) and Mount Tayawan (north-northeast caldera rim). Several patches of high, erosion-resistant terrains outside that caldera (e.g., Mount Dorst) were part of the dip slopes of ancestral Pinatubo (Fig. 24). Lava flows on the caldera walls and rim are mostly two-pyroxene-hornblende andesite (augite + hypersthene ± hornblende ± biotite; plagioclase=An_{60}) and are interbedded with pyroclastic flows and near-vent fall breccias (Newhall et al., 1996). Lower on the volcano's flanks, deposits of ancestral Pinatubo are indurated, yellow-brown andesitic and dacitic breccias of mostly lahar origin. An andesitic debris-avalanche deposit exposed along the Sacobia valley east of the volcano may have been derived from the ancestral cone (Geronimo-Catane, 1994).

Deep erosion in the Sacobia, Porac, Marimla, and Porac River valleys, coupled with deep weathering and induration of its products, suggests that activity of the ancestral volcano ended several tens of thousands of years before the caldera-forming eruption and initial growth of the modern Pinatubo.

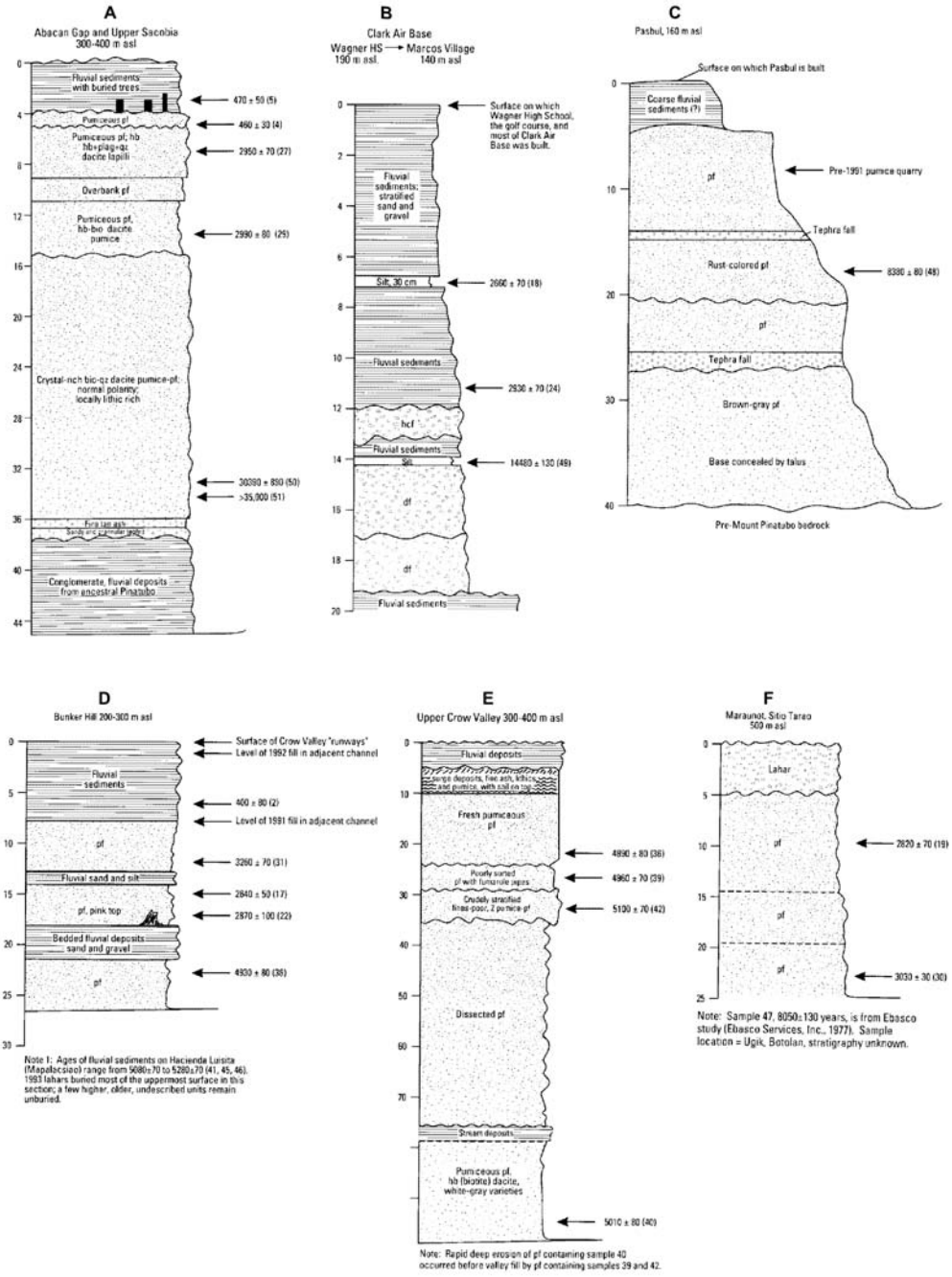

Fig. 25. Composite stratigraphic sections for major rivers of Mt. Pinatubo. (A) Upper Sacobia-Abacan River; (B) Sacobia-Bamban River; (C) Gumain River; (D) O' donnell River; (E) O' donnell River; and (F) Sacobia-Bamban River. Vertical scales are in meters. Modified from Newhall et al. (1996).

Modern Pinatubo

Modern Pinatubo is divided into six eruptive periods. They are: Inararo, Sacobia, Pasbul, Crow Valley, Maraunot, and Buag. The clustering of six eruptive periods for modern Pinatubo was based on radiocarbon ages obtained by Newhall et al. (1996). The samples were from the bark or outermost part of in-situ trees that were rooted in soil underlying the deposits. Each eruptive period is short in relation to intervening repose periods.

Most of the lithologic and tephrochronologic descriptions herein were referred from Newhall et al., 1996. Constructed composite sections from stratigraphic relations and ^{14}C ages of multiple outcrops are shown within the lettered boxes in Fig. 25.

1. Inararo Eruptive Period: >35,000 ^{14}C yBP

Occurring before 35,000 ^{14}C yBP, the Inararo Eruptive Period is known to be the largest eruption in the history of modern Pinatubo, depositing as much as 100 m-thick pumiceous pyroclastic-flow materials on all sides of Mount Pinatubo in the proximal parts of the Sacobia-Pasig-Potrero pyroclastic fan, north to northeast of Mount Dorst, and are buried beneath alluvium at their distal end, at least 21 km from Mount Pinatubo's summit.

The estimated original volume in the Sacobia-Pasig-Potrero fan is about 5 km^3 (bulk), assuming an average thickness of 30 m over an area of 160 km^2 of inferred deposits (Newhall et al., 1996). The 1991 deposits in the Sacobia-Pasig-Potrero system are about one-fifth of the total volume of 1991 pyroclastic-flow deposits, so assuming a similar azimuthal distribution then and now, the Inararo pyroclastic flows might have had a volume of 25 km^3. These deposits are now found as distinctively eroded "pinnacles," erosional remnants within a deep dendritic drainage network between the Abacan and Pasig-Potrero Rivers, between 100 and 500 m above sea level (Section A: Fig. 25).

The Inararo pyroclastic-flow deposit is incipiently welded and exhibits columnar jointing. The deposits contain pumice blocks of biotite-hornblende-quartz dacite with about 64-67 wt% silica. These deposits are distinguished from those of younger eruptive periods by the relative abundance of biotite and quartz phenocrysts, and the only occurrence of euhedral quartz in the Pinatubo sequence. Cummingtonite, present as rims on hornblende phenocrysts in some of the pumice blocks, indicates a pre-eruption magmatic temperature and pressure similar to those in the 1991 magma body. At least two separate pyroclastic-flow units are present within deposits of the Inararo eruptive period, evidenced by the absence of cummingtonite in pumice blocks from some outcrops, slight differences in weathering characteristics, and apparent onlap relations.

2. Sacobia Eruptive Period: ～17,000 yBP

The only known remnant speculated to belong to an eruptive period about 17,000 years ago is the outcrop of two pumiceous, hot(?) debris-flow deposits capped by a silt layer in the north bank of the Sacobia River opposite Clark Air Base (Section B: Fig. 25). These deposited debris-flows and their included pumice clasts closely resemble those of the 1991 eruption.

3. Pasbul Eruptive Period: ～9,000 yBP

Pyroclastic-flow and tephra-fall layers exposed along the road between Sitio Pasbul, Camias, Porac, and the Gumain River, including one pyroclastic-flow deposit with an age of 8380±80 ^{14}C yBP (Section C: Fig. 25), represent a large eruption that overtopped the southeastern rim of the Tayawan Caldera, and nearly or completely filled the valley of the Gumain River.

The dated pyroclastic-flow deposit near Pasbul contains two pumice types, a dominant hornblende plagioclase porphyritic dacite and a subordinate, gray, finer-grained pumice. Biotite occurs only as cores within hornblende phenocrysts, and relict olivine xenocrysts occur as rare cores within hornblende-magnetite reaction clots. Distinguishing features of deposits of the Pasbul eruptive period include a relatively low SiO_2 (63-64 wt%) and scarce quartz and biotite.

4. Crow Valley Eruptive Period: ～6,000-5,000 yBP

The most prominent exposures of major eruptions about 5,500 years ago are the deeply dissected pumiceous pyroclastic-flow deposits along both sides of upper Crow Valley, and upstream from Bunker Hill (Section D: Fig. 25).

Pyroclastic-flow deposits of the Crow Valley eruptive period within the O'Donnell River watershed covered an area of about 20 km^2 to an average depth of about 30 m, for a volume of about 0.6 km^3. The 1991 pyroclastic-flow deposits in the same watershed were about 0.3 km3, or 0.05 of the total 1991 pyroclastic-flow deposit. Assuming the same azimuthal distribution of deposits, the volume of Crow Valley pyroclastic-flow deposits had been about 12 km^3.

At least four thick pyroclastic flows separated by erosional unconformities were identified along Crow Valley and in small valleys just to its west. The two oldest units occur in dissected, topographically high deposits along the walls of the valley. The lower unit is a crudely stratified, 20-m-thick, fine grain-poor pyroclastic-flow deposit with abundant charcoal (Section E: Fig. 25). The upper unit, as much as 40 m thick, contains at least three pyroclastic-flow layers. Two additional pyroclastic-flow deposits are found topographically

below, but stratigraphically above the aforementioned 40-m-thick deposits, in recently eroded cuts into the valley floor. Of these, the lower unit yielded a ^{14}C age of 5,100±70 years (Section E: Fig. 25); the upper one is typically a massive, poorly sorted pyroclastic-flow deposit that yielded a ^{14}C age of 4,960±70 (Section E: Fig. 25).

Almost all pumice fragments sampled from deposits of the Crow Valley eruptive period are cummingtonite-bearing hornblende dacite. Cummingtonite occurs as relatively thick rims on hornblende phenocrysts with two subtypes; a phenocryst-rich white pumice and a phenocryst-poor gray pumice, occuring in deposits of the Sacobia and Pasbul. Both pumice types contain the same phenocryst minerals and are chemically similar, with 65-66 wt% SiO_2. The fine-grained gray type contains dominantly broken crystal fragments rather than the mostly intact phenocrysts seen in the coarser grained white samples.

5. Maraunot Eruptive Period: ～3,900(?)-2,300 yBP

A widespread, moderately well-preserved deposits of pyroclastic flows, lahars, and streamflows that have yielded ages from 3,590±110 to 2,330±110 ^{14}C yBP, or about 3,900-2,300 calendar yBP (Section F: Fig. 25), characterize the Maraunot eruptive period. Pyroclastic flows also traveled far down the O'Donnell, Sacobia, Abacan, Pasig-Potrero, and Marella Rivers.

About 3,000 yBP, a series of eruptions produced the largest known pyroclastic flows of the Marella drainage. During the same period, other pyroclastic flows filled the Sacobia valley to such a depth that lahars and fluvial sediments spilled onto and covered most of today's Clark Air Base. Bulk volume of deposits of the Maraunot eruptive period was roughly equal to that of the Crow Valley eruptive period, an estimated 10 to 15 km^3.

The dominant pumice type in deposits of this eruptive period is cummingtonite-bearing hornblende dacite. Most of the analyzed samples have about 65 wt% SiO_2. Dacite pumice fragments with mingled andesite bands are present in several pyroclastic-flow deposits of the Maraunot eruptive period; the andesite bands are finer grained and contain resorbed olivine xenocrysts rimmed by hornblende. Also as products of other eruptive periods, the dacite pumice occurs in two forms: a dominant, white, coarsely vesicular, and coarsely porphyritic pumice, and a subordinate, gray, finely vesicular, and finer grained pumice.

6. Buag Eruptive Period: ～500 yBP

Primary deposits of this period include a pumiceous pyroclastic-flow deposit high in the Sacobia drainage, a little-dissected lithic-rich pyroclastic-flow deposit in the Marella drainage, and little-dissected pyroclastic-surges or blast deposits in the O'Donnell and Bucao wa-

tersheds, near and beneath the village of Patal Pinto. From these three primary deposits, only the pumiceous unit yielded charcoal with an age of about 500 yBP.

Radiocarbon ages of pumiceous lahar deposits imply that explosive eruptions of this period began at least by 600 yBP and perhaps as early as 800 yBP.

During this period, lahars filled channels of the abovementioned rivers to levels equal to or slightly higher than the 1991 to 1993 fill. Because lahars of the Buag eruptive period filled the Abacan valley, eruption(s) of this period were approximately the same size as that of June 15, 1991.

A lahar deposit of the Buag eruptive period in the Pasig River drainage contains blocks of biotite-, cummingtonite-, and quartz-bearing 65 wt% SiO_2 dacite pumice. Cummingtonite is present as relatively thin rims on hornblende crystals. Quartz and biotite are relatively abundant in several of dacite samples of the Buag eruptive period. In contrast to the biotite- and quartz- rich samples of the Inararo period, quartz phenocrysts in the Buag samples are resorbed. Mafic inclusions and mingled dacite pumice blocks with dark olivine-augite bearing andesite bands and mafic inclusions are also present within this deposit. In contrast to the hybrid andesite of 1991, olivine crystals in samples of the Buag eruptive period lack hornblende reaction rims, their absence being suggestive of entrainment immediately prior to eruption.

The late-Buag summit dome from the undated but morphologically young lithic pyroclastic-flow deposit in the Marella valley, is a biotite- and quartz-bearing high-silica andesite (62 wt% SiO_2) with highly resorbed xenocrysts of olivine and augite (both rimmed by hornblende). This disequilibrium mineral assemblage suggests that the pre-1991 summit dome represents a mixed magma, possibly analogous to the mixed andesite lava dome that, in 1992, began to refill the 1991 caldera (Daag et al., 1996).

4.3.3 The 1991 Mt. Pinatubo eruption

At 1342H of 15 June 1991, after more than five centuries of repose, the Pinatubo climactic eruption began (Fig. 26A), lasted for nine hour, led to the collapse of the volcano's summit, and ultimately formed a 2.5-kilometer-diameter caldera (Fig. 26B) (Wolfe and Hoblitt, 1996). The gigantic plume rose to heights of more the 40 km before drifting to the South China Sea. Although Rosi and others (2001) claimed that the climactic eruption deposits were substantially derived from both Plinian and co-ignimbrite clouds, Dartevelle and others (2002) concluded that they originated from co-ignimbrite clouds through a giant ash cloud.

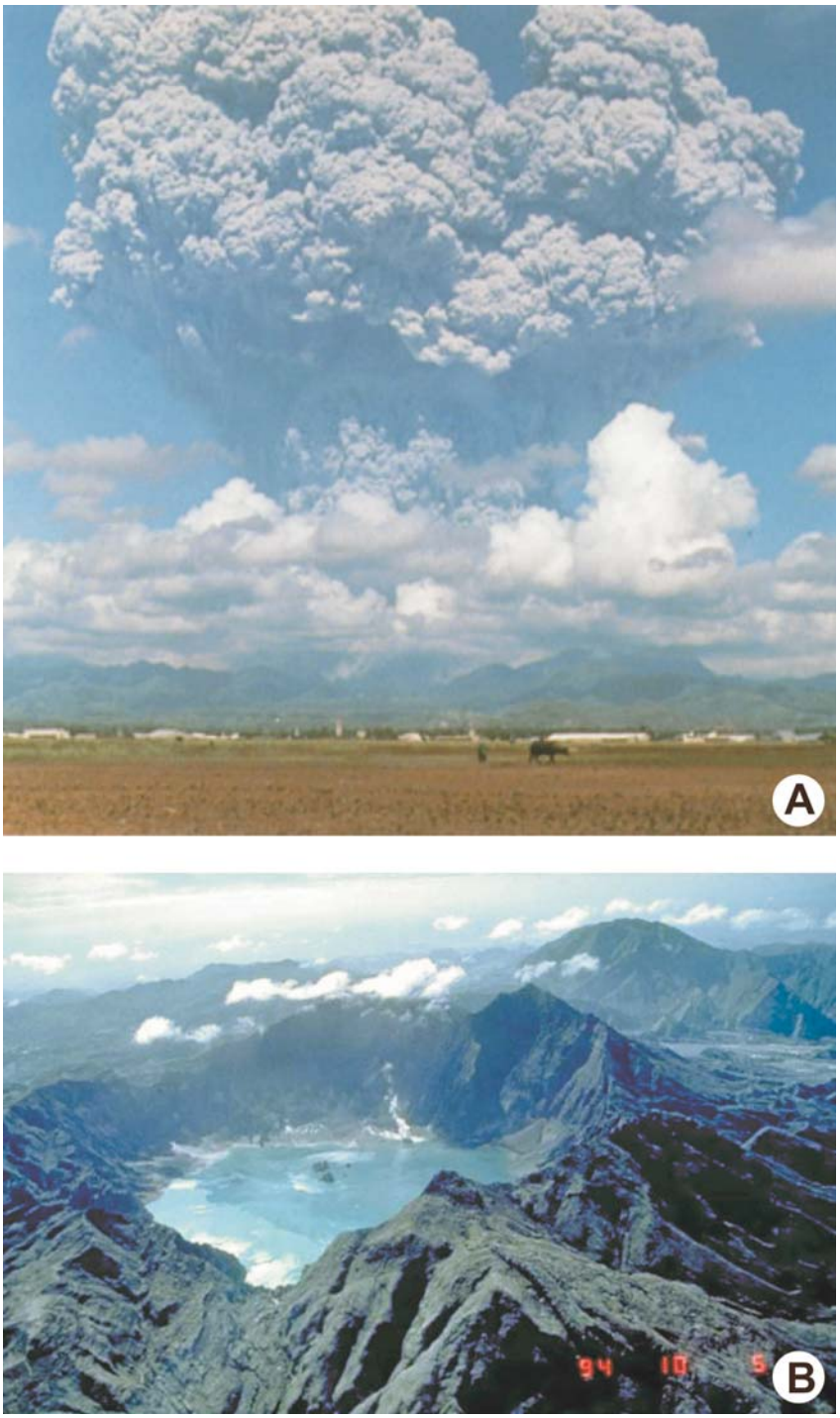

Fig. 26. (A) Giant ash cloud during the Mt. Pinatubo 12 June 1991 eruption. USGS Photo by D.H. Harlow, 1991: *In* Newhall and Punongbayan (1996); (B) Caldera resulting from the 15 June climactic eruption. From Punongbayan et al, (1996).

Estimated erupted magma is between 3.7 to 5.3 km^3 depositing 8.4 to 10.4 km^3 total bulk volume of ejecta composed of 5 to 6 km^3 ignimbrite (Scott et al., 1996) and 3.4 to 4.4 km^3 fall-out deposits (Paladio-Melosantos et al., 1996). Based on numerical models using remote sensing data, Holasek and others (1996) provided an estimate of 4.8-7.8 km^3 DRE. In a more recent study, Wiesner and others (2004) came up with a volume of 4.8-6.0 km^3 DRE on the basis of combined South China Sea deep-sea cores and on-land data.

Hoblitt and others (1996) divided the 1991 to 1992 Pinatubo eruption into eight phases as summarized in Table 6. Precursory activities were characterized by seismic swarms, intense steaming activity, and phreatic explosions that culminated about three months before the main eruption in June 1991. On 02 April 1991, vigorous steam vents opened on the upper north slope of the volcano. Steam jetted to heights of 300 to 800 m and sporadic ash emissions reached heights of 1,500 to 3,000 m. In late May, steaming intensified and amounts of ejected ash increased. By 09 June, continuous ash emission and occasional small explosions produced ash clouds dense enough to flow slowly down the volcano's western slopes. A series of strong explosive eruptions began at 0851 on 12 June 1991, and, starting at 2218 on 14 June, the eruptions slowly became more frequent and culminated in the violent climactic eruption of 15 June (Sabit et al., 1996).

Table 6. Mt. Pinatubo 1991-1992 eruption chronology. Modified from Hoblitt et al. (1996).

Phase	Duration/Date	Description
1991 Eurption Phases		
Phase I	March 15 - 31	Felt earthquakes beginning on March 15, phreatic explosions on April 2, continuing emission of steam and minor ash, constant release of seismic energy, and generally increasing SiO_2 emission.
Phase II	June 1 - 7	Escalating seismic-energy release, concentration of shallow earthquake hypocenters beneath Pinatubo's summit, diminution in SiO emission, inflationary tilt, and increasing ash emission culminating in birth of a lava dome on June 7.
Phase III	June 7 - 12	Dome growth, increasingly heavy emission of ash, escalating seismic-energy release.
Phase IV	June 12 - 14	Four vertical eruptions with minor pyroclastic flows, continued dome growth, and heavy emission of ash.
Phase V	June 14 - 15	Multiple surge-producing eruptions beginning at about 1516 on June 14 and continuing until the climactic phase.
Phase VI	June 15	The climactic phase of activity, beginning at 1342, consisting of a large vertical eruption with the production of voluminous pumiceous pyroclastic flows. This phase culminated in formation of a collapse caldera.
Phase VII	June 15 - early September	Postclimactic phase of activity wherein initially voluminous, continuous ash emissions slowly waned through the middle of late July; intermittent small ash eruptions continued until early September.
1992 Eruption Phase		
Phase VIII:	July - October	Growth of small dome of andesite lava

Caldera Formation

The collapse of Mount Pinatubo's edifice during its explosive eruptions on 15 June 1991, created a 2.5-kilometer wide caldera. By early September 1991, water accumulating through spring discharge from the walls of the caldera, rainfall, and surface runoff led to the formation of a caldera lake (Fig. 26B). From October 1991 to December 1992, the lake's pH dropped from 6 to 1.9. Lake temperature remained constant at 38±2°C during the same period (Campita et al., 1996).

A panoramic sketch by Newhall and others (1996) was made from photos taken from various points inside the caldera from October 1991 to November 1992. From vantage points inside the caldera, many of the units appear stratified, with little apparent dip and considerable lateral continuity, some stretching almost halfway around the caldera. Stratified units are locally cut by domes and many small faults.

Pyroclastic Flows

Scott and others (1996) provided the detailed characteristics and distribution of the 1991 pyroclastic flows. Pyroclastic flows of 15 June traveled as far as 12 to 16 km in all directions from the vent located near the head of Maraunot valley, about 1.3 km northwest of the old summit (Fig. 27). The estimated volume of pyroclastic-flow deposits during the climactic eruption is 5-6 km^3. These directly impacted an area of almost 400 km^2 and altered the landscape dramatically. In proximal areas, flows were highly erosive and left little deposits, whereas in medial and distal areas, valley fills and fans of ponded pyroclastic-flow deposits were thick and broad, forming veneers on ridges and uplands.

Identified pyroclastic flow deposits comprise three facies. First, and by far the most voluminous, are massive pumiceous deposits that form the valley fills and fans. Little evidence exists for individual flow or emplacement units except in some upland areas and near distal limits. Second are stratified pumiceous pyroclastic-flow deposits that veneer uplands in medial areas and consist of numerous beds several centimeters thick. Stratified deposits grade laterally into, and are therefore co-genetic with, massive pyroclastic-flow deposits. Third is a prominent lithic-rich facies formed of clasts of Pinatubo's former summit dome overlying, or interbedded in the upper parts of, pumiceous pyroclastic-flow deposits in medial areas of all major drainages.

Scott and others (1996) hypothesized that a large amount of lithic debris was created as the summit dome foundered. The collapse disrupted the vent and forced fragmenting pyro-

clastic material to escape through growing fractures and faults in the old summit dome. Large amounts of dome rocks were then entrained during this process. Some of the dense lithic materials settled through the flows near the vent and some traveled farther to form lithic-rich pyroclastic-flow deposits. The great bulk of these deposits are sandy and pumiceous. The minor and aerially restricted lithic-rich facies is composed of gravel-size, dense lithic clasts.

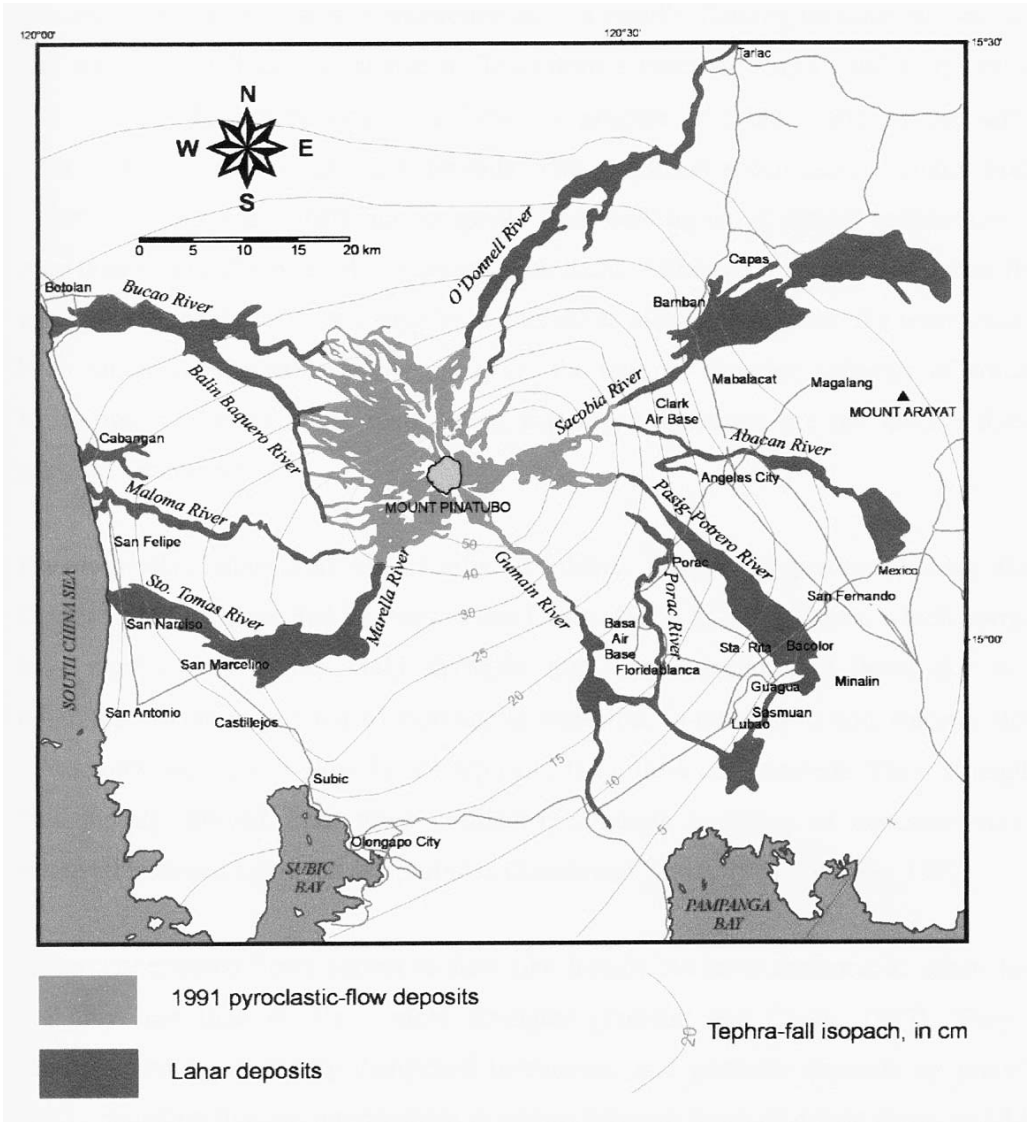

Fig. 27. Distribution of pyroclastic flow, lahar, and tephra deposits of the 1991 Pinatubo eruption by PHIVOLCS.

The asymmetric distribution of the pumiceous pyroclastic flows was controlled chiefly by the preexisting topography (Fig. 27). The June pyroclastic flows were able to spread out towards the western broad, lower relief terrain, consequently burying large parts of the preexisting landscape. Distal areas also contained broad, thick fills of up to 200 m of ponded pyroclastic flow deposits. In contrast, deposition towards the mountainous eastern sector occurred only in distal Sacobia and Pasig valleys and in several narrow canyons.

The thickest pumiceous pyroclastic-flow deposits occur in broad ponds that cover areas of 10 to 30 km^2 and bury former valley floors to depths of 100 to 200 m. Terraces and interfluves between the former valley floors have thinner, discontinuous accumulations. As a result, thick valley fills of pyroclastic-flow deposits blocked numerous tributaries to major drainages and created flooded or poorly drained areas, some of which became temporary lakes. Most lakes were shallow and short lived; many drained early in the rainy season of 1991 as they overflowed, and outlet channels were rapidly incised through poorly consolidated pyroclastic-flow deposits. Such events produced lahars (Pierson et al., 1996; Umbal and Rodolfo, 1996). Some lakes filled and drained repeatedly as secondary pyroclastic flows, generated by avalanching of thick pyroclastic-flow deposits (Torres et al., 1996), or lahars rebuilt blockages. Lakes and poorly drained areas in tributaries were also sites of secondary steam explosions driven by heated surface and shallow ground water; such areas were characterized by numerous craters with aprons of surge and fall deposits.

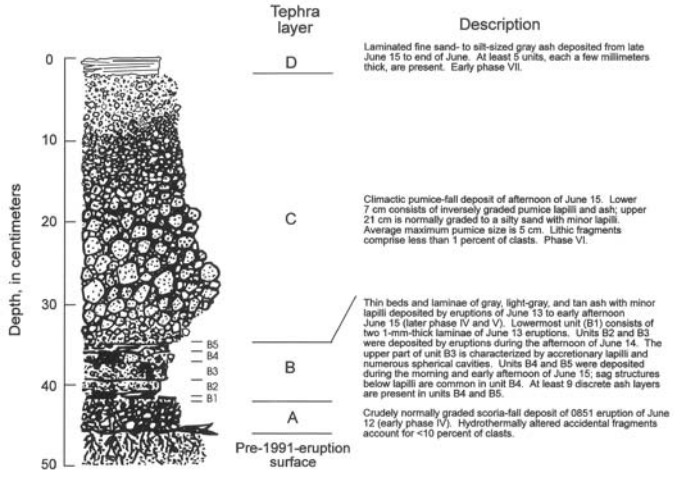

Fig. 28. Representative stratigraphic section of the 1991 tephra-fall deposits southwest of Mt. Pinatubo. Sketch of section located at Sitio Upper Kakilingan, San Marcelino, about 13 km south-southwest of the volcano. From Paladio-Melosantos et al. (1996).

Tephra Fall Deposits

The major eruptions of Mount Pinatubo is reflected in the stratigraphy of the fall deposits, which consists generally of a fine ash layer, a lapilli layer commonly including pumice grains of >1 cm in diameter, and a lapilli-bearing volcanic sand layer, in ascending order. The giant eruption cloud covered an area of 60,000 km^2 and expanded radially for five hours to an area more than 300,000 km^3 (Koyaguchi, 1996).

The stratigraphic section shown in Fig. 28 indicates the typical tephra-fall deposits of southwest of Mt. Pinatubo. The most voluminous deposit of the 1991 eruption is layer C (Fig. 28), composed of dacitic pumice-fall deposit with a bulk volume of about 3.4 to 4.4 km^3 (Paladio-Melosantos et al., 1996).

Each layer of the stratigraphic section was produced by an eruptive phase. Layer A was deposited during a brief explosive eruption on the morning of 12 June. Bulk volume is estimated at 14 M m^3 of andesitic scoria, ash, and some lithic fragments southwest of the volcano. The numerous pyroclastic-surge producing eruptions on 14 to 15 June emplaced about 0.17 km^3 of laminated, mostly fine-grained ash-fall deposits referred to as layer B. The wide dispersal of this layer was induced by ash clouds convecting upward from the pyroclastic surges that moved radially outward (>10 km) from the vent, and by the onset of low-altitude northerly to westerly winds as a tropical storm approached the area. Layer C, the most voluminous deposit, was produced during the climactic eruption on the afternoon of 15 June 1991 (Paladio-Melosantos et al., 1996). Most of Luzon Island and a 3 to 4 M km^3 area of Southeast Asia were affected by the tephra fall. Slowly reducing ash emissions continued from several vents in the caldera for about six weeks after the climactic eruption, depositing a fine-grained laminated tephra-fall layer D that has a bulk volume of about 0.2 km^3.

These Plinian fall deposits are relatively thin and inconspicuous partly due to the passing of Typhoon Yunya during the eruption, which spread the ash in all directions over a broad area. Near-source tephra were scoured by pyroclastic flows and the tephra along the main lobe was blown into South China Sea (Fig. 29).

The ash blown into South China Sea were dispersed in a southwesterly elongate lobe with inflection to west-northwest, reflecting both an upper-level wind field and the northeasterly moving Typhoon Yunya, during the climactic phase (Wiesner et al., 2004). Fully automated collection devices (sediment traps), designed to collect particulate matter settling through the water column for a designated period in a preprogrammed sequence, provided a rare opportunity to study the transport of ash in the water column. The sediment traps

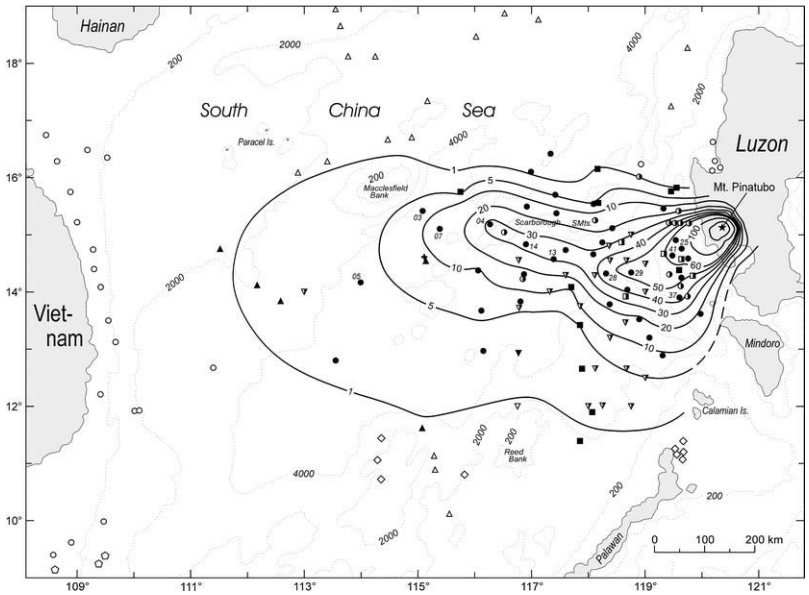

Fig. 29. Thickness contours (in mm) of the 15 June 1991 Mt. Pinatubo ash fall deposit in the South China Sea (isobaths in m) and on Luzon Island (unlabeled isopach is 200 mm). On-land thicknesses (layer C) were taken from Paladio-Melosantos et al. (1996) and E. Listanco (unpublished data, 1991). Marine core sites are denoted as follows: *circles* R/V Sonne cruises SO-132 in 1998 and SO-140 in 1999 triangles SO-95 in 1994 (Wiesner and Wang, 1996); *squares* SO-114 and R/V Ocean Researcher 1 cruise OR-455, both in 1996 (Kuhnt et al., 1996; Wiesner et al., 1997; Wang, 1999); pentagons SO-115 in 1996/1997 (Stattegger et al., 1997); *diamonds* 1997 cruises of R/V Explorer (F. Siringan, 1998); *inversed triangles* 1998 cruises of R/V Xiangyanghong-14 cross 1990-1992 sediment trap mooring station SCS-C (Wiesner et al., 1995). *Filled symbols* ash thickness measured; *half-filled symbols* ash observed, thickness not reliable due to core disturbance or postdepositional redistribution; *open symbols* no macroscopically visible ash. *Numbers* at core sites refer to those sections that were analyzed by sieving/pipetting. From Wiesner et al. (2004).

were attached to fixed mooring array at depths of 1,190 and 3,730 m and laid out in the South China Sea prior to the eruption. Within less than three days after the release of the major eruption plume, each of these traps simultaneously intercepted a total amount of 9 kg/m^2 of ash (Wiesner et al., 1995). On the basis of the mean grain density (2.34 g/cm^3) and average porosity (52.5%) of this material, the calculated depositional thickness is 0.8 cm at about 500 km from Pinatubo Volcano.

The tephra falls from the 15 June 1991 climactic eruption deposited a discrete layer on Luzon Island and across the South China Sea, covering an area of about 4×10^5 km^2 (Fig. 30) (Wiesner et al., 2004). The submarine facies consists of two units, a basal layer (Unit I), and

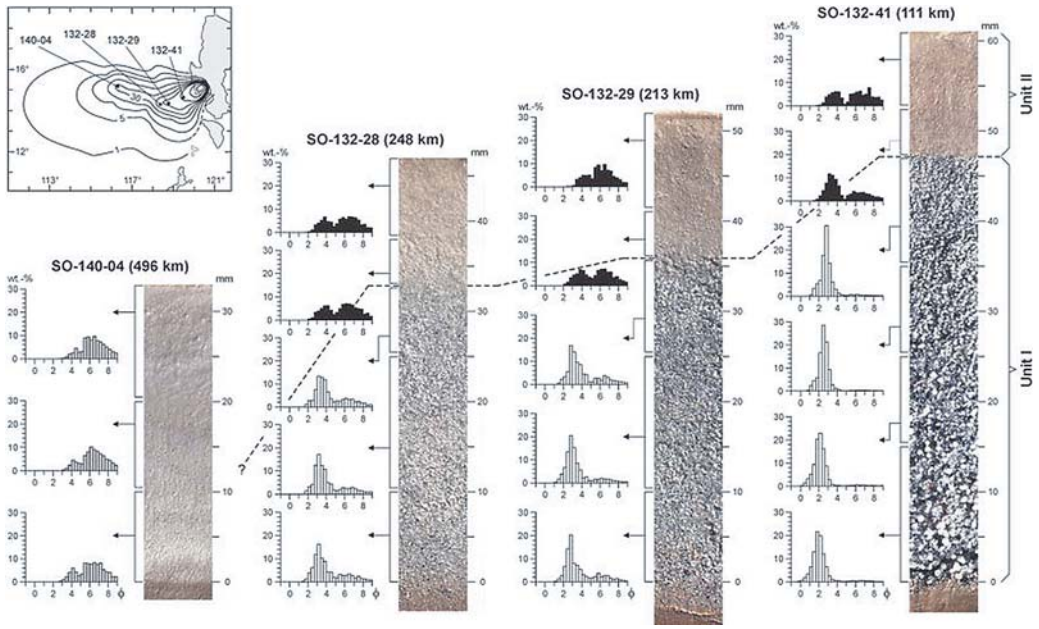

Fig. 30. Stratigraphy and grain size distributions of the submarine Mt. Pinatubo ash fall deposit in four representative cores downwind along the main dispersal axis (distance from source is given in *brackets*; see inset for core locations). *Open bars* unit I; *black bars* unit II; grey bars single ash layer. From Wiesner et al. (2004).

an upper layer (Unit II), separated from each other by a sharp contact. Unit I is a normally graded unit with unimodal grain size while the overlying Unit II is a finer-grained, structureless layer showing grain size bimodality. Unit I correlates with the subaerial tephra fall deposit, layer C, whereas the upper unit does not appear to have an on-land counterpart.

To explain the origin of the units, Wiesner and others (2004) proposed two distinct depositional processes. Unit I was deposited as discrete particles following Stokes' Law. The coarse-grained fraction of Unit II may have settled in the same manner as Unit I. However, to account for the short settling time for the fine-grained fraction of Unit II a separate mechanism was sought. Comparison of field data with earlier experimental observations and tephra flux records in the deep sea (Wiesner et al., 1995; Carey, 1997; McCool, 2002) suggests that fine ash was transported via vertical density currents (Wiesner et al., 2004). In spite of this, convection sedimentation did not affect the order of arrival of tephra onto the sea floor, allowing the preservation of the original stratigraphy. Atmospheric processes, rather than oceanic processes, largely determined the depositional mode of the tephra units in the South China Sea.

Lahars

East Side Lahars

The tropical climate of the Philippines provided ample rainfall to trigger lahars in all major watersheds east of Mt. Pinatubo. Alteration of watershed hydrology by volcanic deposits was also a necessary condition for the formation of these lahars. Disturbed catchment headwaters prior to the climactic eruption, played a key role in the formation of peak-discharge lahars, damaging vegetation, reduced infiltration capacity of the substrate, smoothened the natural relief of the hillslopes, and impacted channels along the mountain front from Porac River to Sacobia River (Major et al., 1996).

The total volume of volcaniclastic sediments deposited in 1991 in the east side basins is about 0.38 km^3, equivalent to about 30% of the total volume of 1991 pyroclastic source deposits in the upper basins (Pierson et al., 1996). Along the mountain front, peak flows were as deep as 6 m or more with instantaneous velocities of 6 m/s. In distal areas, peak flows were less than 1-3 m deep and mean peak flow velocities were less than 4 m/s (Major et al., 1996).

East side drainages have contributing catchment areas of 50-250 km^2. Typical post-eruption lahars were estimated to be 2-3 m deep, 20-50 m wide, and moved at 4-8 m/s. Peak discharges range about 200-1,200 m^3/s with flow durations of two to four hours (Pierson et al., 1996). In effect, sediment aggradation on the east side fans, ranging 0.5 to 5 m thick, caused rivers to avulse out of existing channels and spread deposition in broad, braided channels over large areas of countryside.

Worse than sediment aggradations, densely populated alluvial fans of Tarlac and Pampanga were heavily damaged by lahars that triggered lateral bank erosion and aggraded mainstream channels leading to backflooding of stream channels (Major et al., 1996).

Southwestern Lahars

The 1991 eruption of Mount Pinatubo deposited about 6 km^3 of pyroclastic debris on the volcano's slope, of which 1.3 km^3 was emplaced as the Marella Pyroclastic Fan covering 25 km^3 of the southwest sector (Umbal and Rodolfo, 1996). The fan is drained by the Marella River, along which numerous hot lahars, generated by intense monsoon rains from July to November 1991, transported about 185 M m^3 (14%) of the new pyroclastic-fan deposits downstream, and thus affected an area of 46 km^2.

Approximately 15-25% of the materials remaining in the new Marella Pyroclastic Fan will need to be remobilized before lahars aggrade the Marella-Santo Tomas channel to the

level of the highest prehistoric river terraces (Umbal and Rodolfo, 1996). Typically, sediment delivery rates are highest during the first few years after the eruption and are expected to decline exponentially over the next five to ten years. Typhoons delivering intense rain over the volcano, however, may modify this predicted schedule by generating lahars of catastrophic proportions.

Enhanced surface runoff from the tephra-fall- and pyroclastic-flow-impacted watershed, coupled with the steeper stream gradient of the Marella channel, enabled hot laharic debris flows and hyperconcentrated streamflows to block outflow from the Mapanuepe River. A bedrock constriction just below the confluence of these two rivers, created a backwater effect that promoted deposition from hyperconcentrated streamflows. Later, the constriction was repeatedly plugged by hot debris flows, which caused subsequent lahars to flow upstream and deposit in the Mapanuepe Valley. As each episode of lahar activity in the Marella waned, rising lake waters eventually overtopped and breached the debris dam and released floodwaters that bulked to hyperconcentrated streamflows by incorporating sediments from previous lahar deposits. At its maximum extent in 1991, the lake flooded an area of 6.7 km^2, and impounded an estimated 75 M m^3 of water.

4.3.4 Pinatubo Crater Lake Artificial Breaching − A Mitigation Measure

The 1991 cataclysmic eruption of Mt. Pinatubo resulted to the formation of a summit caldera of approximately 2.5 km in diameter, the lowest point of which is known as the Maraunot Notch, which drains into the Maraunot River on the northwest quadrant of the volcano. This topographic low will serve as the spillover point once lake level reaches this elevation. The Maraunot Notch and upper reaches of the Maraunot River coincide with the northwest-southeast trending Maraunot Fault related to the Iba Fracture Zone proposed by De Boer and others (1980).

Over the last decade, the crater has impounded water and has risen at a rate of 13.3 m/yr (Campita et al., 1996). PHIVOLCS has been closely monitoring the lake level rise since 1998. Also, Oxfam Great Britain (Oxfam GB), a non-government organization, commissioned a group of geologists to assess the hazards posed by the inevitable breakout of the Maraunot Notch.

The sole municipality that covers the flood path from the notch is Botolan, with a total population of more than 46,000. To put these residents out of danger, several mitigation measures were proposed to reduce the hazards posed by the Maraunot Notch breaching. Fir-

st, a monitoring and warning system must be put in place in order to alert people in case the notch is breached. On the engineering side, the controlled draining of the lake by a drain tunnel/canal, pumping or siphoning, or scraping and reinforcing the notch to allow water to spill harmlessly, would be the preferred measure.

PHIVOLCS and the Department of Public Works and Highways (DPWH) opted to construct the drain canal to induce an artificial breaching. DPWH started working on the notch on 17 August 2001, while evacuation procedures were implemented downstream. The breach was then opened at 6:53 a.m. of 06 September 2001. At the end of the day, the reported discharge was only 0.1 m^3/s. The plan for a deliberate triggering a large flood and lahar did not happen, since the excavators contracted by the DPWH did not leave the planned narrow plug at the lake edge, and that the slope of the canal was too low to induce rapid erosion of the notch.

A year later, presumably on 10 July 2002, the notch was breached. PHIVOLCS had reported peak lahars overtopping the Bucao Bridge and damaging Botolan's river spur dikes. Luckily, the breakout event caused no significant damage and casualty.

Chronology of Events Prior to Breaching

Accumulation of lakewater and spring discharge began as early as September 1991 (Campita et al., 1996). The catchment area of the caldera was calculated to be at 5.4 km^2, and lake area at notch elevation at approximately 3.0 km^2. On February 2001, a study made by undergraduate students from the University of Washington at Maraunot Notch revealed that it was made of loose, poorly consolidated pyroclastic breccia. About ten meters of the notch face was still exposed when the study was conducted.

PHIVOLCS began lake level measurements when freeboard (the remaining height of the dam) was at 45 m on 07 May 1998. Shown in Table 7 is the sequence of free-

Table 7. Freeboard measurements at Maraunot Notch from May 1998 to August 2001. From Rodolfo (2001).

Date	Freeboard (m)	Rise/day (cm/day)	Source
07-May-98	45.00		PHIVOLCS
27-Apr-99	27.00	5.1	PHIVOLCS
10-May-00	18.00	2.4	PHIVOLCS
28-Jun-00	16.00	4.1	PHIVOLCS
05-Aug-00	14.30	4.5	PHIVOLCS
16-Aug-00	14.10	1.8	PHIVOLCS
16-Sep-00	11.60	8.1	PHIVOLCS
13-Oct-00	11.35	0.9	PHIVOLCS
23-Nov-00	10.78	1.4	PHIVOLCS
27-Dec-00	10.33	1.9	PHIVOLCS
26-May-01	8.30	1.4	Oxfam-GB
27-Jun-01	6.50	5.6	PHIVOLCS
11-Jul-01	5.00	10.7	Nippon Koei
30-Jul-01	4.50	2.6	Oxfam-GB
30-Aug-01	2.00	8.1	Oxfam-GB

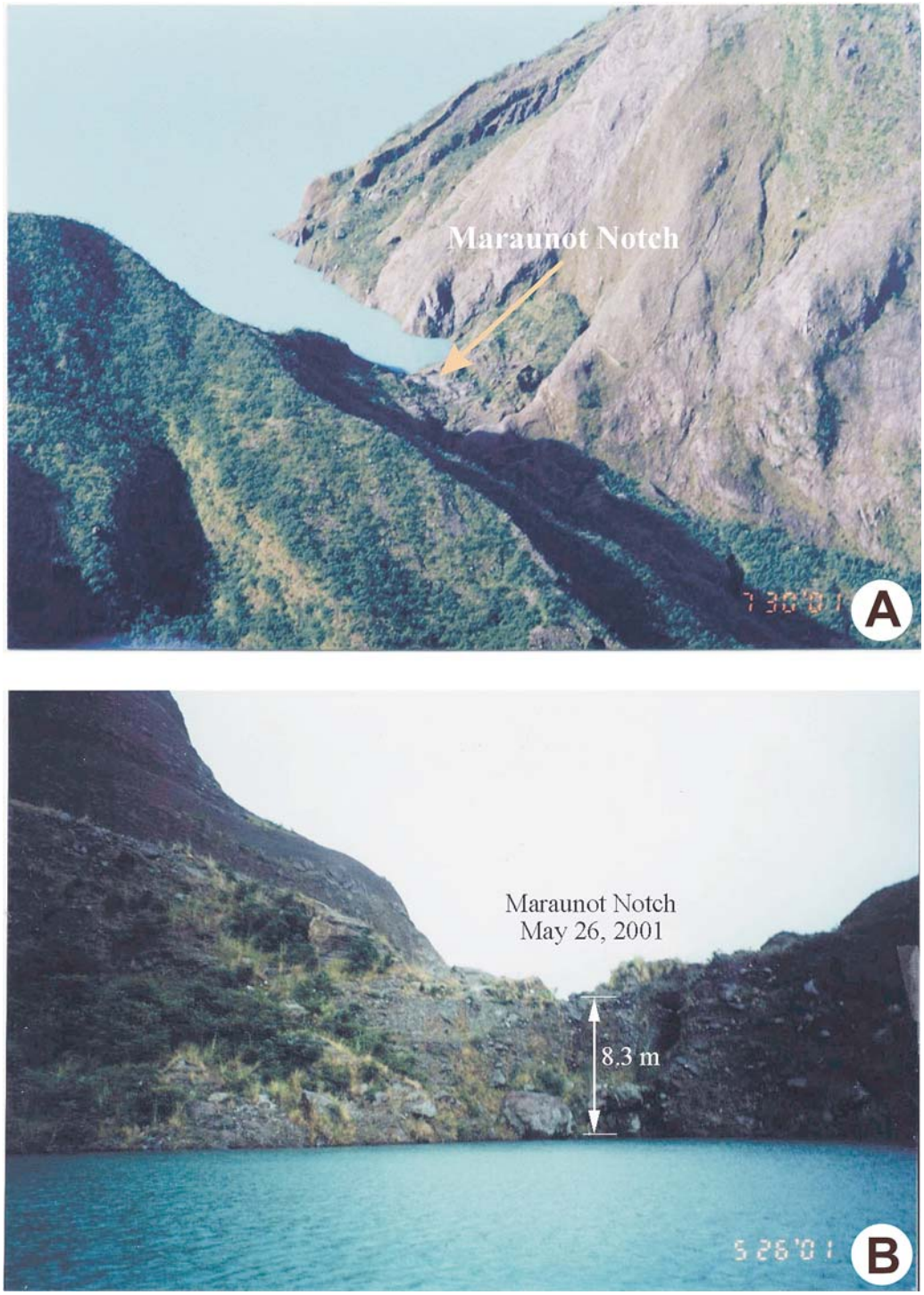

Fig. 31. Mt. Pinatubo summit caldera (A). Also shown is the Maraunot Notch (B). Photos taken on 26 May 2001 by Oxfam-GRT (2001).

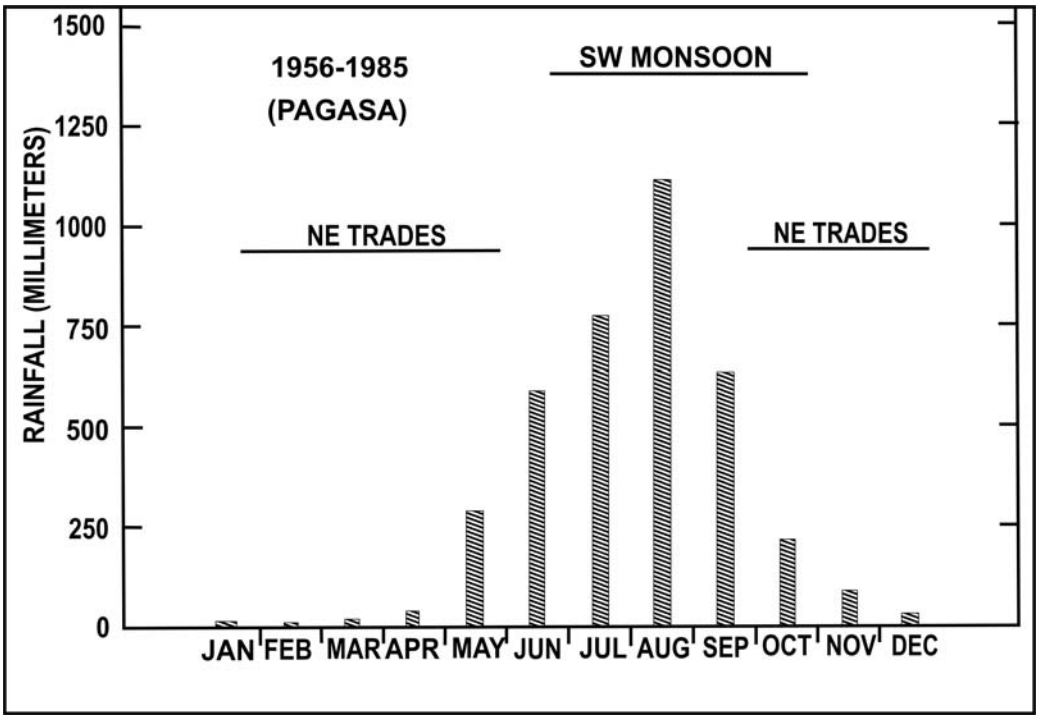

Fig. 32. Monthly average rainfall in Zambales based on data from PAGASA at Iba (1956-1985). From Rodolfo et al. (1996).

board measurements and rate of lake level rise since May 1998. Roughly a year, from May 1998 to April 1999, a lake level rise of 18 m was recorded. In about the same length of time from April 1999 to May 2000, an 8-m rise in lake level was recorded (Fig. 31). More frequent measurements taken in 2000 allowed for a better view of lake level rise during the southwest monsoon season. As shown in Table 7, lake level rise per day followed a similar pattern, with minor variations, on the months of May to September for the years 2000 and 2001. The monthly average rainfall indicates that during the month of August, Iba, the nearest rain gauging station to Mt. Pinatubo, experienced the highest amount of rainfall, causing maximum lake level rise (Fig. 32).

From 26 May to 30 August 2001, lake level rise averaged 1.2 m/mo. With a remaining freeboard of 2 m on 30 August 2001, it was expected that a breaching event would occur before 2001 ended.

Mitigation Measures/Engineering Intervention

Based on the general strength (erodability and level of compaction) of the notch, it will

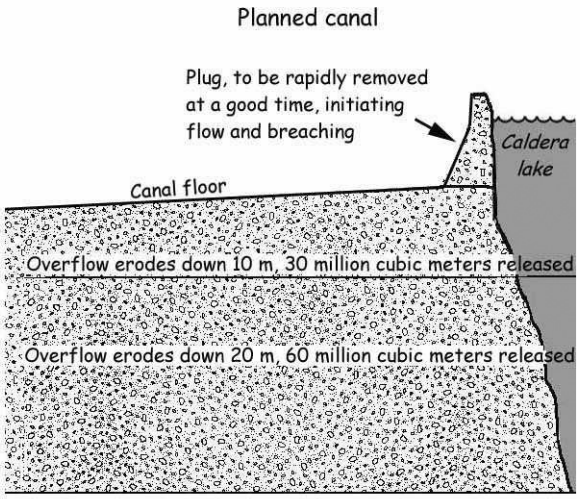

Fig. 33. The planned canal of Maraunot Notch. A narrow plug at the lake edge was proposed and will serve as the trigger for breaching. Also shown is the expected released lake water volume once overflow erodes down 10 or 20 m of the notch. From Rodolfo (2001).

be unable to remain intact once water begins to overtop, and will erode to a maximum depth of 20 m (Fig. 33). If this happens, a total of 60 M m^3 of water will be released (Bornas et al., 2001). It will then bulk up five times once it flows downstream, incorporating all materials that crosses its path. With this bulking up factor, a total of 300 M m^3 of a rapidly flowing mixture of rock debris and water would flow down to the Maraunot River, then to the Balin Baquero and Bucao Rivers, breaching the dikes and then wiping out barangays in Botolan, before finally exiting to South China Sea.

With such a worst-case scenario, evacuation plans were implemented to put at least 46,000 residents of Botolan out of the flood paths. People were gathered on topographically high areas where they can be safe from consequent lahar/flood inundation.

06 September 2001 Artificial Breaching

To prevent a deadly deluge on the town of Botolan, workers (primarily Aetas) with high-pressure water hoses, started blasting the notch on 17 August 2001 (Fig. 34). On 30 August 2001, Oxfam GB-commissioned geologists discovered that the diggers did not leave the planned narrow plug at the lake edge.

At first, the canal was intended to reduce the size of a possible flood. Since the canal was dug much too late when lake water was already close to spilling, it was then planned to

Fig. 34. (Top) Oblique photo of the Maraunot trench looking northeast, taken before unplugging day. Top righthand inset shows the mouth on 01 September 2001, about 2 m above lake level; bottom lefthand inset is the profile of the trench. (Right) View of the mouth of the terraced inner geometry of the trench, 06 September 2001. From PHIVOLCS: *In* Bornas and the Quick Response Team (2001).

deliberately trigger a large flood and lahar, at a specific time when people have evacuated already. On 06 September 2001, the notch was opened at 6:53 a.m. with a water discharge of only 0.1 m^3/s. Apparently, the slope of the constructed canal was too low to induce rapid erosion.

10 July 2002 Natural Breaching

A PHIVOLCS Quick Response Team (PHIVOLCS-QRT) sent to the Pinatubo area observed hyperconcentrated flows (HCF; "dilute lahars") to muddy stream flows (Bornas et al., 2002) and debris flows (Rodolfo, 2003, pers. comm.) in several channels in Pampanga and Zambales, on 10 and 11 July 2002. Peak lahars reportedly overtopped the Bucao Bridge in

Fig. 35. The Mt. Pinatubo crater lake after the 10 July 2002 breakout. A lake drop is evident from the distinet high-water mark circumscribing the crater walls. The high-water mark (yellow arrows) represents the crater lake level prior to breakout and lowering and is distinguished by the lack of vegetation at the crater walls. Photo by PHIVOLCS (2002).

Botolan, Zambales between 1030H and 1100H of 10 July, prompting local officials to close it until noon. Peak lahars also damaged Botolan's spur dike and nearly overtopped its principal dike at San Juan. PHIVOLCS team confirmed that the peak dilute lahars experienced along Bucao on 10 July were in fact triggered by a massive breach at the Maraunot Notch. Approximately 65 M m^3 of lake water (Bornas et al., 2002) drained through the breach, as deduced from lake level drop indicated by a distinct high water mark circumscribing the crater walls (Fig. 35). The measured lake level drop was 23 m. The lake level drop also led to the resurfacing of talus fans at active landslide sites around the crater. Downstream, the breakout flood generated 160 M m^3 of lahars, remobilizing loose materials along the contiguous Maraunot, Balin-Baquero, and Bucao Rivers. Consequently, the produced lahars buried the entire 50-km^2 river valley with sediments three to five meters thick (Bornas et al., 2002).

A survey of the Maraunot Notch confirmed that it has been breached down to bedrock or dacite formation. Specific observations at the Maraunot Notch are summarized as follows (Bornas et al., 2002):

1. All breccia and ash comprising the eroded channel dam have been removed, such that the notch valley is now wholly comprised of bedrock (dacitic dome rock).
2. Lakedrop resulted in the lakeward movement of the shoreline by approximately 20 m.

3. The new outlet channel is approximately two to four meters wide in the first 20 m-reach before spreading 20 m to 30 m wide across a U-shaped valley. The width of the outlet channel at the mouth of the outlet was measured at 3.7 m. Observed discharge at the outlet was 2-4 m^3/sec, which is greater than the <1 m^3/sec discharge measured last 18 June 2002 (Fig. 36).

Fig. 36. Before (A) and after (B) view of the Maraunot Notch, taken 30 September 2001 and 02 August 2002, respectively. Note excavated breccia and ash dam in (A) has been eroded off the notch in (B). From PHIVOLCS: *In* Bornas et al., 2002.

4. Preliminary data from the PAG-ASA Iba Station indicated that potentially 740 mm of rain fell in the crater watershed from 1 to 9 July, contributing 4 M m^3 of water to the lake. An additional 121 mm of rain equivalent to 0.6 M m^3 fell on 10 July, the likely day of breaching.

5. Based on GIS calculations, approximately 65 M m^3 of lake water was released from

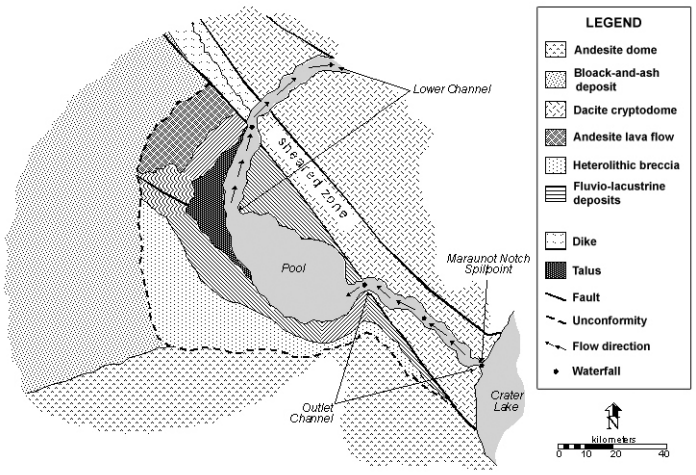

Fig. 37. Post-breakout geology of Maraunot Notch. From Bornas et al. 2002: *In* Catane et al., 2003.

Fig. 38. The Maraunot Fault exposed along the notch after the 10 July 2002 lake breakout. Photo by S. Catane.

the lake.

The 10 July 2002 lake-breakout lahars were sufficient to threaten inundation to Botolan (Bornas, 2002). With the presence of the drain canal constructed a year before, the rate of breaching, the volume of breakout lake water, and the magnitude of consequent lahars were greatly reduced (Bornas et al., 2002).

The breaching of the Maraunot Notch provided an opportunity for geologic mapping. Figure 37 shows the different lithologic units and the Maraunot Fault (Fig. 38).

4.3.5 Volcanic Hazards

The hazards related to Pinatubo Volcano eruptions include ashfall, pyroclastic flows, lahars, and crater-lake breakout. The apparent recurrence interval of explosive eruptions ranges from 500 to a few thousands of years. Lahar is considered as the most persistent hazard of Pinatubo Volcano. After the 1991 eruption, lahar activities prevailed for several years

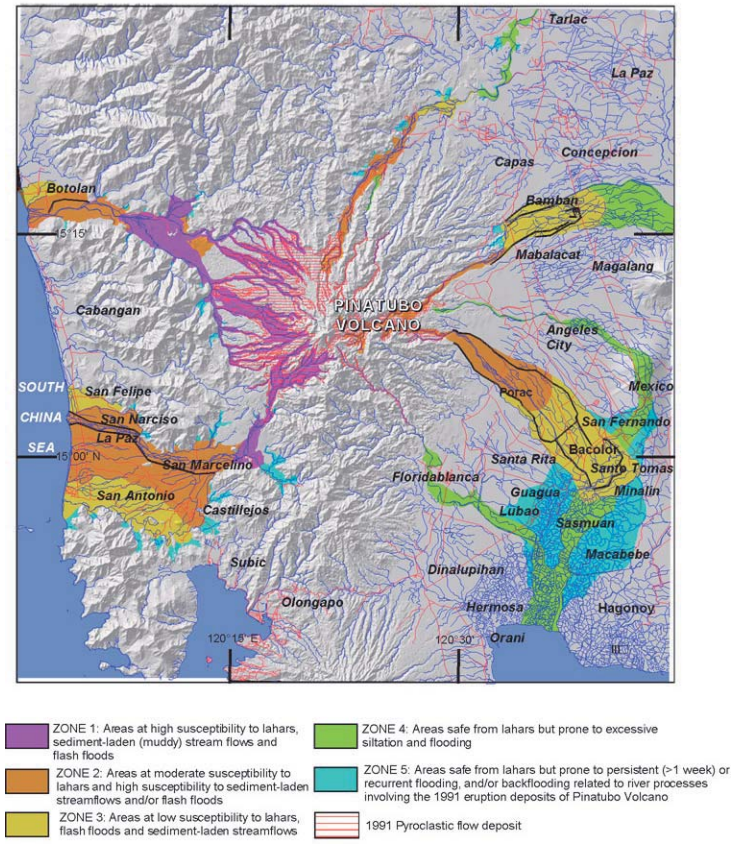

Fig. 39. Pinatubo Volcano hazard zones by PHIVOLCS as of February 2002.

until 1999 (Fig. 39). Some of the post-eruption lahars and floods were associated with the breakout of small temporary lakes formed by the damming of tributaries by 1991 pyroclastic-flow deposits at the upper slopes of the volcano.

Still-hot pyroclastic-flow deposits from the 1991 eruption were sources of secondary pyroclastic flows. They were generated by the collapse of channel walls due to lateral scouring, or secondary explosions related to rainwater infiltrating into the hot pyroclastic-flow deposits. Secondary pyroclastic flows persisted until 1996.

Another hazard, crater-lake breakout, has been recognized in association with the rising level of the caldera lake. Lake breaching on 10 July 2002 produced 160 M m^3 of lahars and damaged structures downstream. Renewed breaching may occur if: (1) blockage of the Maraunot Notch will occur anew; or (2) significant displacement occurs along the Maraunot fault (which coincides with the notch) in an event of an earthquake. Exposures of lake depos-

its along the crater walls suggest the existence of ancient crater lakes roughly in the same location as the present crater. This implies that Pinatubo has a cyclic history of lake formation and modification, either by draining or sedimentation. On the basis of crater-wall stratigraphy, lake sedimentation, crater breaching, dome intrusion, and faulting appear to be inherent in the Pinatubo crater evolution.

4.3.6 Volcano Monitoring

In the absence of historical eruptive activities of Pinatubo Volcano, no monitoring network was established prior to its 1991 eruption. Distant stations detected few earthquakes in the vicinity of Mount Pinatubo following the 7.8-magnitude Luzon earthquake of July 1990. On 02 April 1991, Pinatubo was reactivated from nearly five centuries of repose, with phreatic explosions and vigorous fumarolic activity. PHIVOLCS responded by setting up a temporary monitoring network, consisting of several analog and digital seismometers, in the village of Yamut in Botolan, Zambales (west side of Pinatubo) on 05 April 1991. The temporary station closely monitored the volcano's growing unrest. In May 1991, the Yamut station was transferred to Burgos and then to Poonbato. The temporary station was responsible for issuing daily updates and hazard warnings on the volcano's activity. As the volcano's unrest persistently increased, the Pinatubo Volcano Observatory (PVO) was established inside the Clark Airbase compound in Pampanga, with assistance from the U.S. Geological Survey's Volcano Crisis Assistance Team (VCAT). The first state-of-the-art seismic telemetry and ground deformation networks were set up, with Pinatubo Volcano Observatory as its central station. The seismic telemetry network was linked to computers for effective and rapid location of earthquakes. Other significant monitoring activities included gas studies using Correlation Spectrometer, and periodic aerial surveys. However, due to the difficulty and harsh environmental conditions in maintaining remote monitoring stations, the telemetry system was pulled out after Pinatubo Volcano's activity returned to quiet and normal conditions.

At present, there are two seismic stations: a vertical component seismic station at P12 high on the volcano's slopes, and the JICA Kelungi three-component seismic station at PVO. As of late 2001, there are no working rain gauges or AFM's. For ground deformation, occasional GPS recordings has been conducted jointly by M. Hamburger and PHIVOLCS. Most of the monitoring work since the 1991 eruption has been to track potential lahar and flood activities. Lake levels have been constantly monitored since 1998. Crater-lake breakout

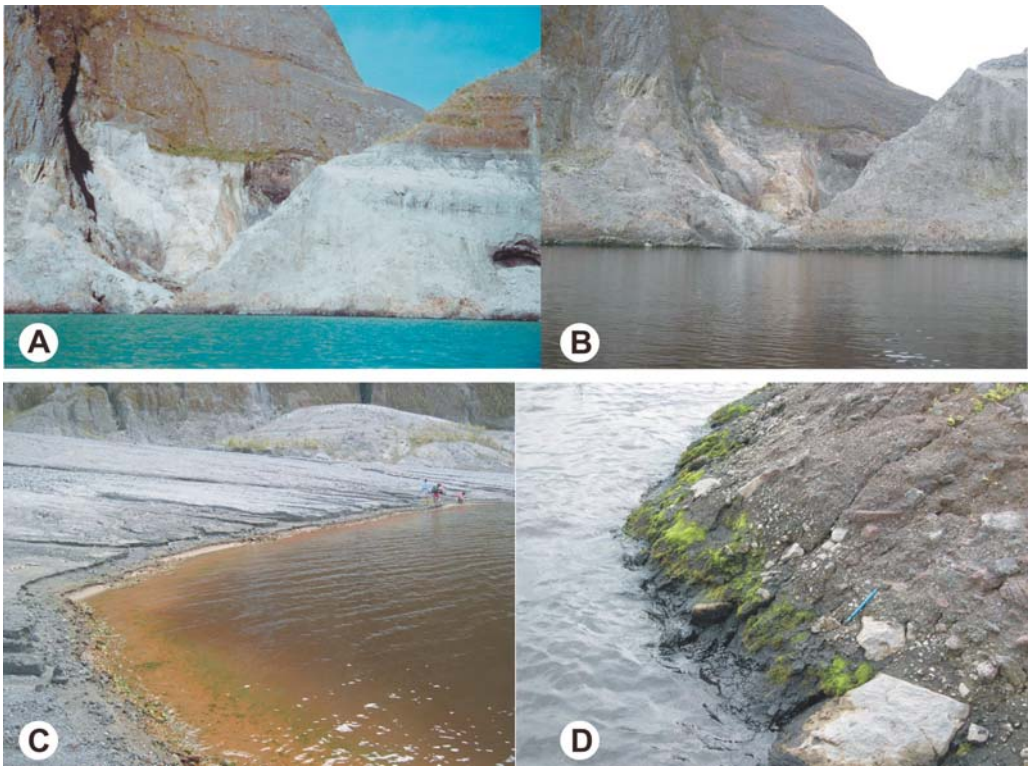

Fig. 40. Crater lake water color changes noted in January 2004. (A) Lake water had a bluish-green colour (photo taken on November 2003). (B) Lake water changed to brown to blackish color on Janauary 2004. (C) Brown precipitates along the lakeshore. (D) Algal growths on lakeshore rocks. Photos C and D were also taken on January 2004. From PHIVOLCS (28 September 2004).

at the Maraunot Notch on 10 July 2002 generated lahars and floods on the northwest side of the volcano. On January 2004, the previous emerald green crater-lake water color turned to brownish black (Fig. 40). The lake water's color, chemistry, possible biological activity, and their causes are currently being monitored and studied by PHIVOLCS and collaborating agencies. By May 2004, the water gradually shifted back to its original emerald green color (Mirabueno, 2005, pers. comm.).

4.4 Hibok-Hibok Volcano

4.4.1 Volcano Profile and Summary of Recent Activities

Hibok-Hibok (09° 12.2' N, 124° 40.5' E) is a 1,330-m high active composite volcano located at the northwestern end of Camiguin Island, an island province approximately 10 km off the

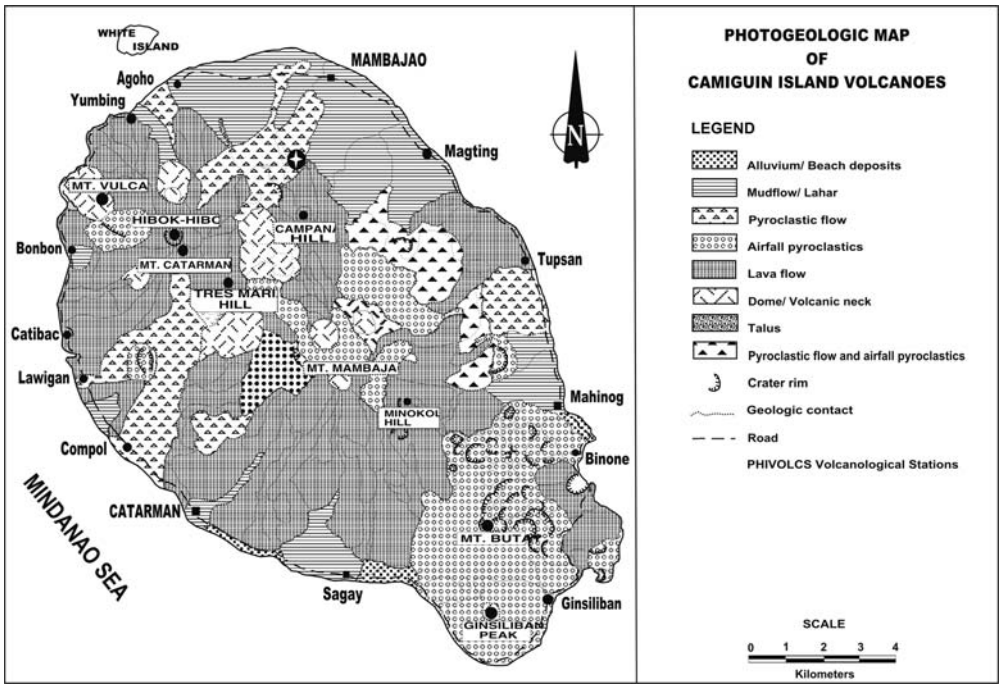

Fig. 41. Photogeologic map of Camiguin Island volcanoes. From PHIVOLCS (1991c).

north coast of Mindanao in southern Philippines. Camiguin is a volcano island consisting of other prominent volcanic centers that include Mt. Vulcan, Mt. Mambahao, Mt. Uhay and Ginsiliban Peak (Fig. 41). Of the five most prominent volcanoes in the island, Hibok-Hibok is at present, the only volcano manifesting activity. Its first recorded eruption occurred in 1827. It is not yet fully established whether the volcanism in Hibok-Hibok and the rest of volcanoes in the island is related to the currently active Philippine Trench (about 200 km to the east) or to an older volcanic arc, the Mindanao Central Cordillera (northern segment of the Sangihe Arc).

The most recent activity of Hibok-Hibok started in September 1948 and lasted until 1953 (Alcaraz et al., 1952). The most violent phase of the eruption occurred in December 1951 when pyroclastic flows (glowing avalanche or *nuee ardente*) rolled down swiftly toward Mambahao, the provincial capital. The eruption claimed about 500 lives (Alcaraz et al., 1952). The hurricane speeds and the high temperatures of the pyroclastic flows caused widespread damage to properties and structures on the north-northeast side of the volcano. A 1,280-high new dome at the summit marked the end of the 1948-1953 eruption. The violent eruption of Hibok-Hibok Volcano in 1951 led to the creation of the Commission on Volcanology, the predecessor

of PHIVOLCS, on June 1952, with the foremost objective of safeguarding life and property against volcanic eruptions.

The eruptions of Hibok-Hibok have been classified as Pelean, an eruption type considered to be very dangerous because it is characterized by explosive disruption of viscous lava dome and the formation of hot, swiftly moving pyroclastic flows. Both the 1871 and 1948-1953 eruptions followed this eruption style.

4.4.2 Evolution of Hibok-Hibok Volcano

Mt. Hibok-Hibok has a bare summit consisting of coherent and loose volcanic rocks. It has several small craters at or near its crest, some forming shallow lakes. Andesitic lava flows, which radiate outwards, predominantly constitute the summit area. Fallout deposits are also exposed on the summit and flanks of the volcano, while pyroclastic flows and lahars are found on its basal slope (PHIVOLCS, 1991c; PHIVOLCS, 1997). A 1,280-m high dome was formed during its most recent activity (1948-1953). Another 150-m wide unnamed crater, bounded by two 1,300-m high old domes, sits at Hibok-Hibok's summit. On the volcano's flanks are three other domes: Mt. Carling, Mt. Tibane and Piyakong Hill. On the northwest base of Hibok-Hibok is Mt. Vulcan, a volcanic dome that grew to a height of 671 m above sea level during the 1871-1874 eruptive period. Mt. Vulcan's base measures 1.4 km x 1.8 km. (PHIVOLCS, 1997).

Punongbayan and Solidum (In: PHIVOLCS, 1991c) proposed the evolution of Camiguin Island, including Hibok-Hibok Volcano, mainly on the basis of photogeologic interpretation. The sequence of evolution is summarized in Fig. 42 (A-I). They envisioned that volcanism started from the seafloor of Mindanao, continued build-up via submarine eruptions, until it emerged as an island (Fig. 42A). The volcano named Camiguin Tanda Volcano continued to grow subaerially by the piling up of lava and pyroclastic materials. Flank cones on its southeastern slopes, Mt. Butay and Guinsilaban Peak, were formed through phreatic eruptions (Fig. 42B, 42C). The activity of Guinsilaban appeared to have been short-lived. However, Mt. Butay continued on, through the ejection of pyroclastic materials from its central vent and flank eruptions, mostly monogenetic, although some with associated lava flows (Fig. 42D). Mt. Mambajao grew initially as a flank eruption on the southeastern slopes of Camiguin Tanda (Fig. 42E). Mt. Mambajao ejected mainly lava flows and domes and less pyroclastic materials. Dome building activities were significant in its growth and evolution (Fig. 42F).

Mt. Catarman started to build its cone at the northwestern flank of Camiguin Tanda,

when its southeastern half got almost fully covered by Mt. Mambajao (Fig. 42H). Mt. Catarman, through the effusion of lava flows and pyroclastic materials, and the formation of lava

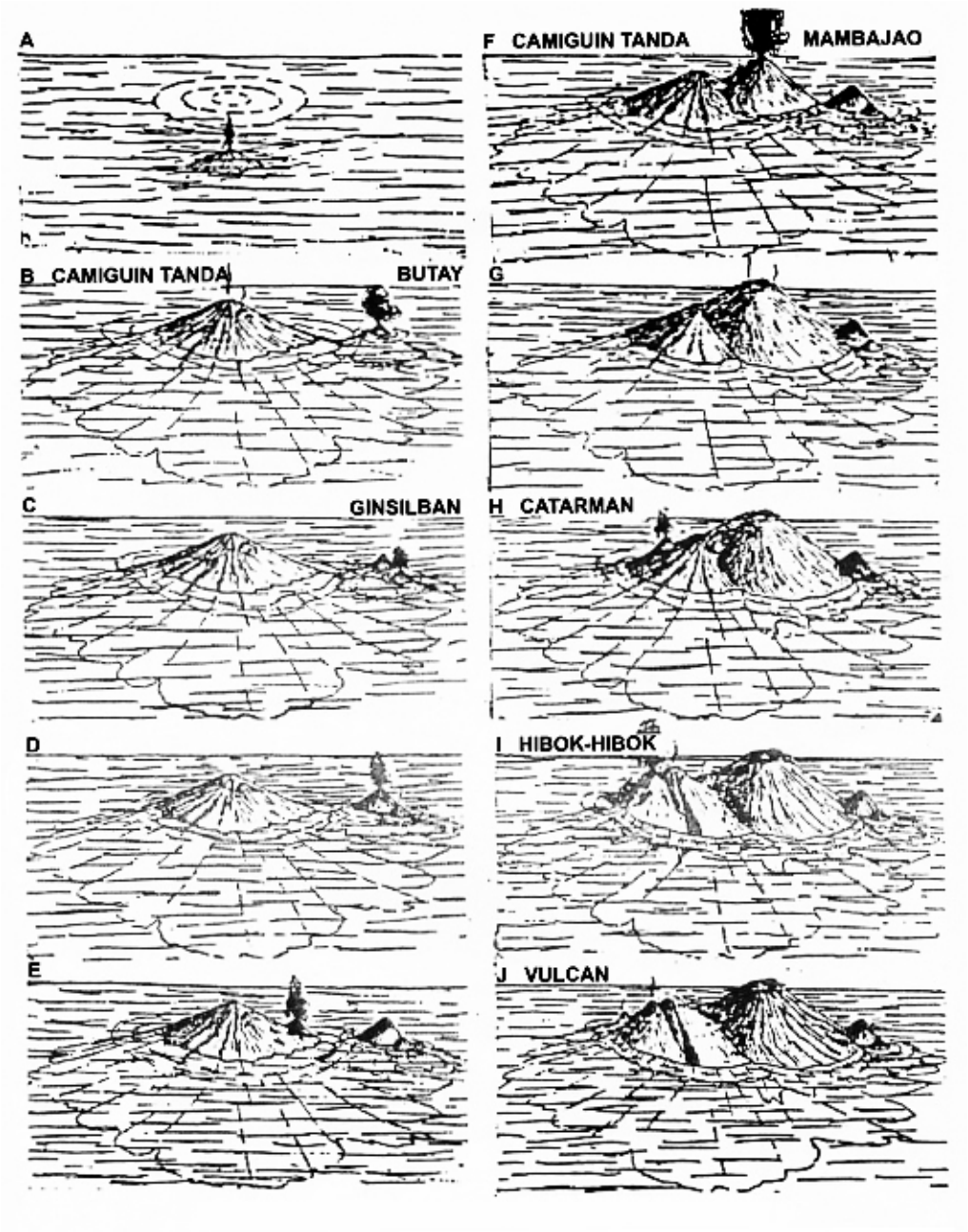

Fig. 42. Proposed evolution of Camiguin Island by R. Punongbayan and R. Solidum. From PHIVOLCS (1991c).

domes, buried almost completely the remaining northwestern half of Camiguin Tanda. Its subsequent activities shifted to its northwestern slope, to form the Mt. Hibok-Hibok (Fig. 42I). Hibok-Hibok Volcano continued to build-up by the ejection of lava and pyroclastic materials. A large lava dome, Mt. Vulcan, subsequently formed on its northwestern basal slope (Fig. 42J). Hibok-Hibok is the only active center in the entire Camiguin Island.

Despite the destruction brought by Hibok-Hibok's eruption in the early 1950s, Camiguin Island has flourished on its volcanic soils, the fertility of which has made the island suitable for the cultivation of coconut, copra, and other agricultural products. Camiguin is now a major copra producer in the region.

4.4.3 Historical Eruptions and Eruptive Patterns

There are no available written records of volcanic activities prior to 1871. The first reported eruption of Hibok-Hibok was in 1827, followed by a similar activity in 1862, which both caused destruction to agricultural lands. A Spanish friar, Sadera Maso, wrote a detailed description of the 1871 eruption and succeeding solfataric activities of Hibok-Hibok Volcano from 1897-1902 (PHIVOLCS, 1997).

The January－April 1871 event began with earthquakes and subterranean rumbling sounds on the north end of Camiguin Island. Earthquakes triggered landslides and fissuring, and destroyed trees and plantations. When the seismic activity ceased, an explosion occurred, veleasing gases, volcanic ash, and larger pyroclasts. A new crater was formed at the base of Hibok-Hibok, about 13.5 km to the southeast. The explosion completely destroyed everything within a 3-km radius from the new vent (PHIVOLCS, 1997). The eruption lasted for a week and a lava dome began to grow. For four years, lava dome building, with small, intermittent dome disruption, ensued, giving rise to Mt. Vulcan. Since then, Mt. Vulcan's activity has been limited to steam emissions from the crevices of its summit (PHIVOLCS, 1991c;PHIVOLCS, 1997).

In 1897, white sulfurous vapors issued out from the area occupied by the present dome (1948-1953) of Hibok-Hibok. This destroyed farmlands on the northeastern and southwestern slopes of the volcano. As described by Maso, a new solfataric vent was subsequently formed opposite the crest of the volcano, and solfataric activity continued up to 1902 (PHIVOLCS, 1997). Frequent subterranean sounds were noted during the activity, which lasted for 8-10 days.

The 1948-1953 eruptions

The most recent activity of Hibok-Hibok Volcano was preceded by tremors that started on 31 September 1948. On the next day, a violent explosion, accompanied by a strong earthquake occurred. A steam blast opened a crater (Kanangkaan) at the norhteastern slope of the volcano. Eruption clouds overwhelmed the town of Mambahao and adjacent areas.

On June 1949, steam blast eruptions of relatively weaker intensities occurred. A new extrusion of incandescent material from the crater area was observed to have flowed towards Barrio Itum, forming the Itum Flow adjacent to the Kanangkaan Flow. The cycle recurred in September 1950. On 15 September 1950, steam blasts similar to those in 1948 occurred. During the 1950 activity, the third blocky lava flow was formed, the Ilihan Flow, and then in December 1951 a fourth cycle took place (PHIVOLCS, 1991c).

On 04 December 1951, the steam blasts exceeded those in the earlier eruptive phase in intensity and destructiveness, and had temperatures much higher than in previous blasts. No attendant tremors or unusual crater activity were observed. The steam blast produced what has been referred to by volcanologists at that time as *nuee ardente* − a dense, boiling, heavily charged, ash-laden glowing cloud seen as cauliflower shaped cloud from a distance (PHIVOLCS, 1991). High-speed and high-temperature (estimated up to 800℃) pyroclastic flows rolled down swiftly toward Mambajao, causing widespread damage along their path. Trees were blown down and charred. Houses were burned down. Animals and people were either charred or mummified. The activity claimed about 500 lives and damaged hundreds of thousands of pesos worth of properties and structures (PHIVOLCS, 1997).

On 06 December 1951, 41 hours after the steam blast, a series of explosions in the crater area illuminated the volcano vicinity. Incandescent materials were emitted and a dense dark eruption cloud formed above the volcano, with strong electrical discharges. Activity shifted toward Itum, adding new extrusives to the 1949 Itum Flow (PHIVOLCS, 1991c). The 1948 to 1952 eruptions of Hibok-Hibok had three eruption sites. These were Kanangkaan Crater (1948), Itum Crater (1949), and Ilihan Crater (1950) (PHIVOLCS, 1997).

Alcaraz (1954) proposed that the 1948-1951 eruption of Hibok-Hibok followed a cycle consisting of four phases (Table 8): Phase 1- a short period of steam explosion and rock avalanches; Phase 2- explosions or steam blasts with a thick steam and ash cloud and high pyroclastic-flow generating possibility: Phase 3- the eruption of incandescent materials and large volumes of ash and steam, and formation of flows and occasional crater explosions; and Phase 4- decrease in the amount of steam and ejecta from the crater. From Phase 4, the

Table 8. Cycle of activities for the 1948-1953 Hibok-Hibok eruption. Modified from Alcaraz (1952).

Phase	Duration/Date	Activities
Phase I	Approximately on the last week of Aug. 1948	Emission of steam from the crater and rockfalls/slides of volcanic materials, with or without accompanying tremors.
Phase II (Main gas phase)		Explosions, or steam blasts, with release of heavy clouds, ashes and other volcanic fragments. Strong possibility of development of *nuee ardentes*
	01 Sept. 1948 5:00 PM	First steam blast - explosive outburst, with the extrusion of dense black cloud described as a cauliflower- or mushroom-shaped cloud that dissipated in about 0.5 hour.
		First lahar occurred simultaneously with or immediately after the initial blast.
	02 Sept. →	Two similar but weaker outbursts occurred.
	03 Sept. →	Intensity III earthquake followed by tremors of moderate intensity; two eruption clouds observed - one vertical, the other laterally directed to the south.
	04 Sept. →	Eruption clouds reached maximum heights, rising every 10 min. with increasing volume; sulfuric smell noted.
Phase III		Extrusion of incandescent materials; emission of ash-laden steam in large amounts; formation of block-and-ash flows and occasional minor crater outbursts.
	Possibly started on 04 Sept.	Increased frequency of rockfalls.
	On the evening of 04 Sept.	Crater glow was observed for 4 nights.
		Extrusion of blocky lava started after the initial steam blast of 01 Sept. 1948. Lava broke off from the crater area and cascaded down the volcano slope; lava broke further into smaller pieces as it hit protruding points or other obstacles. (This describes the generation of block-and-ash flows)
Phase IV	Could have started on 08 or 09 Sept.	Decrease in amount of steam and pyroclasts from the crater.
	09 - 10 Sept. →	Gas emission continued in Catarman main crater; at Hibok-Hibok, extrusion of viscous lava piled up to plug the crater; fumarolic activities prevailed.
		Kanangkaan lava flow was formed; moved at an average of 19.7 meters per day and reached a distance of 4.8 km; stopped upon encountering a spur of Mount Mambajao in April 1949.
		Build-up of a cone at the crater area to a height of 60 m.

activity can start again with Phase 1 and a cycle is completed in a period between 9 to 14 months.

4.4.4 Volcanic Hazards and Hazard Zones

Hazards posed by Hibok-Hibok's eruptions include tephra falls, pyroclastic flows (steam blasts, nuees ardentes or glowing avalanche), earthquakes, and lahars. Fissuring, subsidence, and tsunamis may likewise be triggered by volcanic eruptions. Figure 43 shows the hazard zonation map for pyroclastic flows and lateral blasts of Hibok-Hibok Volcano.

For Hibok-hibok, the area within a 3-km radius from the crater area is the Hibok-Hibok Restricted Area. It is considered a high danger zone because of its constant exposure to dan-

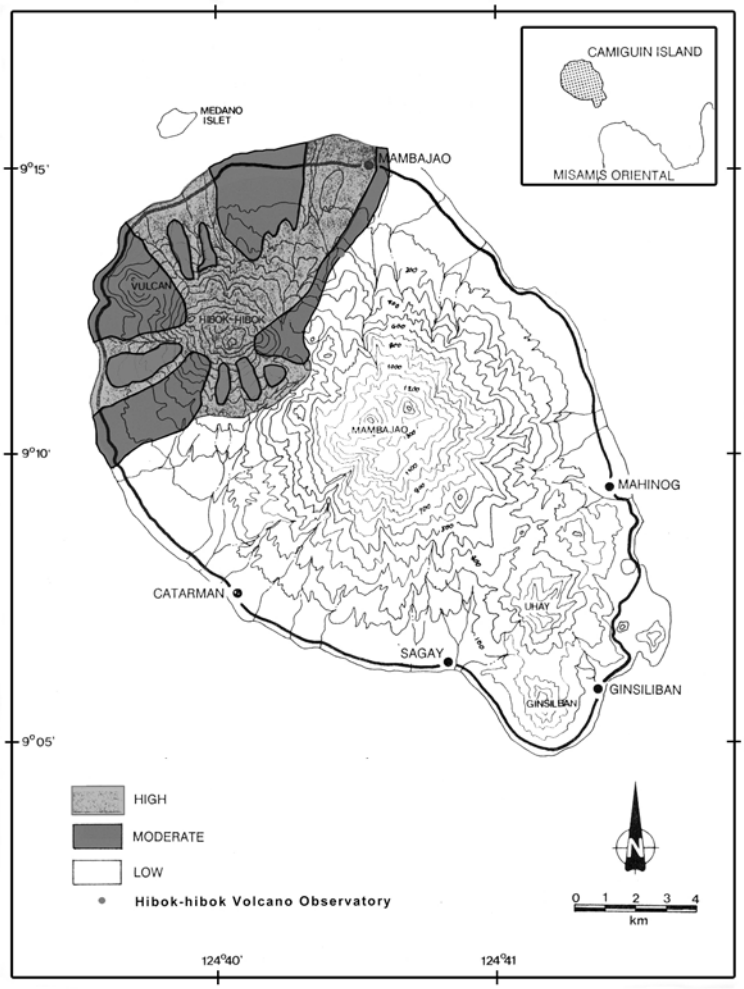

Fig. 43. Hazard zonation map for pyroclastic flows and lateral blasts of Hibok-Hibok Volcano. From PHIVOLCS (1997).

ger from landslides, lahars or gas emissions, even when the volcano is not in an eruptive state. Permanent human settlement is not allowed in this area. Also vulnerable is the Potentially Dangerous Area, which covers the entire portion of Camiguin Island, north of a line connecting the village of Tangaro in Catarman town and Tupsan village in Mambahao. People residing in this area have been advised by PHIVOLCS to be vigilant for signs of volcanic unrest and be prepared to evacuate in the event of renewed activity. The danger zone covers ten villages and the town center of Mambahao and 11 villages of Catarman. Around 21,000 people are living within the danger zone.

4.4.5 Volcano Monitoring and Eruption Precursors

Hibok-Hibok is one of the deadliest volcanoes, with more than 500 casualties in the latest eruption in 1948-1953. Since then, no sign of renewed activity has been noted. PHIVOLCS currently maintains a three-component Hosaka seismograph and watertube tiltmeter at Hibok-Hibok Volcano Observatory, 4.7 km from the summit. Ground deformation (EDM and precise levelling) surveys are conducted periodically to determine swelling or inflation of the volcanic edifice. Installation of sea gauges and additional levelling and EDM lines around the island are underway. Hotspring geochemistry is also being monitored.

Precursory signs such as localized earthquakes, crater glow, and others, preceded the past eruptions of Hibok-hibok. The following precursors were observed prior to Hibok-Hibok eruptions:

1. *Increased seismicity and rumbling*. Local earthquakes and volcanic tremors, some of which were felt, occurred several months before an eruption. These gradually, but progressively, increased in number and intensity as eruption approached. Some of these quakes were accompanied by subterranean rumbling sounds.
2. *Ground deformation*. In May 1949, a dome-like structure was extruded through the Itum crater. This later collapsed, probably due to lifting of earth materials around the base of the dome, resulting in the steepening of the slope (inflation or swelling) and consequent sliding. A 30-m long fissure was also observed on the northwest side of the summit crater.
3. *Increased steaming activity*. Moderate to strong emissions of steam were manifested most of the time prior to the eruption.
4. *Crater glow*. Based on the crater glow observed after 1952 eruption, it is expected that Hibok-Hibok will manifest crater glow, weeks or months prior to its eruption, as a result of magma migration to the surface.

4.5 Parker Volcano

4.5.1 Volcano Profile

Parker Volcano (6°6.8' N, 124°53.5' E) is a complex andesitic-dacitic composite cone located in the south-central Sarangani Region of Mindanao Island, southern Philippines. It belongs to the northern segment (Mindanao Central Cordillera Arc) of the Sangihe Volcanic Arc, a Quarternary volcanic chain running from Sulawesi, Indonesia to Central Mindanao. The summit of Parker Volcano is occupied by a 3-km diameter caldera, onto which the 2-km

wide Maughan Lake lies. Parker, locally known as *Falen*, is 1,784-m high and surrounded by extensive, youthful pyroclastic-flow deposits that suggest similarity to Pinatubo Volcano. Ga-ao River, on the northwest slope, drains the lake.

Because of the apparent absence of historical activity, Parker Volcano was unknown to most volcanologists until only recently. It is now known to be the site of a major explosive eruption in 1641 that was previously attributed to Awu Volcano on Sangihe Island, Indonesia (Delfin et al., 1997). The eruption was huge and caused darkness over the island of Mindanao. The 1641 eruption produced voluminous pyroclastic flows and lahars and resulted in the formation of the summit caldera. This was the last of the three major explosive eruptions from Parker during the last 3,800 years (Defin et al., 1997). Parker Volcano remains quiet since this eruption.

On 06 September 1995, the caldera wall breached and resulted in a disastrous flood that killed nearly 100 people on the northwestern slopes. About 30 M m^3 of lake water was released along Ga-ao and Allah Rivers, and resulted to a lake level drop of about 10 m (PHIVOLCS Quick Response Team, 1995). Floods destroyed 300 houses, nine bridges, and displaced about 50,000 people. High water discharge resulted in undercutting and destabilization of the river walls upstream of the Ga-ao Creek consequently forming several landslides along the channel. In the absence of evidence for renewed activity, PHIVOLCS concluded that the breaching was not, in anyway, associated with volcanic activity. The real cause of the breaching remains controversial and unresolved up to this date.

Only a month later, a large landslide dam was observed along Ga-ao creek. The lake level began to rise again in late 1995, resulting in a net lake level increase of more than 8 m as of January 2002. The dam did not collapse until 06 March 2002 when a Magnitude 6.8 (Ms) earthquake (Palimbang earthquake) jolted Mindanao, affecting the four provinces of Sarangani, South Cotabato, Sultan Kudarat, and Davao del Sur. The tremor induced a breach of the landslide dam at the crater outlet of Parker Volcano. The resulting floods damaged agricultural lands and communities along Ga-ao-Allah River floodplain, but no casualty was incurred. The 2002 Ga-ao Creek landslide dam breached and caused the lake level to drop by 9.1 meters, unleashing about 27 M m^3 of lake water (PHIVOLCS, 2002b). Emplaced deposits from the floods and debris flows were traced at least 80 km downstream of Ga-ao-Allah River.

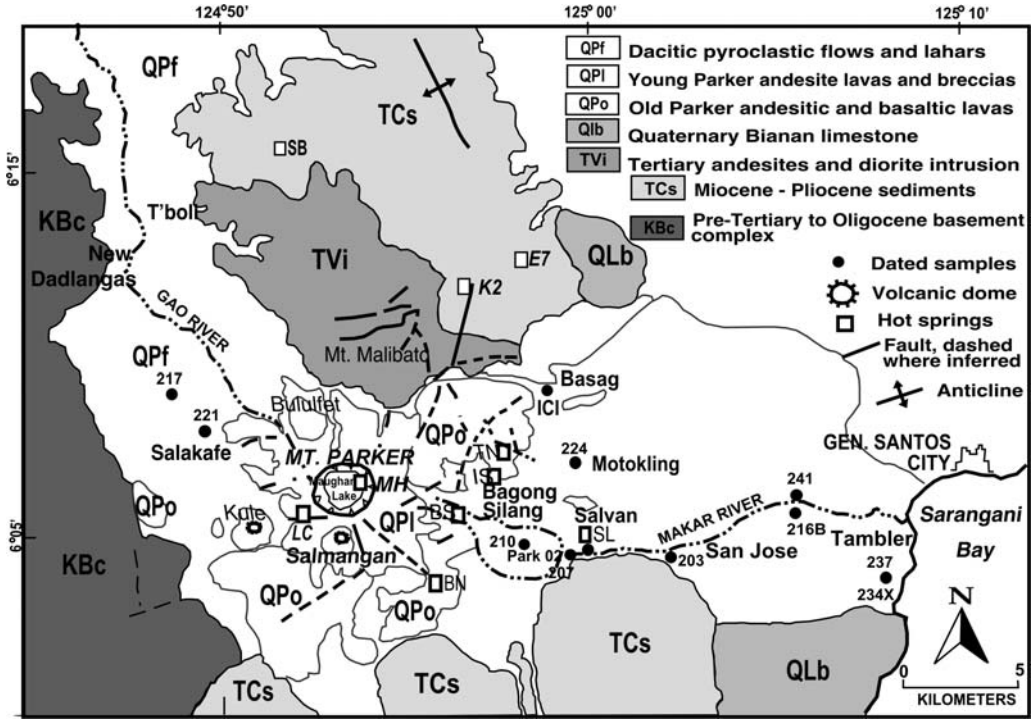

Fig. 44. Geologic map of Parker Volcano and vicinity. From Delfin et al. (1997).

4.5.2 Geology

Parker Volcanic Complex is part of a northerly trending arc of volcanoes in the Mindanao Central Cordillera Arc, which stretches from Hibok-Hibok Volcano to the north to Balut Island volcano to the south. Of the volcanoes along the arc, only the northernmost, Hibok-Hibok, in the island of Camiguin, is presently active.

Parker Volcano consists of a steep-sided cone with a 2.75 km x 2.9 km summit caldera, surrounded by an extensive apron of pyroclastic-flow and related deposits. The caldera floor is occupied by Lake Maughan, the water level of which lies at an elevation of 1,300 m. No hydrologic survey was ever conducted, thus the depth and morphology of the lake bottom is unknown. The lake's only outlet, and the caldera' s lowest point, is in the northwest, where it drains into the Ga-ao River.

Delfin and others (1997) described the geology of Parker as a volcanic cone composed largely of generally fresh hornblende andesite extrusives (QP1: Fig. 44). The predominant lithology is hornblende andesite lava flows, medium-K, and high silica (>60 wt%) (Table 9, Fig 45). Other units of QP1 include crystal lithic tuffs, tuff-breccias, and rare olivine basaltic

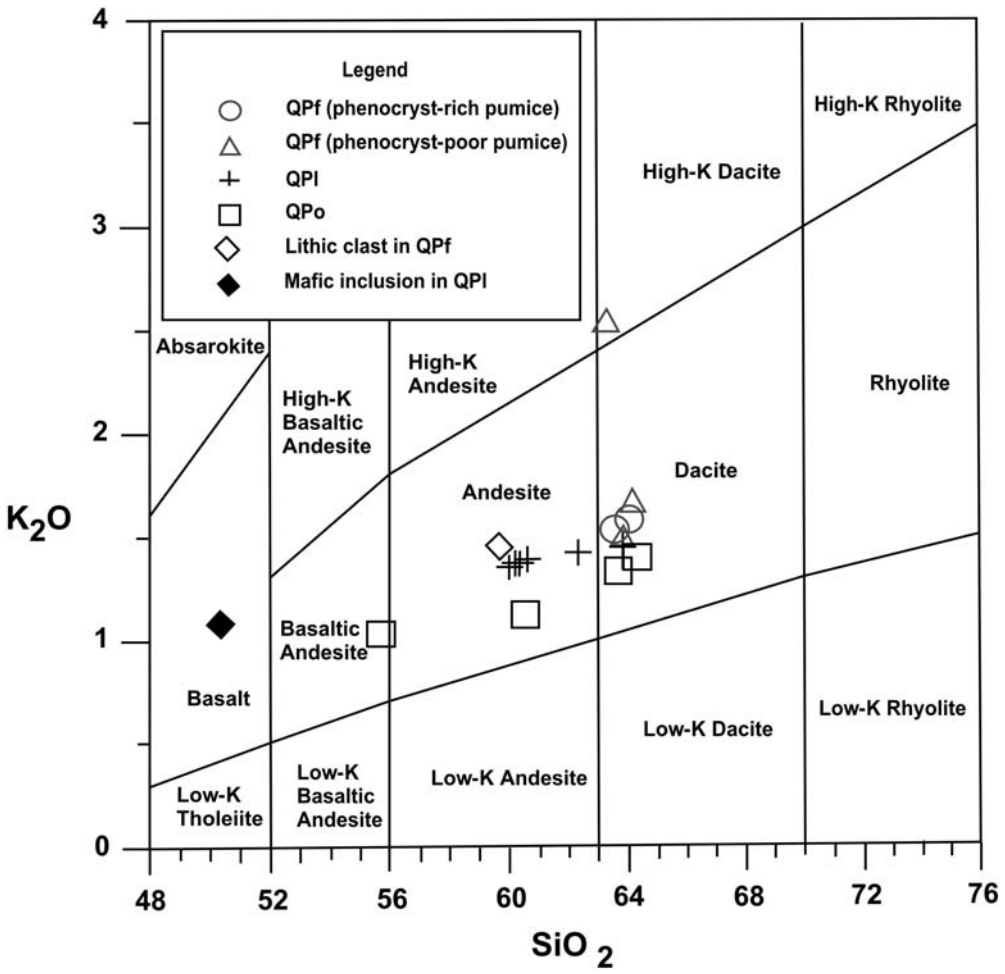

Fig. 45. K_2O vs. SiO_2 variation diagram for selected Parker rock samples. Delfin et al. (1997).

lavas. These deposits overlie an older sequence of the Quaternary Parker volcanics (QPo), whose remnants are expressed as topographically elevated terrain south and east of the Mt. Parker cone. The QPo deposits consist of altered andesitic lavas, breccias, and tuffs erupted from an ancestral Parker Volcano and outlying vents. Chemically, the QPo deposits range from basaltic andesite to dacite.

Extensive fans of pumiceous pyroclastic deposits and lahars (QPf) form the youngest deposits of Mt. Parker. They extend more than 20 km northwest, east, and south of the volcano. In the south, the pyroclastic flows crossed and draped over pre-existing topographic highs composed of QPo and TCs units. The pyroclastic-flow deposits are generally loosely

Table 9. Major element analyses of pumice, lithic fragments, and lava flows from Parker Volcano. From Delfin et al. (1997).

Sample name	SiO_2	TiO_2	Al_2O_3	Fe_2O_3	MnO	MgO	CaO	Na_2O	K_2O	P_2O_5	Sample Description
Maan - 3a*	63.55	0.48	16.43	4.48	0.09	2.88	5.90	4.51	1.53	0.16	Phenocryst-rich QPf pumice
Maan - 3b*	64.16	0.46	16.31	4.31	0.09	2.78	5.60	4.45	1.67	0.16	Phenocryst-poor QPf pumice
PAR 110	60.55	0.63	18.54	6.48	0.11	2.69	5.63	4.07	1.12	0.18	QPo lava from Bluhal Riv.
PAR 211a*	64.06	0.46	16.75	4.10	0.09	2.59	5.56	4.65	1.58	0.15	Phenocryst-rich QPf pumice
PAR 211b*	63.83	0.46	16.95	4.25	0.09	2.58	5.68	4.51	1.50	0.17	Phenocryst-poor QPf pumice
PAR 215*	59.74	0.60	16.10	5.84	0.10	4.71	6.99	4.28	1.45	0.21	Lithic clast in QPf
P93-INC	50.37	0.86	14.38	9.21	0.17	11.41	9.43	2.86	1.08	0.24	Mafic inclusion in QPl
P93-1a	63.83	0.54	17.85	3.58	0.07	2.50	5.47	4.50	1.45	0.20	QPl lava in crater lake
P93-1b	62.32	0.53	17.19	4.81	0.09	3.10	5.91	4.48	1.42	0.16	- do -
P93-2	60.61	0.56	16.66	5.26	0.11	4.09	6.41	4.74	1.39	0.17	QPl lava below crater rim
P93-3	60.20	0.59	17.42	5.57	0.12	3.08	6.92	4.50	1.37	0.22	QPl lava at crater rim
P93-3a	60.36	0.59	17.46	5.54	0.12	3.07	6.89	4.39	1.37	0.21	- do -
P93-4	60.03	0.58	17.47	5.54	0.12	3.41	6.84	4.43	1.35	0.22	QPl lava outside crater rim
P93-5	63.29	0.64	17.34	4.78	0.09	1.68	4.76	4.40	2.55	0.47	Phenocryst-poor QPf pumice
P93-6	55.71	0.71	16.31	7.10	0.14	6.58	8.29	3.88	1.03	0.24	QPo lava at Basag
P93-7	64.27	0.50	17.27	4.35	0.05	2.16	5.19	4.65	1.40	0.14	QPo lava west of Basag
P93-7a	64.35	0.50	17.29	4.27	0.05	2.14	5.15	4.72	1.39	0.14	- do -
P93-8	63.69	0.47	16.89	4.57	0.05	2.47	5.63	4.75	1.33	0.16	QPo lava southwest of Basag

*Analyses by Philipps PW 1404 X-ray fluorescence at Geological Survey of Japan by Y. Kawanabe.
All others done by P. Castillo and R. Solidum at Scripps Institution of Oceanography,
University of California, San Diego, CA, USA.

consolidated, massive, and poorly sorted. The pumice juvenile clasts are composed mainly of dacite, with minor hornblende andesite occurring as lithics. The eruption of voluminous pumiceous pyroclastic deposits of QPf has led to the formation of Mt. Parker's summit caldera (Bayon and Salonga, 1992).

Two pumice types are observed in the field: a phenocryst-rich variety, and a less abundant, finer-grained phenocryst-poor type. These two pumice types, however, differ only texturally as both have similar phenocryst assemblage and bulk rock composition (Table 9, Fig. 45). The phenocryst-rich variety contains 30-40% phenocrysts (0.8-1.1 mm size), while the phenocryst-poor pumices are so fragmental, that it is made up of only 5-10% phenocrysts (0.2 mm median size) by volume. Co-existence of two pumice types that is mineralogically and chemically similar, but texturally distinct, has been reported in the 1991 Mt. Pinatubo dacite (Bernard et al., 1996; Luhr and Melson, 1996; Pallister et al., 1996). The explosive fragmentation of crystals in pumice, particularly during the most explosive phases of climatic eruptions, is regarded to have been the principal mechanism of producing phenocryst-poor

Table 10. ^{14}C ages for Mt. Parker. From Delfin et al. (1997).

Sample name	Radiocarbon age (yBP)	Calendar age range (±1s)	Sample Location / Outcrop Description
PAR 237	27,790 ± 820	---	Tambler quarry, 28 aerial km SE of Parker / lahar deposit
PAR 234X	23,150 ± 310	---	About 3 m above PAR 237 / shell in beach sands
PAR 210	3,780 ± 35	---	Ridge above barrio Salvan, elev. 685 m / pumice-rich pyroclastic flow
PAR 221	585 ± 25	1318 - 1406 AD	Near barrio Salacafe, elev. 940 m / coarse pumice-bearing pyroclastic flow
PARK 02*	505 ± 90	1326 - 1445 AD	Makar river, elev. 495 m / massive pyroclastic flow
BASAG 1-C1	350 ± 30	1473 - 1629 AD	Near barrio Basag, elev. 560 m / massive pyroclastic-flow
PAR 204A	320 ± 35	1492 - 1641 AD	Road cut between Salvan and San Jose, elev. 500 m / masive pyrocastic-flow
PAR 241	320 ± 30	1494 - 1640 AD	Makar river north bank, elev. 140 m / 1m-thick lahar deposit
PAR 216B	315 ± 35	1494 - 1642 AD	Makar river near 'MC Village', elev. 150 m / 2 m-thick lahar deposit
PAR 207	305 ± 35	1516 - 1645 AD	Makar river, elev. 495 m / massive pyroclastic flow
PAR 203	205 ± 40	1651 - 1955 AD	Makar river, elev. 335 m, just below San Jose / pumiceous pyroclastic-flow
PAR 224A	205 + 50	1649 - 1955 AD	Road cut near Motokling, elev. 650 m / pyroclastic flow
PAR 224B	<200	---	Same as PAR 224A
PAR 217	<200	---	Road cut between Laconon and Salacafe / stream deposit below youngest lahar

* Sample analyzed at the Geochron Laboratories (Cambridge, Mass., Phil. Geoth. Inc., pers. comm., 1995). All other samples analyzed at US Geological Survey, Menlo Park.

pumice from the phenocryst-rich parent magma.

^{14}C ages for Mt. Parker volcanics are shown in Table 10. Four major radiocarbon-age groups were identified: 23-27 ka, 3.8 ka, ～600 ybp, and ～300 ybp (Delfin et al., 1997).

4.5.3 Historical Evidence for the 17th Century Eruption of Parker Volcano

Only a few volcanological works have been conducted at Parker Volcano because of the absence of historical eruption. Historical evidence using oral traditions and written records are supported by new ^{14}C ages obtained by Delfin and others (1997). The historical evidence that appeared in the Delfin and others (1997) paper is summarized herein. Translations of historical documents also by Delfin and others (1997), were kept in their original form.

Oral tradition

Stories referring to an eruption of Parker “many generations ago” were told by elders of the B’laan group, on the east slope of Parker Volcano, and two T’boli residents of Salacafe, on the northwest slope of Parker. They described the events as follows: a “torrent lake of fire”, falling of the great tree, and formation of the modern Lake Maughan. One storyteller related that the torrent of fire preceded the modern lake; another claimed that the lake

and the great tree were already in existence prior to the torrent of fire. The following are the accounts paraphrased by Delfin et al. (1997):

> "Long ago, a torrent swept the entire countryside, destroying and burning the forest, and leaving a lake of fire (*lanao lifo*). The torrent carried trees; the lake smelled of burning sulphur."
>
> "There once was a great tree in the middle of a forest where the lake now exists, and it was the stairway to heaven. One day, an evil man who was unfit for heaven tried to climb the tree but couldn't. In anger, he spent the next 40 years chopping down the tree and, when he finally succeeded, the formerly dry place filled with a lake and the land all around Parker was ravaged. Sampulan (or Sanggulan), a person-like god, lives by a large rock that can still be seen above the north side of the lake."
>
> "At around the same time as the *lanao lifo*, there was also on the T' boli side a "*katubo holon*", a (hot?) flood as if the dike of a fish pond has just been opened."

The terms used — *lanao lifo* in B' laan and *lanao ofi* in T' boli — refer to an event, the torrent of fire, or the result, a lake of fire, or both. Local residents do not consider this event a volcanic eruption and claimed that Parker has never erupted, but one storyteller referred to an explosion. Delfin and others (1997) interpreted the *lanao lifo* as pyroclastic flow(s) or fresh pyroclastic-flow deposits. Residents who have seen fragments of charcoal in the pyroclastic-flow deposits ("in the soil") believe that they are pieces of the great tree. The *katubo holon* refer to hot, rain-induced lahars that surely occurred, or to the sudden discharge of the lake. Holon refers to the caldera lake; *kayubo* implies growth (Delfin et al., 1997).

Written historical evidence

Delfin and others (1997) reviewed old historical documents and concluded that a giant eruption occurred in the Sarangani area of south Central Mindanao. Errors of date and place of the eruption must have been due to subsequent, second- and third-hand accounts. Among the documents, the best source is the account of Magisa (1641), who has written an account in the same year as the eruption. The original Spanish version of the following excerpt was translated to English and appeared in Delfin and others (1997):

> In the last days of December of 1640, ash fell strongly twice near the Presidio of Zam-

boanga of the Island of Mindanao, covering fields like a light hoar frost ... On January 3rd, at 7 p.m., we suddenly heard some noise about half a league distant, which created some concern in Zamboanga. It sounded like a musketry, and artillery ... On the following day, January 4th, by 9 a.m., the (supposed) artillery fire increased to such an extent that it was feared that the squadron (sent to investigate) might have run into some Dutch galleons. It lasted for about half an hour. People soon became convinced, however, that the noise originated from a volcano which had opened up, because by noon we saw a great darkness approaching from the south which gradually spread over the entire hemisphere ... By 1 p.m., we found ourselves in total night, and at 2 p.m. is such profound darkness that we could not see our hands before our eyes ... This darkness ... lasted until 2 a.m., when a little moonlight appeared, to the great relief of Spaniards and Indios who had had feared that they would be buried beneath the mass of ash which started to fall on them at 2 p.m.

A fleet was following the coast of Mindanao, headed for Ternate and was already close to Cape San Agustin, near an island called Sanguil, on which a volcano suddenly erupted. Darkness enveloped the fleet earlier than it did Zamboanga, for at 10 a.m., the ships found themselves in such deep darkness and terrible blackness, that they believed that Judgement Day to be at hand. It started raining so much rock, soil, and ash, that the ships considered themselves in grave danger and had to light the lanterns and quickly lighten the heavy load of soil and ash that was accumulating. They observed for sometime that on Sanguil Island, plumes and fiery columns rose rapidly into the sky, setting fire to the neighboring forests when descending.

The darkness spread over the greater part of said island, Mindanao, which is very large, and ash fell as far away as Cebu, Panay, and other surrounding islands. Especially, it fell on Jolo, which is probably more than forty leagues from Sanguil, where the volcano had erupted. There, on account of the darkness, people did not realize where (the ash) was coming from. Later, when it became light, they found that, not only had the first volcano in Mindanao and Sanguil (erupted), but that the elements had rebelled (in Jolo), too, and that a second volcano had erupted on a small island which is opposite the bar of the main river of Jolo, where our presidio is located. A great earthquake had opened the earth, and begun to hurl fire mixed with trees and large

> boulders. So great was the uproar and concussion of the elements that it reached from the bowels of the earth to the sea, vomiting, through the same mouth which had opened at the shore, large numbers of shells and other things from the sea floor. Today the mouth of this volcano remains open, is very large, and the entire outline of the island remains burnt.
>
> ... The latest and most extraordinary and wondrous miracle of this 4th day of January is the noise described in this letter, which commenced in the air between 9 and 10 a.m., and which was heard not only in Manila but also in the provinces of Ilocos and Cagayan, probably 140 leagues distant, as well as all in the Philippine Islands and the Moluccas. (The sound) went as far as the Asian mainland, including the kingdoms of Cochin-China, Champa, and Cambodia, as reported by several members of the clergy and other credible persons who came from these kingdoms to Manila. Within a circle of more than 300 leagues diameter and 900 leagues circumference, the sound was simultaneous and of equal loudness.

Delfin and others (1997) noted that succeeding authors repeated excerpts from Magisa and mentioned the existence of volcanoes in the area after Murillo Velarde (1734). An early on-the-ground reconnaissance was reported by Le Gentil de la Galaisiere (1779-1781), who wrote:

> The island of Mindanao also contains a number of volcanoes, which produce a great deal of sulphur. The King of Mindanao gets this substance from the ancient volcano of Sangil, the mines of which are inexhaustible, for each eruption of the volcano adds a new stratum of sulphur to the old deposit.
>
> In January, 1640 (sic), one of the mountains of Mindanao, situated in the territory of the King Buyaen, sixty leagues from Zamboanga, made a frightful noise and spread alarm and terror far and wide. The eruption was so violent that the summit was blown into the air and was carried by two leagues or more away ... different errors concerning the true place from which the sound of the explosion came were doubtless due to the echoes from the mountains of these Islands. But the truth soon became known in Zamboanga. The sky was completely overcast and the people were enveloped

in a darkness so obscure that they were obliged to have recourse to artificial light ... The mountain cast forth such vast quantities of ash, and it was carried to such a height that the wind was able to transport it to incredible distances, for it to fell on the distant parts of the Philippine archipelago, in the Spice Islands, in Borneo, and in Manila. Zamboanga suffered severely, and at the present time one may still see evidence of the damage in all parts of the town. Whenever a spade is stuck into the ground, volcanic ash is encountered.

... The destruction of that mountain formed a lake at its foot, the water of which was white for a long time thereafter, because of the great quantity of ash it contained; but finally this lake, through its overflow, carried away the ash so that at the present time its water is as clear as crystal.

The same eruption was also related by Perry (1860) in detail but added a new interpretation when he wrote:

... As for the (location), which we believed to be Sanguil, and was generally considered as being situated on Mindanao Island, is for us the volcano of Sanguir Island, which Fr. Nieremberg writes as Sanguiz, and which is found between Mindanao and Ternate.

In fact, ... all these circumstances of the (Nieremberg) report then coincide to make us identify in the Island called Sanguiz the present Island of Sanguir, where is found, in fact, a volcano, Awoe or Aboe (pronounced Avou or Abou), whose existence has been well established.

4.5.4 ^{14}C Ages in Support to Historical Evidence

The 300 yBP explosive eruption of Mt. Parker, which formed the present summit caldera, corresponds to the event described by Magisa (1641) and Le Gentil (1779-1781) despite the confusion on date and place brought about by subsequent retelling of the event (Delfin et al., 1997). This is supported by at least seven ^{14}C results.

Analysis of historical documents by Delfin and others (1997) revealed that confusion occurred on the date and the location of eruption. The following is a summary of their their interpretations:

1. Date of eruption

Le Gentil might have unintentionally changed the date of the eruption to 1640 either because he was actually referring to preclimactic eruptions of December 1640 or the voyage that begun in 1640. Subsequent authors (e.g., Von Buch, 1825; Berghaus, 1832; Bowring, 1859; Nieto Aguilar, 1894) inherited Le Gentil's mistake of a large 1640 explosive eruption.

2. Site of eruption

Magisa's (1641) account placed the eruption close to Cape San Agustin, at Sanguil Island. Le Gentil (1779-1781) likewise placed Sangil Volcano in Mindanao but Perry (1860) contended that the Sanguil in Magisa's account refers to Sanguir (Sangihe) Island between Mindanao and Ternate and that the eruption could have come from Awu Volcano. The name "Sanguil", "Sangil", "Sanguir" or "Sanguiz" is common to both Mindanao and the islands to the south. The Sarangani region of Mindanao was also referred to as Sanguir in the 17th century. Nevertheless, if the Spanish squadron observing the eruption was off Cape San Agustin, then the volcano must be closer to Mindanao than to Sangihe Island to the south. Cape Sarangani might have been mistaken for Cape San Agustin. Jagor's (1873) interpretation of a Sarangani source for the 1641 event is supported by Le Gentil's claim that the eruption occurred in the territory of the Kingdom of Buayen, sixty leagues from Zamboanga. Sixty leagues distance is roughly equal to 300 km, the distance of Parker to Zamboanga. In addition, Buayan today is a district of General Santos City located where the Buayan (Crocodile) River flows into Sarangani Bay. Forrest (1780) described an area along the west coast adjacent to the "Great Bay of Sugud Boyan" (Sarangani Bay) as "remarkable land of an even outline". Forrest must be referring to the surface of the young, 300 year-old lahar deposits forming smooth, gently sloping apron around Parker Volcano.

3. Eruption of Awu volcano (?)

No independent report was obtained prior to the one by Alexis Perry (1860), reporting of a large eruption of Awu Volcano in 1641. Instead all reports of the 1641 eruption of Awu seem to derive from Perry (1860). Moreover, Indonesian volcanologists doubt that such a large eruption occurred. Matahelumual (1985) described an eruption in Awu Volcano between December 1640 and January 1641, but there were no fatalities, and the eruption was phreatic.

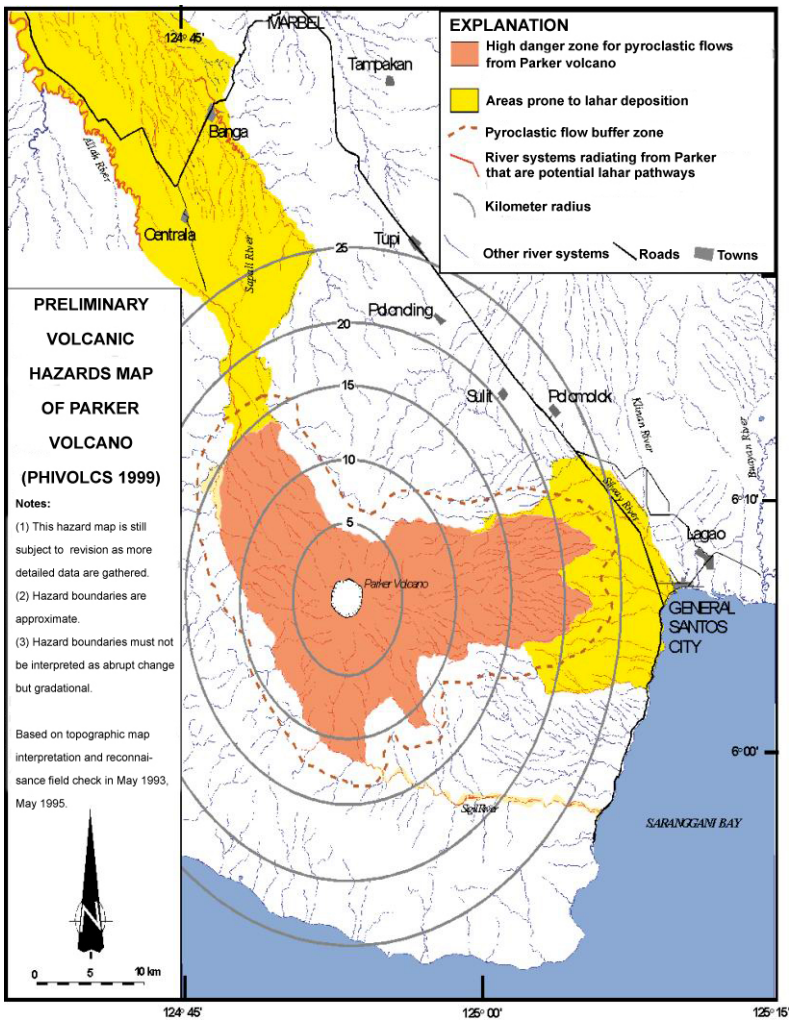

Fig. 46. Preliminary hazards map of Parker Volcano by PHIVOLCS as of 1999.

In summary, primary historical reports favour a Sarangani Peninsula source for the 1641 eruption, near or at what is presently known as Parker Volcano.

4.5.3 Volcanic Hazards and Monitoring

Delfin and others (1997) has established a 1641 eruption of Mt. Parker and a 300-year interval, at least, for the last two eruptions. The number of ^{14}C ages though is insufficient to determine the frequency of events. The historical and geological evidence clearly demonstrates the explosive activity of Parker, and thus requires a greater level of study and volcano monitoring. Figure 46 shows the preliminary hazard map of Parker Volcano.

As demonstrated by the 06 September 1995 and 06 March 2002 floods, an important hazard of Parker Volcano is due to crater-lake breakout. This can be triggered by an eruption or earthquake, as in the 06 March 2002 landslide dam breakout. After the 1995 flash flood, a permanent remote seismic station was installed at Bagong Silang village, located about 6 km east-southeast of Lake Maughan. This relays data acquired to the manned seismic station of PHIVOLCS at the Mindanao State University (MSU) Campus in Tambler, General Santos City.

5. Philippine Calderas and Their Activities

5.1. Taal Caldera

5.1.1 Geologic Setting

Taal Caldera is a young volcanic center that lies within a fault-bounded volcano-tectonic depression (Fig. 47) within the Macolod Coridor, a cross-arc northeast-trending lineament, comprised of andesitic composite volcanoes and monogenetic basalt tuff cones and maars. The concentration of volcanoes in Macolod Corridor was initially thought to be an expression of a *Bruchlinie* or deep fracture (Von Drasche, 1876). Adams (1910) interpreted the northeast-structural line passing through Balayan Bay, Taal Volcano Island, and the southern border of Laguna de Bay, as the southern margin of the elevated fault block that includes Mt. Batulao, Tagaytay Ridge, and Mt. Sungay. Forster and others (1990) and Oles (1991) placed the boundary of Ma-

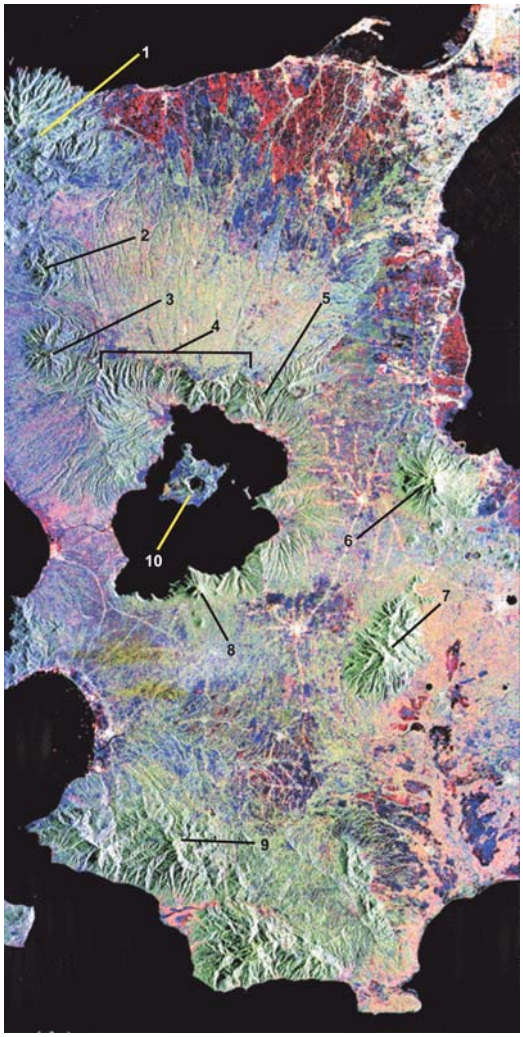

Fig. 47. Satellite image showing Taal Caldera, Taal Lake, and the Volcano Island. Volcanic centers: 1-Mt. Palay-palay/Mataas na Gulod, 2-Mt. Carilao, 3-Mt. Batulao, 4-Tagaytay Ridge, 5-Mt. Sungay, 6-Mt. Makiling, 7-Mt. Malepunyo, Mt. Macolod, Mt. Panay, Mt. Macapili. Image by NASA-JPL.

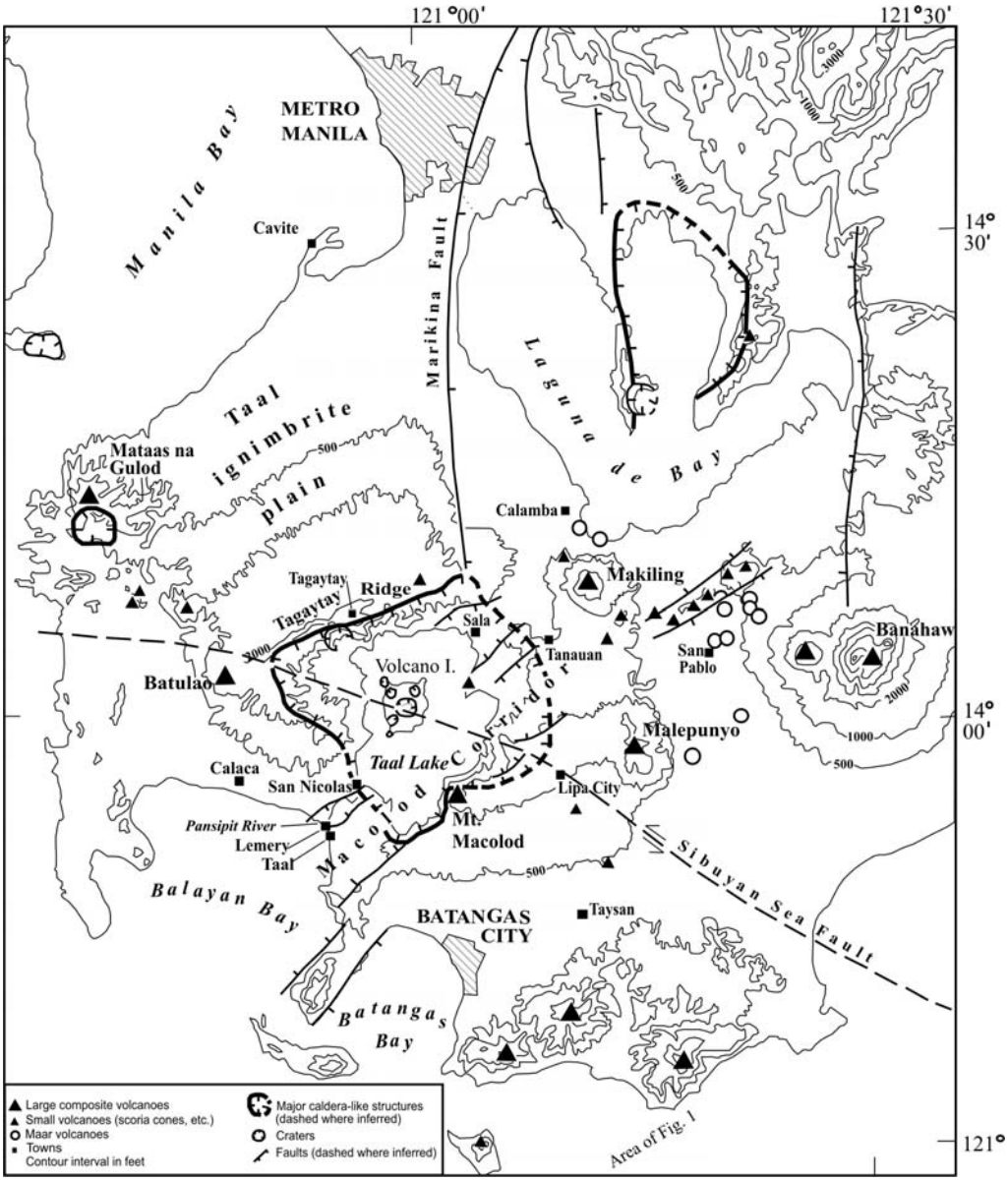

Fig. 48. Map of Taal Caldera and other volcano-tectonic structures of the Southern Tagalog Volcanic Field.

colod Corridor between the Tagaytay Ridge and the northeast-trending normal fault west of the Batangas mountains. The roughly north-south trending southern terminus of the Marikina Fault System extends to the Cavite highlands, near the vicinity of Mt. Sungay. Alcaraz and Datuin (1975) and Lim (1983) interpreted that a northeast-southwest and a northwest-southeast trending lineament, control the location of eruption centers at the Taal

Volcano Island, which is located within Taal Caldera. On the basis of aeromagnetic and seismic data, Bischke and others (1990) concluded that the Sibuyan Sea branch of the Philippine Fault cuts across Taal Caldera, but concealed by younger Taal deposits.

The 20 x 15 km Taal Caldera is bounded by several pre-caldera basaltic-andesitic stratovolcanoes namely Mt. Batulao, Mt. Sungay, Mt. Macolod, Mts. Malepunyo, and Mt. Makiling (Fig. 48). Mt. Batulao is a dissected andesitic stratovolcano located at the northwestern rim of the caldera. K-Ar date for a lava sample yielded an age of 3.40 Ma (De Boer et al., 1980; Oles, 1991). Another stratovolcano, Mt. Sungay, sits at the northern rim of the Caldera. Deposits of Mt. Sungay are draped by early-stage dacitic ignimbrites of Taal caldera (Listanco, 1994). To the east and northeast are two volcano complexes, Mts. Malepunyo and Makiling. Both centers are partially mantled by Taal Caldera ignimbrites (Listanco, 1994). The oldest dated andesite lava from Mt. Malepunyo is 1.10 Ma (De Boer et al., 1980; Oles, 1991). Likewise, dacite and andesite samples from the highly dissected Mt. Makiling yielded 0.51 and 0.18 Ma, respectively. The maar field and other volcanoes of the Macolod Corridor, lie farther east of Mts. Malepunyo and Makiling.

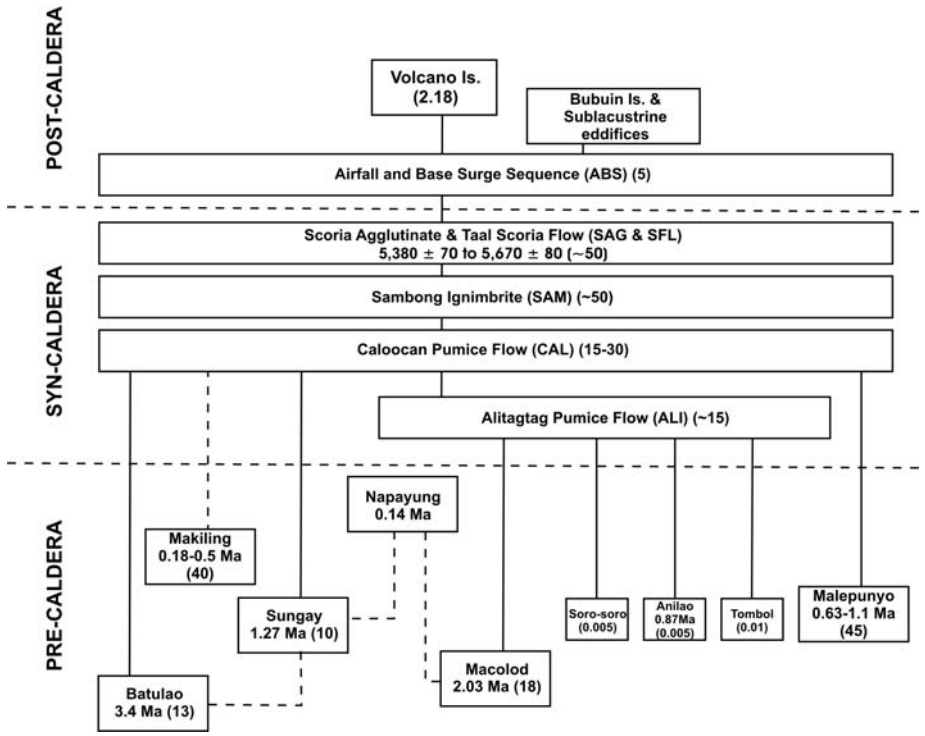

Fig. 49. Block diagram showing time-stratigraphic relationship for Taal Caldera units and related edifices. From Listanco (1994).

5.1.2 Caldera Features and Stratigraphy

Taal Caldera has an asymmetrical topographic rim. The Tagaytay Ridge on the north is the highest, with an elevation of 500-600 m above sea level. The southern caldera rim is vertical at Mt. Macolod and Alitagtag, but generally gently sloping elsewhere. Except at the faulted centers of Mt. Macolod and Mt. Sungay, the walls of the caldera are composed of thick ignimbrite-airfall-surge sequences. Younger airfall-surge sequences mantle the lower half of the walls (Geronimo, 1988; Listanco, 1994). The base of the oldest ignimbrites is exposed close to lake water levels on the southern side of the caldera (Listanco, 1994). They can be traced at about 50 m above sea level at the northern side. The volume of the tectonic depression (that includes the caldera) was estimated at 120 km^3 (Listanco, 1994).

Intra-caldera deposits, consisting of well-bedded fallout and banded andesite lava at the

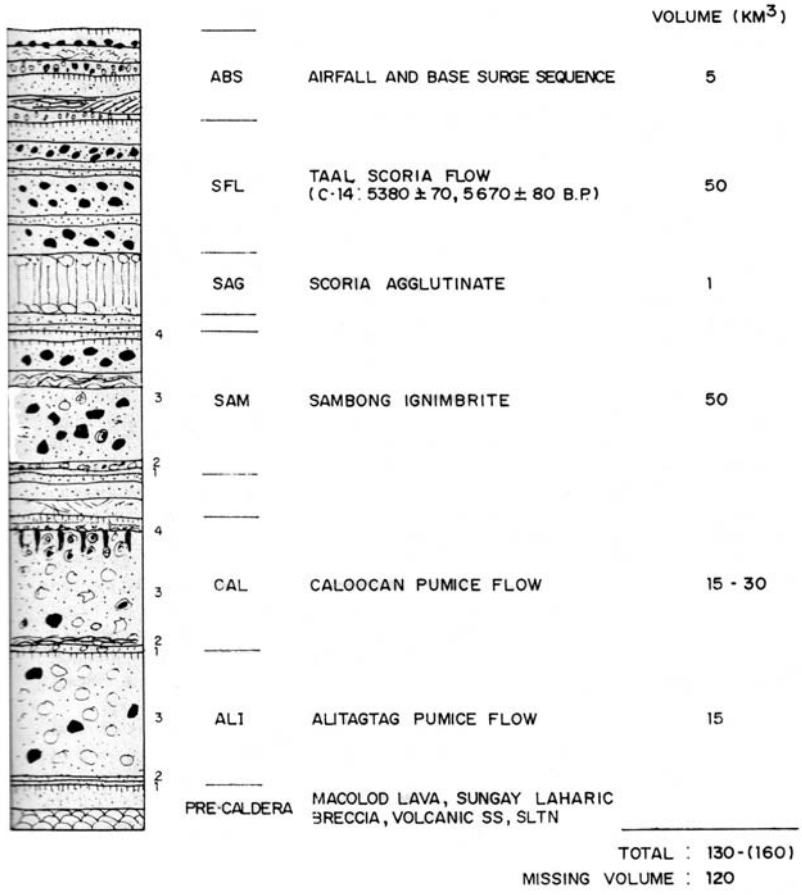

Fig. 50. Standard section of Taal Caldera. From Listanco (1994).

base, are exposed at Napayung Island (a small island inside Taal Lake located northeast of Taal Volcano Island). These deposits were dated 140 ka (Oles, 1991), and are draped by Taal Caldera ignimbrites.

Listanco (1994) subdivided the Taal Caldera-related events into six stages (Figs. 49, 50). Each stage produced a physically and compositionally distinct set of deposits. The first four stages are: the Alitagtag (ALI) and Caloocan (CAL) pumice flows, Sambong (SAM) ignimbrite and scoria agglutinate (SAG), and Taal scoria flows (SFL). They are characterized by voluminous extrusion of calc-alkaline andesitic to dacitic magma. The ^{14}C age of the youngest calderagenic deposits (SFL) is 5,380-6,830 yBP (Listanco, 1994; Martinez and Williams, 1999). Post-caldera emplacement of airfall and base surge sequences (ABS) characterize the fifth stage. The sixth, and currently the active phase, is related to the formation of the Taal Volcano Island and probably the other sublacustrine eruption centers.

5.2 Laguna Caldera

5.2.1 Geologic Setting

The 20 x 10 km elliptical-shaped Laguna Caldera sits on the margin of the 40-km wide young volcanic field (Fig. 51), the Macolod Corridor. It is located within the dinosaur foot-shaped Laguna de Bay, known to be the largest lake of Luzon Island. The Laguna de Bay has three basins, the west, middle and east bay, and covers a total area of 922 km^2. The middle bay/central lobe has been ascribed by previous workers as the Laguna Caldera. Oles and others (1991) described the structure as the largest volcano-tectonic depression formed by caldera eruptions within an extensional setting. The caldera belongs to the Southwest Luzon Volcanic Field (SLWVF) that also includes Mts. Makiling, Batulao, Malepunyo, Banahao and Taal Volcano and its caldera.

Volcanoes and faults border the caldera (Fig. 52). To the north-northeast direction lies the Sierra Madre Range. It is a Paleogene volcanic arc in response to the west-dipping subduction east of Luzon Island during the Cretaceous and Paleogene (Lewis and Hayes, 1982; Karig, 1973; Murphy, 1973). Northwest of the caldera is Metro Manila and the Central Valley Basin. Both are underlain by thick a volcaniclastic sequence from Laguna Caldera. On the eastern caldera margin is Mt. Sembrano, an old and dissected andesitic volcanic center and a pre-caldera feature. To the east is the fault-bounded Talim Island, which is interpreted to be a remnant (flank) of an old volcanic center. A morphologically young-looking crater exists on the southeast portion of Talim Island. Taal Volcano and Taal Caldera lie further to

the south-southwest. Two prominent tectonic structures trending northwest-southeast and north-south, abound the caldera. The north-south fault system forms a nearly vertical wall at the eastern edge of Talim Island.

Fig. 51. Satellite image of the Laguna-Taal-Metro Manila area. From http://earthrise.space.com/dataSpark/earthrise.

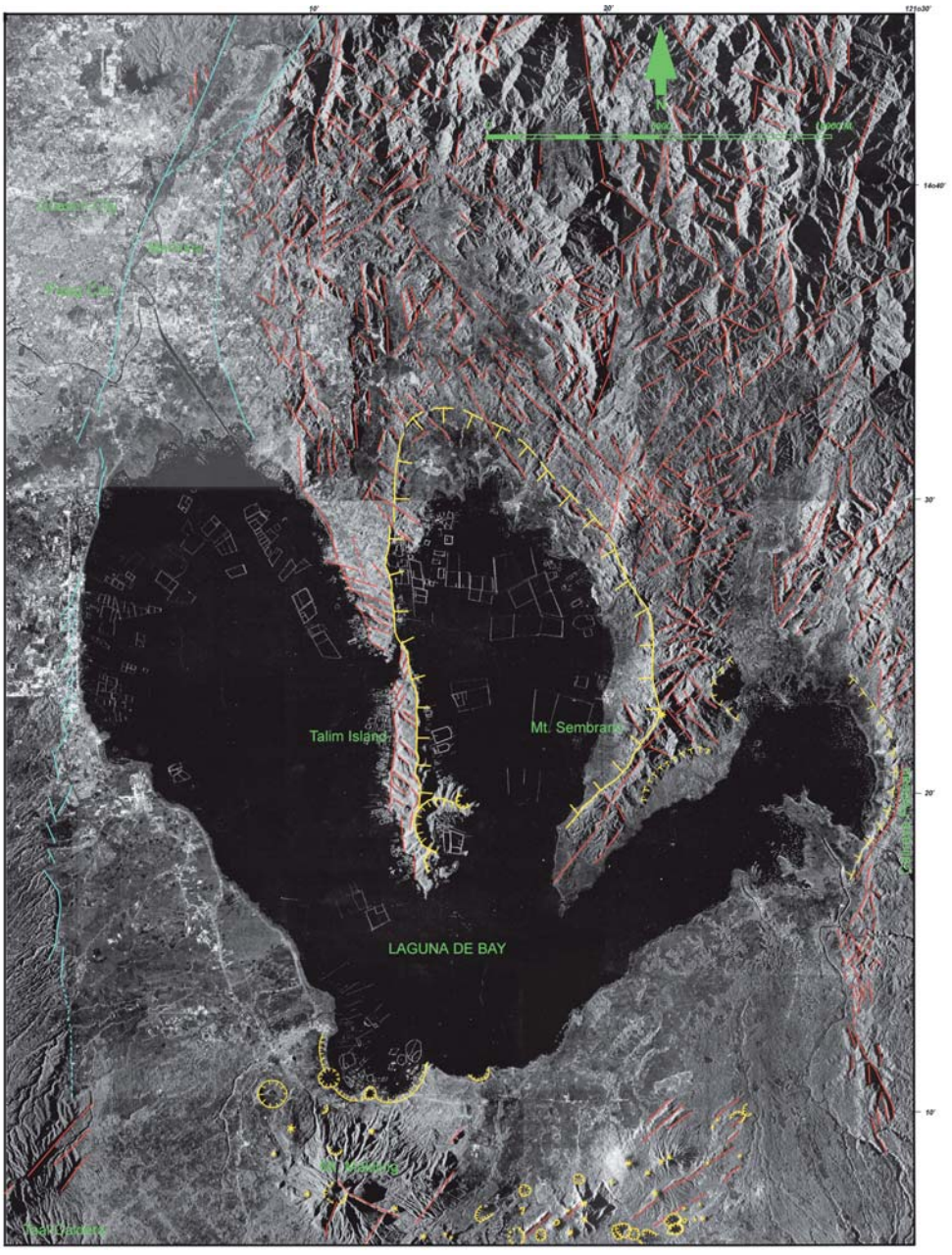

Fig. 52. SAR image of Laguna Caldera, Laguna de Bay, and other geologic structures. The caldera rim is indicated by the prominent yellow hactured line (dashed when inferred) at the middle bay. Cluster of smaller craters (also in yellow), at the bottom of the image, is the San Pablo monogenetic field. Mt. Makiling prominently rises within this field. The two parallel blue lines (left side of image) mark the trace of the Marikina Valley Fault System. Numerous NE-SW and NW-SE lineaments (red lines) on the upper part of the image are older structures inherent in the basement rocks of the Sierra Madre Range. From Catane and Arpa (1999).

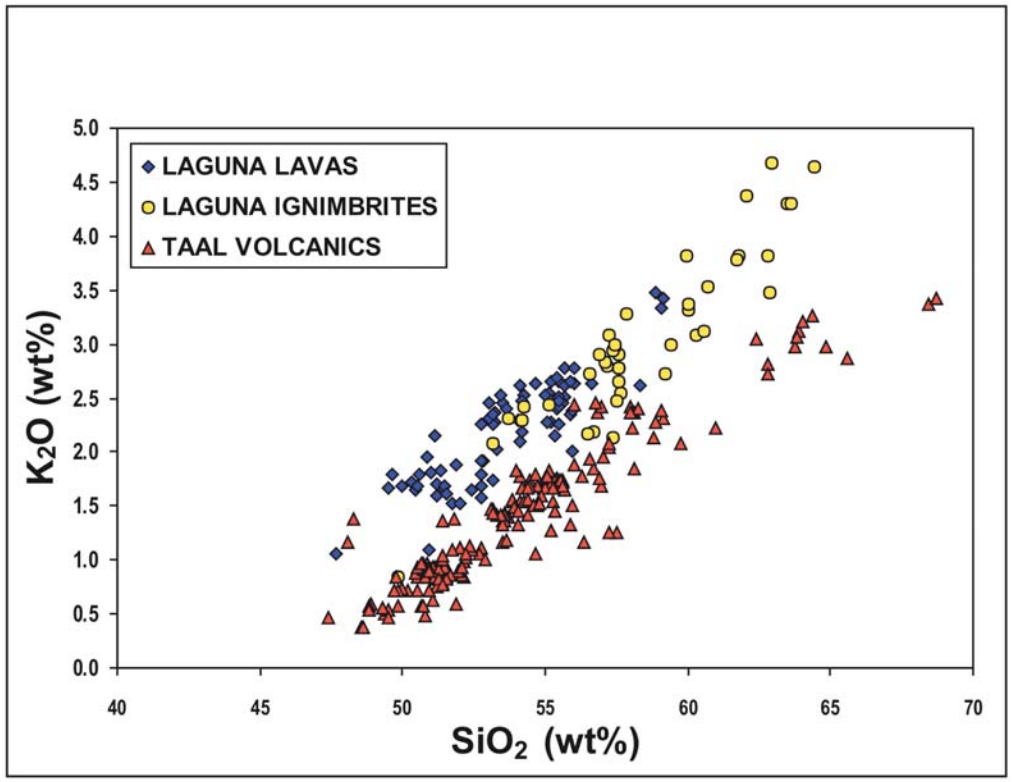

Fig. 53. Taal-Laguna geochemical data. Taal data was compiled by Knittel (1998) from published and unpublished works; Laguna data from Catane and Arpa (1999) and unpublished data of Catane (2004).

Laguna Caldera is one of the few identified, but less studied caldera volcanoes in the Philippines. Wolfe and Self (1983) identified the caldera structure on the basis of topographic expression. A recent gravity survey, jointly conducted by PHIVOLCS and a Japanese collaborator, reaffirmed the location of the caldera in the middle bay (Arpa, pers. comm., 2000). Gravity anomaly indicates asymmetry of sediment thickness inside the caldera, where thick pile of sediments underlies the eastern edge, as opposed to the thin sediments on the western edge of the bay, suggesting that caldera floor is dipping to the east. Subsequent studies such as flow lineation analysis and lag-breccia facies distribution indicate the middle bay as the locus of vents (Catane et al., 2004). Deposits from Laguna and Taal overlap on the southern side (of Laguna), but deposits can be discriminated by their distinct geochemical signatures. Both the lavas and pyroclastic flow deposits of Laguna have distinctly higher K^2O, MgO, Rb and Zr contents compared to Taal (Fig. 53). In spite of the few studies available, Laguna Cal-

dera is of importance because it is the source of pyroclastic and epiclastic deposits covering many parts of Metro Manila and adjacent provinces, Rizal, Laguna, and Bulacan (Catane and Arpa, 1999).

5.2.2 Age, Stratigraphy and Caldera History

C-14 and K-Ar Ages

Radiocarbon dating revealed at least three clusters representing episodes of younger calderagenic eruptions in the vicinity of Laguna caldera (Catane and Arpa, 1999). These are: (1) 5,000 yBP, (2) 27,000-29,000 yBP, and (3) >42,000 yBP. All carbon samples were obtained from massive pyroclastic-flow deposits. The sample which yielded 5 ka was collected from a boring core retrieved at 18 m depth from a massive pumice flow unit in Aurora, Quezon City. Listanco (1994) reported a 27 ka age of carbon sample obtained in Cubao, Quezon City. A similar age of 29 ka was obtained from samples taken from a massive pumice flow from an excavation in Ortigas City, Metro Manila. Samples were analyzed in the ^{14}C laboratory of USGS and by Beta Analytic Inc., Florida, USA. Wolfe and Self (1983) earlier reported ages of 1.7 Ma and 1.0 Ma, respectively, for an andesitic lava flow and andesitic tuff at the northern edge of the caldera. Subsequent K-Ar ages were provided by Oles (1991) to be 2.3 Ma and 2.24 Ma, from andesitic lavas, and 1.1 Ma, from a rhyolitic tuff. Additional K-Ar dates by Sudo et al. (2000) yielded a 1.67-2.19 Ma range for andesite lava flows on the northeast and southern rim of the caldera. Oldest volcanic rocks (>1 Ma) were obtained from andesite flows of old pre-caldera volcanic centers, whereas ages for the oldest tuffs are about 1.0 Ma. Although the ^{14}C and K-Ar ages are difficult to reconcile at present due to the difference of dating methods and materials used by different workers, Catane and others (2004) put 1 Ma as a reasonable upper limit of the earliest caldera activity. This maximum age is supported by field observation that at least some of the younger pyroclastic units are fresh to slightly altered and virtually undeformed. Considering the high weathering rates, active tectonism and volcanism in the area, the deposits are most likely to be <1 Ma.

Caldera History

The geologic history of Laguna may be subdivided into three stages namely: (1) pre-caldera volcanism, (2) caldera-forming stage, and (3) post-caldera volcanism (Catane et al., in preparation). Each stage is characterized by eruption of intermediate volume trachytic pyroclastic flows, surges, and Plinian falls. Associated lahars, fluvial, and lake deposits are em-

placed in each episode. Between some explosive eruptions, non-explosive activity prevailed in the form of lava flows. Stratigraphic studies showed that some lava flows may be related to caldera activity, such that they mark the end of the explosive eruption. At least three calderagenic eruptions occurred at Laguna. Extensive reworking to form lahars and stream deposits immediately followed each of them. Each caldera episode is marked by a period of repose, allowing soil profile or weathered horizon to develop.

Pre-caldera volcanoes

Pre-collapse volcanism is characterized by the formation of basaltic to andesitic stratovolcanoes. Two small, dissected, pre-caldera volcanoes, Talim Island and Mt. Sembrano, found at the east and west of the caldera margin, were formed at this stage. The surface topography of these volcanoes is partly obscured by erosion and a thick blanket of pyroclastic flow deposits. Talim Island is interpreted to be a remnant of a stratovolcano that collapsed following voluminous extrusion of magma in one of the caldera-related eruptions of Laguna. Its asymmetrical cross-section suggests that the island formed the flank of a stratovolcano. Furthermore, surface parallel drainage pattern in Talim Island suggests that ancient rivers flowed from an elevated area, further east of the island. K-Ar dating of basaltic to andesitic lava flows from Talim Island and Mt. Sembrano yielded 1.67-1.19 Ma ages (Sudo et al., 2000).

Caldera-forming eruptions

There are more than 20 pyroclastic-flow units identified on the basis of stratigraphy and physical characteristics. The three youngest calderagenic events based on ^{14}C dating are 5,000 yBP, 27,000-29,000 yBP, and >42,000 yBP (Catane and Arpa, 1999). At least one of the caldera-related events, the 27-29 ka eruption, had an associated lava flow.

There were five samples that yielded an age of 42 ka or >50 ka, which is beyond the detection limit of ^{14}C dating method. Among the dated units of this range, Binangonan Pumice Flow appears to be the youngest, on the basis of the degree of deposit preservation. It consists of a lower Plinian fall and surge unit, followed by series of massive pyroclastic flows, and capped by pyroclastic surges (Catane et al., 2004). It is pumiceous and nonwelded, but shows co-occurrence with more mafic clasts in some massive flow units. It forms as a thick proximal flow unit in Binangonan, Rizal.

At least two samples fell within the 27-29 ka range. One sample was collected from a

Fig. 54. Exposure of the youngest Laguna ignimbrite, Teresa scoria flow (upper columnar jointed unit), in Tanay, Rizal. Photo by S. Catane.

scoria-flow deposit in Ortigas, and another from a pyroclastic-flow deposit in Cubao, both in Quezon City, Metro Manila. These pyroclastic flows are correlated with the Teresa Scoria Flow, proximal pyroclastic-flow deposits that extensively outcrop in Teresa, Rizal (Fig. 54). The Teresa Scoria Flow is regarded as the youngest event clearly associated with Laguna caldera. The eruption is characterized by the emplacement of surges and falls, followed by a series of pyroclastic flows and ash cloud surges. In some places, the sequence is capped by andesitic lava flows. Deposits are non-welded to welded, of intermediate composition, varying from dacitic to more mafic compositions within a single flow unit. Some outcrops contain banded pumices, indicating magma mingling during the eruption.

In exposures, the Teresa Scoria Flow consistently lies above the Binangonan Pumice Flow. Teresa Scoria Flow can be distinguished from Binangonan Pumice Flow by its lower degree of deformation and the predominance of mafic clasts. Geochemical analysis of the juvenile clasts for both units revealed andesitic-dacitic compositions.

Microscopic examination of juvenile scoria and pumice clasts from Teresa and Binangonan units revealed an aphyric magmatic source (Catane and Arpa, 1999). Both scoria and pumice are very glassy, constituting to about 40-60 % of the volume. Only about less than 10% comprise the minerals, and 30-50% is occupied by vesicles. For scoria, the mineral assemblage is plagioclase and clinopyroxene. Pumice clasts have the same mineral assemblage, ex-

cept that the percentage of clinopyroxene is very small, and the percentage of total crystal content is also low compared with scoria. Pumices are highly vesiculated and often exhibit a fibrous texture. Both scoria and pumice are fresh, and no evidence for vapor-phase crystallization was observed. Bulk chemical analysis revealed SiO_2 values of 56-58 wt% and 59-63 wt% for scoria and pumice, respectively.

Lava flows are more basic in composition than most of the juvenile pyroclasts, with a SiO_2 range of 51-54 wt%. Clinopyroxene, plagioclase, and rarely olivine, exist as mineral phases in the lavas. Although most lava flows lies within the K-Ar age range of 1-2 Ma, some andesite to basaltic andesite lava flows are interbedded with caldera-related pyroclastic-flow units. This implies that some lava flows might have been emplaced as a terminal event during the caldera-forming stage. The old ages of lavas, however, are inconsistent with the ^{14}C ages of pyroclastic flow deposits. A difficult aspect in establishing the stratigraphy of Laguna Caldera is largely due to the discrepancies of ages provided by ^{14}C and K-Ar methods. The absolute age range of most calderagenic deposits probably lies within the time span that is not precisely detected by both methods.

The most recent large-scale eruption event that affected the Metro Manila and Laguna areas occurred about 5 ka. However, deposits seem to be too young for a relatively dissected Laguna Caldera source. Instead, this eruption may be related to the last calderagenic eruption of Taal Caldera that occurred about the same time.

Post-caldera volcanism

Except for the well-preserved young maar vents at the southern margin of Laguna de Bay, other young vents at the vicinity of the caldera include the small vents at the southern point of Talim Island. It appears that no large-scale eruption occurred in Laguna during the Holocene. Small phreatic/phreatomagmatic explosion craters in Talim Island typify post-collapse volcanism in Laguna.

5.3 Irosin Caldera

5.3.1 General Geologic Setting

Irosin Caldera belongs to the Mt. Bulusan Volcanic Complex (BVC) located at the southern end of the Bicol Arc. Magmatism along the arc is related to the westward subduction of the Philippine Sea Plate down the Philippine Trench (Cardwell et al., 1980; Divis, 1980; Hamburger et al., 1983). The BVC includes the active Bulusan Volcano and surrounding vents,

the Irosin Caldera, and other older volcanic centers. Volcanism in the BVC is subdivided into three stages: precaldera, syn-caldera, and postcaldera (Panem and Delfin, 1988; Delfin, 1991). The first stage, which began at least 2.14 Ma, is characterized by a stratovolcano building stage along regional fractures. It is characterized by the eruption of high-K basaltic andesites and andesites, tuff-breccias and tuffs that built the Gate Mountains in the southern part of the complex. This eruptive phase is believed to have structural control, as inferred from the northwest alignment of eroded craters and vents. The early stage was followed by a period where large-volume ignimbrite sheets were erupted, resulting to caldera formation. Renewed volcanism after the caldera collapse formed several stratocones and domes during the postcaldera stage. Young volcanism and recent activity of Bulusan Volcano also belong to this stage.

5.3.2 Geologic of Irosin Caldera

Irosin Caldera is an 11 km-wide volcanic depression located in the province of Sorsogon, southern Luzon Philippines. Along with the active Bulusan Volcano, its surrounding vents,

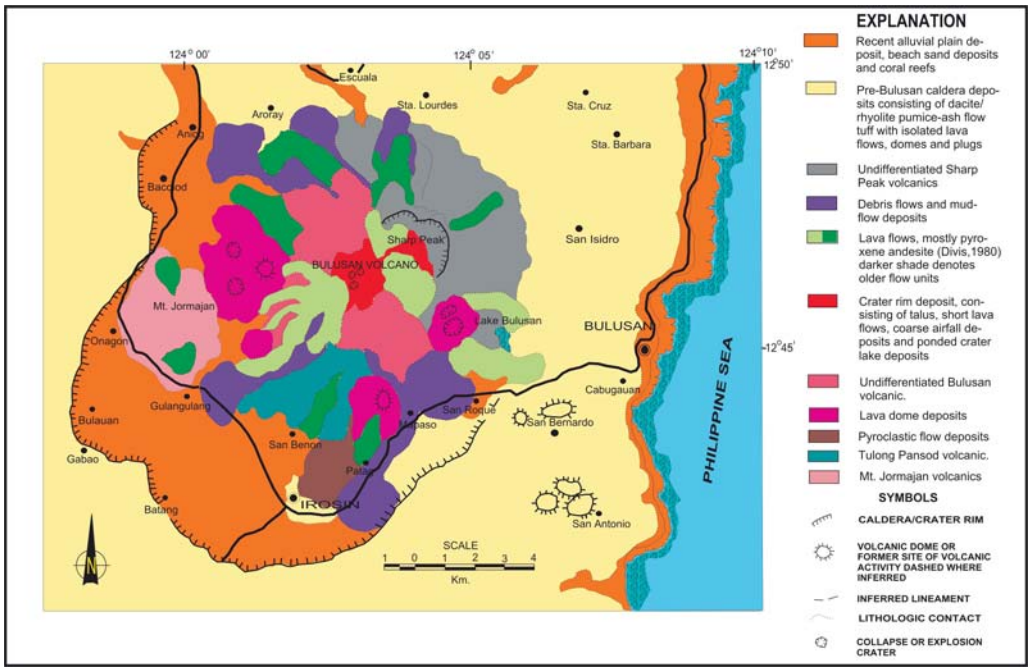

Fig. 55. Geologic map of Bulusan Volcano and Irosin Caldera based on airphoto and reconnaissance field mapping by J. Umbal and J. Cruz (PHIVOLCS, 19?_).

Fig. 56. A view of the sediment-filled Irosin Caldera floor, post-caldera Mt. Jormajan (offcenter right) and pre-caldera volcanoes (left). Photo by S. Catane.

and associated older volcanic centers in various erosional stages, they occupy an area of about 900 km^2 and are collectively known as the Mt. Bulusan Volcanic Complex (BVC) (Fig. 55).

The Irosin Caldera was formed during the second stage of volcanism in the BVC. After a long period of inactivity, highly silicic magmas were erupted, that led to caldera collapse (Fig. 56). ^{14}C ages of samples embedded in ignimbrites erupted during the caldera-forming stage, revealed an age of ～35-40 ka (Delfin, 1991). A volume of probably >10.4 km^3 of dacitic to rhyolitic pumiceous pyroclastic flows were erupted, deposits of which reached at least 20 m thick in flat lying areas. Delfin (1991) deduced that this eruption was the largest single extrusion of rhyolitic magma in the entire Bicol Arc. This event removed a large volume of magma from the chamber, leading to a collapse, and the formation of the 11-km wide Irosin caldera. Pyroclastic flows were emplaced in all directions around the caldera.

The caldera is bounded by walls of varying relief - about 100 m on the west, 150 m on the southwest, and 560 m on the southeast (Panem and Delfin, 1988). This variable relief of the

caldera wall may be explained by the manner of edifice collapse, wherein the wall rocks collapsed asymmetrically into a funnel-shape central vent, following the mechanism proposed by earlier workers for island-arc calderas (e.g., Aramaki, 1984; Walker, 1984; Scandone, 1990. There is no visible caldera rim in the north; either because collapse in this area was not accommodated through a ring fracture contiguous with the southern fault, but through down sagging of the land, unless it is buried by postcaldera extrusives (Panem and Delfin, 1988).

The last stage, the postcaldera, occurred after a period of quiescence and lake sedimentation, the latter presumably ended by uplift and renewed volcanism. Assuming that the BVC follows the typical timing for onset of postcaldera magmatism in intermediate-sized caldera, which is about 5-10 ka after caldera collapse (Mahood, 1980), then post-caldera magmatism in the BVC will fall between 25-30 ka. This will be the age of the Sharp Peak Volcano, which was formed by lavas, pyroclasts and lahars of the earliest mafic post-caldera magma in the BVC. These lavas were dark, sparsely-porphyritic and vesicular basalts and basaltic andesites that include the most primitive melts erupted in the BVC. Succeeding post-caldera eruptions had more differentiated lavas that formed the Taripungso andesite, Agoho andesite, and Jormajan dome, edifices less eroded than Sharp Peak but more degraded than Bulusan

Table 11. Summary of volcanic activities at Irosin Caldera. From Delfin (1991).

Eruptive unit	Age (Ma)	Basis
Precaldera Eruptive Stage		
Gate volcanics	2.14	K-Ar
Tabon-tabon volcanics	<2 - >1.1	Stratigraphic correlation
Calunan andesite	1.1	K-Ar
Homajan basalt	0.4	K-Ar
Bintacan volcanics	<0.4 - >0.04	Stratigraphic and geomorphic correlation
Caldera Eruptive Stage		
Malobago dome	~0.035 - 0.04	Petrological and geochemical correlation
Irosin ignimbrite	0.035 - 0.04	^{14}C
Postcaldera Eruptive Stage		
Sharp Peak volcanics	~0.025 - 0.035	Stratigraphic correlation
Agoho andesite	~0.02 - 0.01	Stratigraphic and geomorphic correlation
Taripungso andesite	~0.02 - 0.01	Stratigraphic and geomorphic correlation
Jormajan dome	~0.02 - 0.01	Stratigraphic and geomorphic correlation
Talatak dome	~0.01	Stratigraphic and geomorphic correlation
Bulusan volcanics	>0.006 - present	^{14}C and historic activity

Volcano.

The post-caldera stage is still continuing today. It built several coalescing domes and stratocones within the caldera, including the active Mt. Bulusan, a composite cone predominantly built of andesite lava flows and subordinate breccias and tuffs. Interbeds of airfall tuff and lahars on its northern and southern slopes were erupted between 1 to 5 ka (Delfin, 1991). It has fifteen recorded eruptions that are mostly mild ash ejections, the earliest being in 1852, and the latest in 1995 (PHIVOLCS, 2002). A summary of eruptive history of Mt. Bulusan Volcanic Complex is given in Table 11.

The Bulusan andesites, and those of the other volcanoes in the Bicol Arc, are believed to be fractionated magmas derived from the mantle wedge below the arc, rather than primary slab-derived melts. The mantle wedge is most probably a depleted N-type MORB mantle that has been metasomatised by fluids from the subducted slab, since the most likely source for the BVC magmas must at least contain these two components (Tatsumi et al., 1986). An open system behaviour, wherein both magma mixing and assimilation accompanied fractional crystallization, characterizes the evolution of BVC magmas.

6. Summary and Conclusions

The Philippine archipelago is a host to more than 400 volcanoes. These volcanoes are distributed in nine volcanic arcs/belts associated with subduction zones bordering the Philippines. The two major and active subduction zones, the Philippine Trench and the Manila Trench, are related to the oblique convergence of the Philippine Sea Plate and Eurasian Plate. The presence of oppositely facing subduction zones, compounded by numerous active tectonic elements, makes the Philippines one of the most geologically interesting but complex areas in the world.

Philippine volcanoes are classified as active, potentially active, and inactive, based on their current activities and eruptive histories. There are 22 active, 27 potentially active, and 359 inactive volcanoes. Philippine volcanoes are predominantly andesitic with calc-alkaline affinities. The most active volcanoes which erupted recently include Mayon, Taal, Bulusan, Canlaon, Hibok-Hibok, and Pinatubo.

Philippine volcanoes exhibit various types of eruptive activities: phreatic, phreatomagmatic, Strombolian, Vulcanian, Pelean and Plinian. The most explosive among the active volcanoes are Mayon, Taal, Pinatubo, Hibok-Hibok, and Parker.

With its 48 historical eruptions, Mayon Volcano is considered the most active volcano in the Philippines. Eruption style varies from Strombolian, Vulcanian to Plinian but Pelean- and Merapi-type eruptions associated with domes occur as well. Its most violent Plinian eruption in 1814 killed 1,200 people, while 77 died in a small, unprecedented phreatic explosion in 1993. No casualties were incurred in its most recent eruption in 2001. Eruptive patterns based on historic eruptions and geochemical compositions showed that most explosive activities occur when basaltic magma is erupted, possibly due to basaltic magma injection into a shallow reservoir.

Taal is notorious for its violent phreatic and phreatomagmatic activities (e.g., 1911, 1965) that produce base surges. Ready access to lake water into Taal's vent system makes most of its eruption destructive. There are 47 eruptive centers in the volcano island and 35 other underwater vents. Except for one offshore eruption, all 33 historic eruptions took place within the island. The most violent eruptions occurred in 1754, 1911, and 1965. A total of 1,525 casualties were incurred during the 1911 and 1965 eruptions. Rare Strombolian eruptions took place only twice in 1968 and 1969. The foremost hazards related to Taal eruptions are base surges.

The Plinian eruption of Pinatubo Volcano in 15 June 1991, the third largest in the 20^{th} century, has inflicted long-term, widespread damage in the surrounding provinces. The eruption released about 6 km^3 volume of tephra, and covered an area of $4x10^5$ km^2 mostly over Luzon Island and the South China Sea. Pinatubo's giant eruption plume intruded the stratosphere, reached heights of more than 40 km, and caused a decrease of global temperature by 0.5℃. Lahars around Pinatubo persisted for years after the 1991 eruption. Accumulation and rising of meteoric water inside the caldera after the 1991 eruption, posed continuing hazards most especially at the northwest sector of the volcano. On 10 July 2002, the Maraunot Notch was breached, resulting to the release of 65 M m^3 of lake water and formation of 160 M m^3 of lahars down valley. An unusual change in lake-water color, from emerald green to dark brown, occurred in January 2004. However, it gradually returned to its original emerald green color on May 2004. The cause of the color change is still being investigated by PHIVOLCS and its collaborators.

The explosive eruptions of Hibok-Hibok in 1948-1953 marked the beginning of volcano monitoring in the Philippines. COMVOL, the predecessor of PHIVOLCS, was created to avert the loss of life and properties. The eruption claimed the lives of about 500 people by pyroclastic flows associated with dome explosions and collapse. Since then, the volcano re-

mained quiet. Hibok-Hibok historical eruptions are characterized by lava dome building and generation of Pelean-type pyroclastic flows.

Parker Volcano was recently associated with the 1641 explosive eruption previously attributed to Awu Volcano in Indonesia based on ^{14}C ages, geologic and historic evidence. Its last two eruptions occurred in an interval of 300 yrs. Explosive activities of Parker are demonstrated by historical and geological evidence, the size, composition, and type of eruptive activities of which are similar to Pinatubo Volcano.

Extensive flooding along the Ga-ao-Allah River system occurred due to breaching of landslide dams along Ga-ao creek in September 1995 and March 2002. While the cause of the September 1995 flooding remains unresolved, an earthquake triggered the March 2002 breaching. Landslide dams will form anew and earthquakes will persist, thus Parker Volcano's crater lake remain a threat to surrounding communities.

Taal, Laguna, and Irosin are, so far, the only identified calderas in the Philippines. They are of intermediate size typical of island-arc calderas. Taal Caldera's latest calderagenic activity occurred 5-6 ka. Laguna Caldera, whose deposits formed the landmass of Metropolitan Manila, has had young eruptions, the youngest of which is probably 26-29 ka. Thick population surrounds both Taal and Laguna, with the most populated area Metro Manila (12 M) sitting only 20 km away from Laguna Caldera. Taal and Laguna calderas are andesitic in composition, while Irosin is dacitic. Irosin Caldera was probably formed about 35 ka. In as much as only a few studies are available on these calderas, reconstruction of their eruptive histories and determination of the frequency of explosive events must be carried out.

References

Adams, G.I., 1910. Geological reconnaissance of southwestern Luzon. *Phil. J. Sci.*, Sec. A, 5: 57-116.

Adriano, R., Brevante, B., Bristol, M., Cambaliza, R., Collantes, M.G., Cortez, R., Erlano, J., Garcia, M.C., Givero, A., Marbebe, D., Padrique, A., Anacio, X., Cabria, H., Forbes, M., Zamora, P., Arcilla, C., Catane S., de Silva, L., Siringan, F., and Tejada, M.L., 2002. Pleistocene volcanism in North Palawan: implications and problems. *In: Proc. Geol. Soc. Phil. 2002 Geological Convention*, Quezon City, Philippines.

Aguila, L.G., Newhall, C.G., Miller, C.D., and Listanco, E.L., 1986. Reconnaissance geology of large debris avalanche from Iriga Volcano, Philippines. *Phil. J. Volcanol.*, 3:54-72.

Alcaraz, A. and MacDonald, G., 1954. Report to the Commission on Volcanology regarding the present condition of Hibok-Hibok Volcano. *The Phil. Geol.*, 8 (2):71-73.

Alcaraz, A., Abarquez, R., Abad, L., Quema, J., and Teves, J., 1952. A preliminary report on the recent eruptions of Hibok-Hibok Volcano, Camiguin island, Philippines. *Phil. Geodetic and Geophys. Inst.*, Report to the Committee on Volcanology, Dept. of Agriculture and Natural Resources, 216-223.

Andal, E.S., 2002. Geological and geochemical characterization of the Plio-Pleistocene to Recent volcanic rocks of the southeastern Luzon volcanic arc chain: implications to arc evolution. M.Sc. Thesis, *University of the Philippines - National Institute of Geological Sciences*, 154 p.

Aramaki, S., 1984. Formation of the Aira Caldera, southern Kyushu, about 22,000 years ago. *J. Geophy. Res.*, 89:8485-8501.

Arculus, R.J., 1994. Aspects of magma genesis in arcs. *Lithos.*, 33, 189-208.

Arpa, M.C., 2000. Personal communication. Arpa, M.C., 2001. Mapping of the deposits from the July 2001 Mayon Volcano eruptions. Philippines. *Phil. Inst. Volcanol. and Seis. (PHIVOLCS-GGRDD) internal report*, 3 p. + figs.

Arpa, M.C., Bornas, M.A., Abigania, M.I., Delos Reyes, P., Panol, M., Solidum, R., Listanco, E., Tagami, T., Matsumara, A., and Obata, M., 2001. Petrology and chemistry of lava flow and pyroclasts from the February to March 2000 eruption of Mayon Volcano, Philippines. *Phil. Inst. Volcanol. and Seis. (PHIVOLCS-GGRDD) internal report*, 31 p.

Aurelio, M., 2000. Tectonics of the Philippines revisited. *J. Geol. Soc. Phil.*, 55(3-4):119-183.

Balce, G., Magpantay, A., and Zanoria, A., 1979. Tectonic scenarios of the Philippines and northern Indonesian region. *In: Ad Hoc Working Group Meeting on The Geology and Tectonics of Eastern Indonesia*, Bandung, Indonesia, 9-14.

Bautista, C., Bautista, M.L., and Garcia, D., 1986. Seismic monitoring: a useful tool for mudflow detection at Mayon Volcano, Albay, Philippines. *Phil. J. Volcanol.*, 3(2):90-110.

Bayon, F. and Salonga, N., 1992. Surface geology and hydrothermal systems of Mts. Parker and Matutum geothermal prospects. *Phil. Nat' l. Oil Co. (PNOC-EDC) internal report*, 57 p.

Berghaus, H.K.W., 1832. Geo-hydrographisches Memoir zur Erklärung und Erlaüterung der reduzirten Karte von den Philippinen und den Sulu-Inseln: Gotha, Jusrus Perthus, 114 p. (Berghaus Atlas von Asia, no. 13)

Bernard, A., Knittel, U., Weber, B., Weis, D., Albrecht, A., Hattori, K., Klein, J., and Oles, D., 1996. Petrology and geochemistry of the 1991 eruption products of Mount Pinatubo.

In: Newhall, C.G. and Punongbayan, R.S., eds., *Fire and Mud: Eruptions and Lahars of Mount Pinatubo, Philippines*, Philippine Institute of Volcanology and Seismology, Quezon City and University of Washington Press, Seattle, 767-797.

Besana, G.M., Shibutani, T., Hirano, N., Ando, M., Bautista, B., Narag, I., and Punongbayan, R.S., 1995. The shear wave velocity structure of the crust and uppermost mantle beneath Tagaytay, Philippines, inferred from receiver function analysis. *Geophy. Res. Lett.* 22:3143-3146.

Bischke, R.E., Suppe, J., and Del Pilar, R., 1990. A new branch of the Philippine Fault system as observed from aeromagnetic and seismic data. *Tectonophy.* 183:243-264.

BMG, Bureau of Mines and Geosciences, 1981. Geology and mineral resources of the Philippines, Manila, 1:361-378.

Bornas M.A.V., Paladio-Melosantos, M.L., and Rañola, J.S., 2001. Conditions for natural breaching of the Maraunot Notch and catastrophic drainage of Pinatubo crater. *Phil. Inst. Volcanol. and Seis. (PHIVOLCS-GGRDD) internal report*, 15 p.

Bornas, M.A.V., Delos Reyes, P., Arpa, M.C., Abigania, M.I., Panol, M., and Solidum, R., 2000. Mapping and characterization of pyroclastic flow deposits from the 2000 Mayon Volcano eruption project. *Phil. Inst. Volcanol. and Seis. (PHIVOLCS-GGRDD) internal report*, 14 p.

Bornas, M.A.V., and the Quick Response Team, 2001. The 2001 Mount Pinatubo crater lake breakout crisis. *Phil. Inst. Volcanol. and Seis. (PHIVOLCS-GGRDD) internal report,* 10 p.

Bornas, M.A.V., Tungol, N.M., Maximo, R.P.R., Paladio-Melosantos, M.L., Mirabueno, M.H.T., and Javier, D.V., 2002. The 10 July 2002 Pinatubo crater lake breakout: preliminary fieldwork results. In: *Proc. Geol. Soc. Phil. 2002 Geological Convention*, Quezon City, Philippines.

Bowring, J., 1859. A visit to the Philippine Islands. *Smith, Elder and Co.*, London, 434 p.

Bruinsma, J.W., 1983. Results of potassium-argon age dating on twenty rock samples from the Pinatubo, southeast Tongonan, Bacon-Manito, Southern Negros, and Tongonan, Leyte areas, Philippines: Proprietary report by *Robertson Research Ltd.* to the Philippine National Oil Company-Energy Development Corporation, 24 p.

Campita, N.R., Daag, A.S., Newhall, C.G., Rowe, G.L., and Solidum, R.U., 1996. Evolution of a small caldera lake at Mount Pinatubo. *In:* Newhall, C.G. and Punongbayan, R.S., eds., *Fire and Mud: Eruptions and Lahars of Mount Pinatubo, Philippines*, Philippine Institute of Volcanology and Seismology, Quezon City and University of Washington Press, Seat-

tle, 647-664.

Cardwell, R., Isacks, B., and Karig, D., 1980. The spatial distribution of earthquakes, focal mechanism solutions and subducted lithosphere in the Philippine and northern Indonesian regions. *In:* D.E. Hayes, ed., *The Tectonic and Geologic Evolution of Southeast Asian Seas and Islands*, AGU Monograph Series 23:1-35.

Carey, S.N., 1997. Influence of convective sedimentation on the formation of widespread tephra fall layers in the deep sea. *Geology*, 25:839-842.

Catane, S.G. and Arpa, M.C., 1999. Large-scale eruptions of Laguna Caldera: contribution to the accretion and other geomorphic development of Metro Manila and adjacent provinces. *Phil. Inst. Volcanol. and Seis. (PHIVOLCS-GGRDD) internal report*, 30 p.

Catane, S.G. and Mirabueno, M.T., 2001. Characteristics and origin of the pyroclastic flows and surges of the 1993 Mayon Volcano eruption. *J. Geol. Soc. Phil.*, 56 (3-4):125-143.

Catane. S.G., Listanco, E., Corpuz, E., Lagmay, M., Bornas, M.A.V., Cabria, H., and Panol, A., 2003. Active volcanoes in the Philippines − Mayon, Pinatubo and Taal. Field Trip Guidebook A5, IUGG 2003, *The Volcanol. Soc. Japan*, 198 p.

Catane, S.G., Ui, T., Cabria, H.B., Arpa, M.C., and Taniguchi, H., 2004. Potential hazards from the youngest explosive eruptions of Laguna Caldera to Metropolitan Manila, Philippines. *In: Proc. of the 2004 Western Pacific Geophysics Meeting (WPGM)*, Hawaii, USA

Centeno y Garcia, J., 1885. Estudio geologico del volcan de Taal. *Tello, Madrid,* 53 p.

Corpuz, E. and Laguerta, E., 2003. The June and July 2001 eruptions of Mayon Volcano, Philippines. *Phil. Inst. Volcanol. and Seis. (PHIVOLCS) internal report*, 9 p.

Cruz, J., 1987. Volcanism and associated hazards in the Philippine setting. *In: Geologic Hazards and Preparedness Systems*, Phil. Inst. of Volcanol. and Seis., National Science and Technology Authority, Manila, 22-37.

Cruz, J.B., Solidum, R.U. Jr., and Corpuz, E.G., 1985. Transport, emplacement and textural characteristics of the Bonga pyroclastic flows of the 1984 eruption of Mayon Volcano. *Phil. J. Volcanol.*, 2 (1-2), 68-93.

Daag, A.S., Dolan, M.T., Laguerta, E.P., Meeker, G.P., Newhall, C.G., Pallister, J.S., and Solidum,R.U., 1996. Growth of a postclimatic lava dome at Mount Pinatubo, July-October 1992. *In:* Newhall, C.G. and Punongbayan, R.S., eds., *Fire and Mud: Eruptions and Lahars of Mount Pinatubo, Philippines,* Philippine Institute of Volcanology and Seismology, Quezon City and University of Washington Press, Seattle, 647-664.

Dartevelle, S., Ernst, G.G.J., Stix, J., and Bernard, A., 2002. Origin of the Pinatubo climactic

eruption cloud: implications for volcanic hazards and atmospheric impact. *Geology*, 30 (7):663-666.

Datuin, R., 1982. An insight on quaternary volcanoes and volcanic rocks in the Philippines. *J. Geol. Soc. Phil.*, 36 (1):1-14.

De Boer, J.Z., Odom, L.A., Ragland, P.C., Snider, F.G., and Tilford, N.R., 1980. The Bataan orogen: Eastward subduction, tectonic rotations, and volcanism in the western Pacific (Philippines): *Tectonophy.*, 67:305-317.

Defant, M.J., De Boer, J.Z., and Oles, D., 1988. The western central Luzon arc, the Philippines: two arcs divided by rifting? *Tectonophy.*, 145:305-307.

Defant, M.J. and Ragland, P.C., 1988. Recognition of contrasting magmatic processes using SB-systematics: an example from the western central Luzon arc, Philippines. *Chem. Geol.*, 67:197-208.

Defant, M.J., Jacques, D., Maury, R.C., De Boer, J., and Joron, J., 1989. Geochemistry and tectonic setting of the Luzon arc, Philippines. *Geol. Soc. Am. Bull.*, 101:663-672.

Defant, M.J., Maury, R.C., Joron, J., Feigenson, M.D., Leterrier, J., Bellon, H., Jacques, D., and Richard, M., 1990. The geochemistry and tectonic setting of the northern section of the Luzon arc (the Philippines and Taiwan). *Tectonophy.*, 183, 187-205.

Defant, M.J., Maury, R.C., Ripley, E.M., Feigenson, M.D., and Jacques, D., 1991. An example of island-arc petrogenesis: geochemistry and petrology of the southern Luzon arc, Philippines. *J. Petrol.*, 32: 455-500.

Delfin, F.G. Jr., 1984. Geology of Mt. Pinatubo geothermal project: *Phil. Nat' l. Oil Co. (PNOC-EDC) internal report*, 35 p.

Delfin, F.G. Jr., 1991. Petrogenesis of Mt. Bulusan volcanic complex, Bicol arc, Philippines. M.Sc. Thesis, *University of South Florida*, 122 p.

Delfin, F.G. Jr., Villarosa, H.G., Layugan, D.B., Clemente, V.C., Candelaria, M.R., and Ruaya, J.R., 1996. Geothermal exploration of the pre-1991 Mount Pinatubo hydrothermal system. *In:* Newhall, C.G. and Punongbayan, R.S., eds., *Fire and Mud: Eruptions and Lahars of Mount Pinatubo, Philippines,* Philippine Institute of Volcanology and Seismology, Quezon City and University of Washington Press, Seattle, 197-212.

Delfin, F.G. Jr., Newhall, C.G., Martinez, M.L., Salonga, N.D., Bayon, F.B., Trimble, D., and Solidum, R., 1997. Geological, ^{14}C, and historical evidence for a 17th century eruption of Parker Volcano, Mindanao, Philippines. *J. Geol. Soc. Phil.*, 3(1):25-42.

Divis, A., 1980. The petrology and tectonics of recent volcanism in the central Philippine

Islands. *In: Petrology and Volcanism in the Philippines*, AGU Geophys. Monogr. 23:127-144.

Divis, A., 1983. The geology and geochemistry of Philippine copper porphyry deposits. *In:* Hayes, D.E., ed., *The Tectonic and Geologic Evolution of Southeast Asian Seas and Islands, Part 2,* A.G.U. Monograph Series 27:176-216.

Ebasco Services Inc., 1977. A report on geochronological investigations of materials relating to studies for the Philippine Nuclear Power Plant I: preliminary safety analysis report, vol.7, section 2.5. H.1, Appendix.

Espinas, M., 1968. A critical study of the Ibalong, the Bicol folk epic-fragment. *Unitas,* 41(2): 173-250.

Faustino, L., 1929. Mayon Volcano and its eruptions. *Phil. Jour. Sci.*, 40(1):1-43.

Fitch, T., 1972. Plate convergence, transcurrent faults, and internal deformation adjacent to Southeast Asia and Western Pacific. *J. Geophy. Res.*, 77(23):4432-4460.

Forrest, T., 1780. A voyage to New Guinea and the Moluccas: London, G. Scott, 411p. (An Oxford Reprint, 1669, with foreword by D.K. Bassett, published by Oxford Univ. Press, Kuala Lumpur)

Forster, H., Oles, D., Knittel, U., Defant, M., and Torres, R., 1990. The Macolod Corridor: a rift crossing the Philippine island arc. *Tectonophy.*, 183:265-271.

Geronimo, S., 1988. Characteristics, depositional facies and emplacement mechanisms of the Buco base surge sequence, Batangas province. M.Sc. Thesis, *University of Philippines*, 81p.

Geronimo-Catane, S., 1994. Features and nature of emplacement of debris-avalanche deposits in the Philippines. Ph.D. Dissertation, *Graduate School of Science and Technology, Kobe University,* Japan, 261p.

Goto, A., 1993. Viscosity measurement of volcanic ejecta of Mayon Volcano. *In: Eruption of Mt. Mayon, Philippines February 1993 and associated hazards.* Research Report of Grants-in-Aid for Scientific Research from the Ministry of Education, Science and Culture, Japan. Faculty of Science, Hokkaido University, 47-52.

Hamada, T., 1976. Rikagaku Kenkyushu N-2337 and N-2338. *In:* Newhall, C.G., 1977. *Geology and petrology of Mayon Volcano, southeastern Luzon, Philippines,* M.Sc. Thesis, *University of California*, 291p.

Hamburger, M., Cardwell, R., and Isacks, B., 1983. Seismotectonics of the northern Philippine island arc. *In:* Hayes, D.E., ed., *The Tectonic and Geologic Evolution of Southeast Asian Seas and Islands, Part* 2, AGU Monograph Series 27:1-22.

Hamilton, W., 1979. Tectonics of the Indonesian region. *USGS Prof. Paper 1078*, 345 p.

Hoblitt, R.P., Wolfe, E.W., Scott, W.E., Couchman, M.R., Pallister, J.S., and Javier, D., 1996. The preclimactic eruptions of Mount Pinatubo, June 1991. *In:* Newhall, C.G. and Punongbayan, R.S., eds., *Fire and Mud: Eruptions and Lahars of Mount Pinatubo, Philippines,* Philippine Institute of Volcanology and Seismology, Quezon City and University of Washington Press, Seattle, 457-512.

Holasek, R.E., Self, S., and Wood A.W., 1996. Satellite observations and interpretations of the 1991 Mount Pinatubo eruption plumes. *J. Geophy. Res.*, 101:27635-27655.

Jagor, F., 1873. Reisen in den Philippinen. Weidmannsche Buchhandlung, Berlin, 381p.

JICA, Japan International Cooperation Agency Metal Mining Agency of Japan, 1999. Report on regional survey for mineral resource in the Bicol area, Republic of the Philippines.

Karig, D., 1973. Plate convergence between the Philippines and Ryukyu Islands. *Marine Geology*, 14:153-168.

Karig, D. and Sharman, G., 1975. Subduction and accretion in trenches. *Geol. Soc. Am. Bull.*, 86:377-389.

Knittel, U., 1998. Personal communication.

Knittel, U. and Defant, M.J., 1988. Sr isotopic and trace element variations in Oligocene to Recent igneous rocks from the Philippine island arc: evidence for recent enrichment in the sub-Philippine mantle. *Earth Planet. Sci. Lett.*, 87:87-89.

Knittel, U. and Oles, D., 1995. Basaltic volcanism associated with extentional tectonics in the Taiwan-Luzon island arc: evidence for non-depleted sources and subduction zone enrichment. *In:* Smellie, J.L., ed., *Volcanism Associated with Extension at Consuming Plate Margins*, Geol. Soc. London Spec. Publ., 81:77-93.

Knittel, U., Defant, M.J., and Raczek, I., 1988. Recent enrichment in the source region of arc magmas from Luzon island, Philippines: Sr and Nd isotopic evidence. *Geology*, 16:73-76.

Koyaguchi, T., 1996. Volume estimation of tephra-fall deposits from the June 1991 eruption of Mount Pinatubo by theoretical and geological methods. *In:* Newhall, C.G. and Punongbayan, R.S., eds., *Fire and Mud: Eruptions and Lahars of Mount Pinatubo, Philippines,* Philippine Institute of Volcanology and Seismology, Quezon City and University of Washington Press, Seattle, 583-600.

Le Gentil, de la Galaisière, Guillaume Joseph Huacinthe Jean Baptiste, 1779-1781. Voyage dans les mers de l'Inde, fait par ordre du roi, a l'occasion du passage de Vènus, sur le disque du soleil, le 6 juin 1761, and le 3 du mème mois 1769: Paris. Imprimerie royale.

Lewis, S. and Hayes, D., 1983. The tectonics of northward propagating subduction along Eastern Luzon, Philippine Islands. *In:* Hayes, D.E., ed., *The Tectonic and Geologic Evolution of Southeast Asian Seas and Islands. Part 2.* AGU Monograph Series 27:57-78.

Lim, J.B., 1983. Correlating the orientation of tectonic stress with the flank eruptions of Taal Volcano. *Phil. J. Volcanol.*, 1(1):41-65.

Listanco, E.L., 1994. Space-time patterns in the geologic and magmatic evolution of calderas: A case study at Taal Volcano, Philippines. D.Sc. Dissertation, *Earthquake Research Institute, University of Tokyo,* Tokyo, Japan, 184 p.

Listanco, E., Sudo, M., Newhall, C., Ohkura, T., Tatsumi, Y., Ando, M., and Punongbayan, R., 1999. Application of per analysis to the magmas of the 1968-1993 eruptions of Mayon volcano. In: *The Mayon Volcano 1993 Eruption Volcanological and Seismological Monograph, Phil. Inst. Volcanol. And Seis. (PHIVOLCS)*, 27-34.

Lizardo, R., 1986. Statistical analysis of the eruptive events of Mayon Volcano, Philippines. *Phil. J. Volcanol.*, 3 (2):1-20.

Lowry, A.R., Hamburger, M.W., Meertens, C.M., and Ramos, E.G., 2001. GPS monitoring of crustal deformation at Taal volcano, Philippines. *J. Volcanol. Geotherm. Res.*, 105:35-47.

Ludwig, W., Hayes, D., and Ewing, J., 1967. The Manila Trench and West Luzon trough － I. Bathymetry and sediment distribution. *Deep Sea Res.*, 14:533-544.

Luhr, J.F. and Melson, W.G., 1996. Mineral and glass compositions in June 15, 1991 pumices: evidence for dynamic disequilibrium in the dacite of Mount Pinatubo. *In:* Newhall, C.G. and Punongbayan, R.S., eds., *Fire and Mud: Eruptions and Lahars of Mount Pinatubo, Philippines,* Philippine Institute of Volcanology and Seismology, Quezon City and University of Washington Press, Seattle, 733-750.

McCabe, R., Almasco, J., and Diegor, W., 1982. Geologic and paleomagnetic evidence for a possible Miocene collision in western Panay, central Philippines. *Geology*, 10:325-329.

McCool, W.W., 2002. Sedimentation from hypopycnal flows. M.Sc. Thesis, *School of Oceanography, University of Washington,* Seattle, 36p.

Magisa, R., 1641. Succeso raro de tres volcanes, dos de fuego, y uno de agua, que rebentaron a 4 de Enero deste año de 1641, a un sismo tiempo en differentes partes de estas islas Filipinas, con grande estruendo por lay ayres como de artilleria, y mosqueteria: Manila, Compania de Jesus, 6 p.

Mahood, G., 1980. Geological evolution of a Pleistocene rhyolitic center－Sierra La Primavera, Jalisco, Mexico. *J. Volcanol. Geotherm. Res.*, 8:199-230.

Major, J.J., Janda, R.J., and Daag, A.S., 1996. Watershed disturbance and lahars on the east side of Mount Pinatubo during the mid-June 1991 eruptions. *In:* Newhall, C.G. and Punongbayan, R.S., eds., *Fire and Mud: Eruptions and Lahars of Mount Pinatubo, Philippines,* Philippine Institute of Volcanology and Seismology, Quezon City and University of Washington Press, Seattle, 895-920.

Martinez, M. and Williams, S., 1999. Basaltic andesite scoria pyroclastic flow deposits from Taal Caldera, Philippines. *J. Geol. Soc. Phil.*, 54 (1,2):1-18.

Masigla, L.M. and Ruelo, H.B., 1987. Interpretation of the historical eruptive activity of Taal Volcano, Philippines. *Phil. Inst. Volcanol. and Seis. (PHIVOLCS) internal report*, Manila.

Matahelumual, J., 1985. Awu. *Bull. Volcanol. Survey of Indonesia*, 107:51 p.

Meyer, R., 1985. *In:* Ramos- Villarta, S., Corpuz, E., and Newhall, C., 1985. Eruptive history of Mayon Volcano, Philippines. *Phil. J. Volcanol.*, 2 (1-2), 1-35.

MGB, Mines and Geosciences Bureau, 1996. Geology and mineral resources of the Philippines, vol. 2, *Mines and Geosciences Bureau*, Manila, 175 p.

Miklius, A., Flower, M.F., Huijsmans, J.P., Mukasa, S.B., and Castillo, P., 1991. Geochemistry of lavas from Taal Volcano, southwestern Luzon, Philippines: evidence for multiple magma supply systems and mantle source heterogeneity. *J. Petrol.*, 32:593-627.

Mirabueno, H.M., 2001. Reconstruction of the February 1814 erupion of Mayon Volcano, Philippines. M.Sc. Thesis, *University of Caterbury*, Christchurch, New Zealand, 84 p.

Moore, J.G., Melson, W.G., 1969. Nuess ardentes of the 1968 eruption of Mayon Volcano, Philippines. *Bull. Volcanologique*, Ser. 2, 33:600-620.

Murillo Velarde, P., 1734. Mapa de las yslas Pilipinas: Manila, Compañia de Jesus.

Murphy, R.W., 1973. The Manila trench－west Taiwan foldbelt: a flipped subduction zone. *Geol. Soc. Malaysia Bull.*, 6:27-42.

Nakata, T., Sangawa, A., and Hirano, S., 1977. A report on tectonic landforms along the Philippine Fault Zone in northern Luzon, Philippines. *Science Reports, Tohoku Univ.*, 7th Series (Geography), Sendai, Japan, 27 (2):69-93.

NASA Jet Propulsion Laboratory. Taal Volcano, Philippines. (Online image) 22 October 2004 http://southport.jpl.nasa.gov/pio/volcanos/srl2-taal.gif

Newhall, C.G., 1977. Geology and petrology of Mayon Volcano, southeastern Luzon, Philippines, M.Sc. Thesis, *University of California*, 291p.

Newhall, C.G., 1993. Preliminary report of collaboration with the Philippine Institute of Volcanology and Seismology on the 1993 eruption of Mayon volcano. *USGS internal report*, 24

p.

Newhall, C.G. and Dzurisin, D., 1988. Historical unrest at large calderas of the world. *USGS Bull. 1855*, 1:599 p.

Newhall, C.G. and Punongbayan, R.S., (eds.), 1996. Fire and mud: eruptions and lahars of Mount Pinatubo, Philippines. Philippine Institute of Volcanology and Seismology, Quezon City and University of Washington Press, Seattle, 1126 p.

Newhall, C.G., Daag, A.S., Delfin, F.G., Jr., Hoblitt, R.P., McGeehin, J., Pallister, J.S., Regalado, M.T.M., Rubin, M., Tubianosa, B.S., Tamayo, R.A., Jr., and Umbal J.V., 1996. Eruptive history of Mount Pinatubo. *In:* Newhall, C.G. and Punongbayan, R.S., eds., *Fire and Mud: Eruptions and Lahars of Mount Pinatubo, Philippines,* Philippine Institute of Volcanology and Seismology, Quezon City and University of Washington Press, Seattle, 165-196.

Nieto Aguilar, J., 1894. Mindanao, su historia y geografia: Madrid, Imprenta del Cuerpo Administrativo del Ejercito, 152 p.

Nishigami, K., Shibutani, T. Ohkura, T., Hirata, M., Horikawa, H., Shimuzu, K., Matsuo, S., Nakao, S., Ando, M., Bautista, B.C., Bautista, L.P., Barcelona, E.S., Valerio, R., Lanuza, A.G., Chu, A.V., Villegas, J.J., Rasdas, A.R., Mangao, E.A., Gabinete, E., Punongbayan, B.J.T., and Punongbayan, R.S., 1994. Shallow crustal structure beneath Taal volcano, Philippines, revealed by the seismic explosion survey. *Bull. Disas. Prev. Res. Inst., Kyoto University,* 44:123-138.

Oles, D., 1991. Geology of the Macolod Corridor intersecting the Bataan-Mindoro island arc, the Philippines. Final report for German Research Society Project No. Fo 53/16-1 to 2 and German Agency for Technical Cooperation Project No. 85.2522.2-06.100.

Oppenheimer, C., 1988. Thermal observations of Mayon Volcano, Sept. 1988. *Phil. Inst. Volcanol. and Seis. (PHIVOLCS) internal report*, 2 p.

Oxfam-GRT, 2001. Potential for crater lake breaching and consequent lahars and flooding, Pinatubo volcano, Philippines, AD 2001. *PDRN internal report*.

Paladio-Melosantos, M.L., Solidum, R.U., Scott, W.E., Quiambao, R.B., Umbal, J.V., Rodolfo, K.S., Tubianosa, B.S., Delos Reyes, P.J., and Ruelo, H.R., 1996. Tephra falls of the 1991 eruptions of Mount Pinatubo. *In:* Newhall, C.G. and Punongbayan, R.S., eds., *Fire and Mud: Eruptions and Lahars of Mount Pinatubo, Philippines,* Philippine Institute of Volcanology and Seismology, Quezon City and University of Washington Press, Seattle, 513-536.

Pallister, J.S., Hobblit, R.P., Meeker, G.P., Knight, R.J., and Siems, D.F., 1996. Magma mixing at Mount Pinatubo: petrographic and chemical evidence from the 1991 deposits. *In:* Newhall, C.G. and Punongbayan, R.S., eds., *Fire and Mud: Eruptions and Lahars of Mount Pinatubo, Philippines,* Philippine Institute of Volcanology and Seismology, Quezon City and University of Washington Press, Seattle, 687-732.

Panem, C.C. and Delfin, F.G. Jr., 1988. Geology of Mt. Bulusan geothermal prospect. *Phil. Nat' l. Oil Co. (PNOC-EDC) internal report*, 49 p.

Peña, O., 1986. Seismic activity of Mayon Volcano prior to its 1984 eruption. *Phil. J. Volcanol.*, 3(2):21-37.

Peña, R. B., 1998. Petrology and geochemistry of the Balungao Group of volcanic centers, Pangasinan-Nueva Ecija, Luzon. *M.Sc. Thesis, University of the Philippines-National Institute of Geological Sciences*, 1-10.

Perrey, A., 1860. Documents sur let tremblements de terre et les phénomènes volcaniques dans l' archipel des Philippines: Memoires de l' Academie Impériale des Sciences. Arts et Belles-Lettres, Dijon, 2nd series, 8:85-194.

Pierson, T.C., Daag, A.S., Delos Reyes, P.J., Regalado, M.T.M., Solidum, R.U., and Tubianosa, B.S., 1996. Flow and deposition of post eruption hot lahars on the east side of Mount Pinatubo, July-October 1991. *In:* Newhall, C.G. and Punongbayan, R.S., eds., *Fire and Mud: Eruptions and Lahars of Mount Pinatubo, Philippines,* Philippine Institute of Volcanology and Seismology, Quezon City and University of Washington Press, Seattle, 921-950.

PHIVOLCS, Philippine Institute of Volcanology and Seismology, 1991a. Volcanoes of the Philippines. *PHIVOLCS Press*, Quezon City, Philippines, 41 p.

PHIVOLCS, 1991b. Taal Volcano Profile. *PHIVOLCS Press*, Quezon City, 90 p.

PHIVOLCS, 1991c. Camiguin Island. *PHIVOLCS Press*, Quezon City, 23 p.

PHIVOLCS, 1992. Operation Taal. *PHIVOLCS Press*, Quezon City, 29 p.

PHIVOLCS, 1995. Volcanoes of the Philippines. *PHIVOLCS Press*, Quezon City, 41 p.

PHIVOLCS, 1997. Catalogue of Philippine volcanoes, vol. 1, active volcanoes. Prepared by Del Mundo, E.T., Sabit, J.P., and Campita, N.R., *PHIVOLCS Press*, Quezon City, 100 p.

PHIVOLCS, 2002a. Volcanoes of the Philippines. Department of Science and Technology (DOST), 41 p.

PHIVOLCS, 2002b. Palimbang earthquake triggers Maughan lake breakout, Jan-June 2002. *PHIVOLCS Observer*, 13 (1-2):7-8.

PHIVOLCS, 2003. Taal Volcano Profile. *PHIVOLCS Press*, Quezon City, 3 p.

PHIVOLCS' Quick Response Team, 1995. The flash flood on Sept. 6, 1995 at the Alah River Valley: observations and interpretations. *In: Proc. Geol. Soc. Phil. 1995 Geological Convention*, Quezon City, Philippines

PHIVOLCS, Sept. 28, 2004. *Pinatubo advisory.* Retrieved 14 October 2004, from http://www.phivolcs.dost.gov.ph/Volcano/VolLatestActivity/PinatuboLatest.htm

Pubellier, M., Garcia, F., Loevenbruck A., and Chorowicz, J., 2000. Recent deformation at the junction between the north Luzon block and the central Philippines from ERS-1 Images. *The Island Arc*, 9: 598-610.

Pubellier, M., Quebral, R.D., Rangin, C., Deffontaines, B., Muller, C., Butterlin, J. and Manzano, J., 1991. The Mindanao collision zone, a soft collision event within a continuous Neogene strike-slip setting. *J. Southeast Asian Earth Sci.*, 6(3-4):239-248.

Punongbayan, R.S., 1985. An approach for estimating ages of active volcanoes. *Phil. J. Volcanol.*, 2 (1-2):191-205.

Punongbayan, R.S., Newhall, C.G., and Hoblitt, R.P., 1996. Photographic record of rapid geomorphic change at Mount Pinatubo, 1991-94. *In:* Newhall, C.G. and Punongbayan, R.S., eds., *Fire and Mud: Eruptions and Lahars of Mount Pinatubo, Philippines,* Philippine Institute of Volcanology and Seismology, Quezon City and University of Washington Press, Seattle, 989-1014.

Quebral, R.D., 1994. Tectonics of the southern segment of the Philippine Fault, eastern Mindanao, Philippines: transition from a collision zone to a strike-slip fault. Ph.D. Dissertation, *l' universite Pierre et Marie Curie (Paris IV)*, Paris, France, 280 p.

Ramos-Villarta, S., Corpuz, E., and Newhall, C.G., 1985. Eruptive history of Mayon Volcano, Philippines. *Phil. J. Volcanol.*, 2 (1-2), 1-35.

Ramos, E. 1986. Lakeshore landslides: unrecognized hazards around Taal Volcano. *Phil. J. Volcanol.*, 3 (1), 28-53.

Ramos, E., De Torres, C., and Calderon, A., 1985. Earth tide influences on the recent activities of Mayon Volcano. *Phil. J. Volcanol.*, 2(1-2):172-190.

Ringenbach, J.C., Pinet, N., Delteil, J., and Stephan, J.F., 1992. Analyse des structures engendreés en régime décrochant par le séisme de Nueva Ecija du 16 juillet 1990, Luzon, Philipppines, *Bull. Soc. Géol. France*, 163:109-123.

Rodolfo, K.S., 2001. A simple post-mortem of the breaching experiment at Pinatubo, and a proposal. *Presented in the NIGS Colloquium, National Institute of Geological Sciences, University of the Philippines,* Diliman, Quezon City, September 14, 2001.

Rodolfo, K.S., 2003. Personal communication.

Rodolfo, K.S., Umbal, J.V., Alonso, R.A., Remotigue, C.T., Paladio-Melosantos, M.L., Salvador, J.H.G., Evangelista, D., and Miller, Y., 1996. Two years of lahars on the western flank of Mount Pinatubo: initiation, flow processes, deposits, and attendant geomorphic and hydraulic changes. *In:* Newhall, C.G. and Punongbayan, R.S., eds., *Fire and Mud: Eruptions and Lahars of Mount Pinatubo, Philippines,* Philippine Institute of Volcanology and Seismology, Quezon City and University of Washington Press, Seattle, 989-1014.

Rosi, M., Paladio-Melosantos, M.L., Di Muro, A., Leoni, R., and Bacolcol, T., 2001. Fall vs. flow activity during the 1991 climactic eruption of Pinatubo Volcano (Philippines). *Bull. Volcanol.*, 62:549-566.

Sabit, J.P., Pigtain, R.C., and De la Cruz, E.G., 1996. The west-side story: observations of the 1991 Mount Pinatubo eruptions from the west. *In:* Newhall, C.G. and Punongbayan, R.S., eds., *Fire and Mud: Eruptions and Lahars of Mount Pinatubo, Philippines,* Philippine Institute of Volcanology and Seismology, Quezon City and University of Washington Press, Seattle, 445-456.

Saderra Maso, M., 1911. The eruption of Taal volcano January 30, 1911. *Weather Bureau Report*, Manila, 45p.

Scandone, R., 1990. Chaotic collapse of calderas: *J. Volcanol. Geotherm. Res.*, 42:285-302.

Scott, W.E., Hoblitt, R.P., Torres, R.C., Self, S, Martinez, M.L., and Nillos, T. Jr., 1996. Pyroclastic flows of the June 15, 1991, climactic eruption of Mount Pinatubo. *In:* Newhall, C.G. and Punongbayan, R.S., eds., *Fire and Mud: Eruptions and Lahars of Mount Pinatubo, Philippines,* Philippine Institute of Volcanology and Seismology, Quezon City and University of Washington Press, Seattle, 545-570.

Sudo, M., Listanco, E., Ishikawa, N., Tagami, T., Kamata, H., and Tatsumi, Y., 2000. K- Ar dating of the volcanic rocks from Macolod Corridor in Southwestern Luzon, Philippines: toward understanding of the Quaternary volcanism and tectonics. *J. Geol. Soc. Phil.*, 55(1-2):89-104.

Sun, S.S. and McDonough, W.F., 1989. Chemical and isotopic systematics of oceanic basalts: Implications for mantle compositions and processes. *In:* Saunders, A.D. and Norry, M.J., eds., *Magmatism in the Ocean Basins*, Geol. Soc. Spec. Pub., 42:313-345.

Tatsumi, Y., Hamilton, D.L., and Nesbitt, R.W., 1986. Chemical characteristics of fluid phase released from a subducted lithosphere and origin of arc magmas: evidence from high-pressure experiments and natural rocks. *J. Volcanol. Geotherm. Res.*, 29:293-309.

Torres, R.C., Self, S., and Martinez, M.L., 1996. Secondary pyroclastic flows from the June 15, 1991, ignimbrite of Mount Pinatubo. *In:* Newhall, C.G. and Punongbayan, R.S., eds., *Fire and Mud: Eruptions and Lahars of Mount Pinatubo, Philippines,* Philippine Institute of Volcanology and Seismology, Quezon City and University of Washington Press, Seattle, 665-678.

Tubianosa, B., Martinez, M.M., Daag, A., and Arboleda, R., 1999. Monitoring SO_2 emission rates during the 1993 eruption of Mayon Volcano. *The Mayon Volcano 1993 Eruption, Volcanological and Seismological Monograph,* Phil. Inst. Volcanol. and Seis. (PHIVOLCS), 15-26.

Umbal, J.V. and Rodolfo, K.S., 1996. The 1991 lahars of southwestern Mount Pinatubo and evolution of the lahar-dammed Mapanuepe lake. *In:* Newhall, C.G. and Punongbayan, R.S., eds., *Fire and Mud: Eruptions and Lahars of Mount Pinatubo, Philippines,* Philippine Institute of Volcanology and Seismology, Quezon City and University of Washington Press, Seattle, 951-970.

Von Buch, L., 1825. Physik. Beschreibung der Canarien Inseln, 376 p.

Von Drasche, R. 1876. Einige Worte uber den geologischen Bau von Sud-Luzon. Tschermaks Mineral. Petrograph. Mittheilungen, 3:157-165.

Walker, G.P.L., 1984. Downsag caldera, ring faults, caldera sizes, and incremental caldera growth. *J. Geophy. Res.*, 89:8407-8416.

Wiesner, M.G., and Wang, Y., 1996. Dispersal of the 1991 Pinatubo tephra in the South China Sea. *In:* Newhall, C.G. and Punongbayan, R.S., eds., *Fire and Mud: Eruptions and Lahars of Mount Pinatubo, Philippines,* Philippine Institute of Volcanology and Seismology, Quezon City and University of Washington Press, Seattle, 537-544.

Wiesner, M.G., Wang, Y., and Zheng, L., 1995. Fallout of volcanic ash to the deep South China Sea induced by the 1991 eruption of Mount Pinatubo. *Geology*, 23:885-888.

Wiesner, M.G., Welzel, A., Catane, S.G., Listanco, E.L., and Mirabueno, H.T., 2004. Grain size, areal thickness distribution and controls on sedimentation of the 1991 Mount Pinatubo tephra layer in the South China Sea. *Bull. Volcanol.*, 66:226-242.

Wolfe, J.A., 1981. Philippine geochronology. *J. Geol. Soc. Phil.*, 243-262.

Wolfe, J.A. and Self, S., 1983. Structural lineaments and Neogene volcanism in southwestern Luzon. *In:* Hayes, D.E., ed., *Tectonic and Geologic Evolution of Southeast Asian Seas and Islands*, AGU Geophys. Monogr., Series 27:157-172.

Wolfe, E.W. and Hoblitt, R.P., 1996. Overview of the eruptions. *In:* Newhall, C.G. and Punongbayan, R.S., eds., *Fire and Mud: Eruptions and Lahars of Mount Pinatubo, Philippines,*

Philippine Institute of Volcanology and Seismology, Quezon City and University of Washington Press, Seattle, 3-20.

Worcester, D.C., 1912. Taal Volcano and its recent destructive eruption. *National Geog. Mag.*, 23:313-367.

Yumul, G.P. Jr., Dimalanta, C.B., Tamayo, R.A. Jr., and Bellon, H., 2003. Silicic arc volcanism in central Luzon, the Philippines: Characterization of its space, time and geochemical relationship. *The Island Arc*, 12:207-218.

EXPLOSIVE VOLCANISM IN THE PHILIPPINES

（東北アジア研究センター叢書 第18号）

2005年 3 月31日発行　非売品

発　行　者　　東北大学東北アジア研究センター

〒980－8576　仙台市青葉区川内41

印　　刷　　株式会社　東北プリント

〒983－0822　仙台市青葉区立町24－24

CNEAS

THE CENTER FOR NORTHEAST ASIAN STUDIES
TOHOKU UNIVERSITY